

**Autonomous Conflict Detection and Resolution for Unmanned Aerial Vehicles  
On integration into the Airspace System**

Jenie, Yazdi

**DOI**

[10.4233/uuid:02965443-f1e5-440c-b9af-0e0648be9552](https://doi.org/10.4233/uuid:02965443-f1e5-440c-b9af-0e0648be9552)

**Publication date**

2017

**Document Version**

Final published version

**Citation (APA)**

Jenie, Y. (2017). *Autonomous Conflict Detection and Resolution for Unmanned Aerial Vehicles: On integration into the Airspace System*. [Dissertation (TU Delft), Delft University of Technology]. <https://doi.org/10.4233/uuid:02965443-f1e5-440c-b9af-0e0648be9552>

**Important note**

To cite this publication, please use the final published version (if applicable).  
Please check the document version above.

**Copyright**

Other than for strictly personal use, it is not permitted to download, forward or distribute the text or part of it, without the consent of the author(s) and/or copyright holder(s), unless the work is under an open content license such as Creative Commons.

**Takedown policy**

Please contact us and provide details if you believe this document breaches copyrights.  
We will remove access to the work immediately and investigate your claim.

# **AUTONOMOUS CONFLICT DETECTION AND RESOLUTION FOR UNMANNED AERIAL VEHICLES**

ON INTEGRATION INTO THE AIRSPACE SYSTEM

## **Proefschrift**

ter verkrijging van de graad van doctor  
aan de Technische Universiteit Delft,  
op gezag van de Rector Magnificus prof. ir. K. C. A. M. Luyben,  
voorzitter van het College voor Promoties,  
in het openbaar te verdedigen op maandag 23 januari 2017 om 10:00 uur

door

**Yazdi Ibrahim JENIE**

Magister Teknik in Aeronautics and Astronautics,  
Institut Teknologi Bandung, Indonesia  
geboren te Surakarta, Indonesia

Dit proefschrift is goedgekeurd door de  
promotor: Prof. dr. ir. J. M. Hoekstra  
copromotor: Dr. ir. E. van Kampen

Samenstelling promotiecommissie:

|                               |   |
|-------------------------------|---|
| Rector Magnificus,            | voorzitter                                |
| Prof. dr. ir. J. M. Hoekstra, | Technische Universiteit Delft, promotor   |
| Dr. ir. E. van Kampen,        | Technische Universiteit Delft, copromotor |
| Prof. dr. ir. J. A. Mulder,   | Technische Universiteit Delft             |

Onafhankelijke leden:

|                         |   |
|-------------------------|---|
| Prof. dr. H. Muhammad,  | Institut Teknologi Bandung              |
| Prof. dr. D. Delahaye,  | École Nationale de l'Aviation Civile    |
| F. J. L. Bussink, B.Sc. | Nederlands Lucht- en Ruimtevaartcentrum |
| Prof. dr. R. Curran,    | Technische Universiteit Delft           |

Reservelid:

|                         |                               |
|-------------------------|-------------------------------|
| Prof. dr. D. G. Simons, | Technische Universiteit Delft |
|-------------------------|-------------------------------|



*Keywords:*      Airspace Management; Airspace Integration; Autonomous Collision Avoidance; Conflict Detection and Resolution; Monte Carlo Simulation; Safety Analysis; Unmanned Aerial Vehicle; Velocity Obstacle Method;

*Printed by:*      Proefschriftmaken, Vianen, The Netherlands

Cover design by Yazdi Ibrahim Jenie

ISBN 978-94-6186-779-7

An electronic version of this dissertation is available at  
<http://repository.tudelft.nl/>.

Copyright © 2017 by Yazdi Ibrahim Jenie. All rights reserved. No part of this publication may be reproduced, stored in a retrieval system, or transmitted, in any form or by any means, electronics, mechanical, photocopying, recording, or otherwise, without prior permission in writing from the proprietor.

# SUMMARY

## **AUTONOMOUS CONFLICT DETECTION AND RESOLUTION FOR UNMANNED AERIAL VEHICLES**

ON INTEGRATION INTO THE AIRSPACE SYSTEM

**Yazdi Ibrahim JENIE**

In the last decade, the commercial values of Unmanned Aerial Vehicles (UAV), defined as devices that are capable of sustainable flights in the atmosphere that do not require to have a human (pilot) on-board, become widely recognized thanks to the advancement of technology in materials, sensors, computation, and telemetry. As UAVs are becoming cheaper and more user-friendly, many companies are motivated to incorporate them in their everyday business, such as for delivery services, journalisms, or providing Internet services.

All of commercial prospective applications for UAVs, however, can only be achieved once the vehicles are fully integrated into the airspace system. This is not the case yet, since UAV operations, in most part of the world, are strictly regulated to fly only within the visual line of sight (VLOS) of the ground pilot, forbidding the otherwise beyond visual line of sight (BVLOS) flight. One main reason for such strict regulations is the apprehension about the safety of UAV operations, which are likely to be heterogeneous due to the possible large variation of UAVs in the airspace, each with their own preference on how to interact with other UAVs and with the current (manned) air traffic. Hence, airspace management, especially in the mitigation of mid-air conflicts and collisions, is expected to become much more complex, compromising the overall safety.

Therefore, the problem of safe UAV integration into the airspace is the selected topic for this research, especially in the development of Conflict Detection and Resolution (CD&R) systems. The particular system describes any procedures and devices for vehicles to mitigate potential mid-air conflicts and collisions. For a UAV, this system needs to consider a wide range of obstacles it might encounter, from a static unmoving object to other vehicles with completely different characteristics. Moreover, there can be interactions between two UAVs with different levels of CD&R system awareness. Only when their CD&R systems are fully defined and regulated to handle such diverse scenarios, can UAVs be fully integrated into the airspace.

The main goal of this research is to define and evaluate systems for detecting and resolving possible mid-air conflicts of Unmanned Aerial Vehicles, specifically to support safe beyond visual line-of-sight operations in an integrated airspace. This goal is achieved by addressing the four research problems, i.e. the airspace incompatibility, the CD&R diversity, the doubt on UAV safety, and the UAV autonomous CD&R inadequacy. Directly from those problems, four research questions are formulated as follows:

1. What structure can be defined to manage the CD&R system for UAVs operating in an integrated airspace?
2. How can the diverse UAV CD&R approaches be classified into a comprehensive taxonomy that is compatible with the current airspace?
3. How can the safety parameters of the integrated airspace, under influence of a heterogeneous CD&R approaches, can be determined?
4. How can an autonomous CD&R system for UAVs be defined to handle potential conflicts, seeing the vehicle as part of the integrated traffic in the airspace?

To address the first question, this research proposes a taxonomy of CD&R approaches for UAV operating in an integrated airspace. Possible approaches for UAVs are surveyed and broken down based on their types of surveillance, coordination, maneuver, and autonomy. The factors are combined back into several 'generic approaches', for example, the Traffic Warning and Collision Avoidance System (TCAS) in manned flight can be seen as CD&R that uses combination of *a distributed dependent surveillance, an explicit coordination, an escape maneuver, and conducted manually*. The approaches that fits the scheme of UAV integration are then selected methodically, resulting in a novel taxonomy of UAV CD&R approaches.

From the generic approaches in the taxonomy, a multi-layered architecture is developed in this research, managing CD&R procedures in the airspace that are compatible with the manned flights, while also embracing those that are unique to UAVs'. The multi-layered feature means that instead of relying on only one CD&R approach, UAVs can implement multiple approach in a fail-safe concept, ensuring that even in a case when one approach fails, there are still available layers that can prevent direct collisions. Six CD&R approaches from the taxonomy are further selected as the safety layers, which included the layer of (1) Procedural, (2) Manual, (3) Cooperative, (4) Non-cooperative (5) Escape, and (6) Emergency approaches.

A brief implementation of the multi-layered CD&R architecture suggesting that its usage depends closely on the type of mission: in a particular mission some layers might become less necessary, while in others they might be important. The proposed architecture, however, is lacking definitions of physical thresholds between layers, such as the distance or time-to-collision, which need to be defined specifically for each type of UAV. This is warranted for the future work for UAVs air traffic management, but might only be truly be defined once the BVLOS flights of UAVs are allowed in the airspace.

Answering the second research question, the previously proposed taxonomy is attributed to available CD&R methods in the literature, in order to determine their fitness and whether they are complementary or interchangeable from one to another. A total of 64 CD&R methods are evaluated, ranging from preflight calculations on determinis-

tic maps, such as a Global Path Planning, to reactive avoidances with on-board sensors, such as by using the Velocity Obstacle method. Using the taxonomy, the position of each approaches in the overall safety management scheme, such as by using a multi-layered architecture, can be defined.

The taxonomy attribution has shown that many of the available methods fall outside the taxonomy, and suggests the need to concentrate research more to parts where representative methods are lacking. On further evaluation, it also becomes apparent that the diversity of CD&R preferences only existed within the walls of laboratories, due to the current UAV flight limitation to only within VLOS. Nevertheless, the taxonomy potentially can aid both developers and authorities in deciding an adequate CD&R approach(es) to ensure safety of an upcoming BVLOS flight in an integrated airspace.

The third question is addressed by setting up a series of Monte Carlo simulation to derive two safety parameters, i.e. the frequencies of near mid-air collisions (NMAC), and of mid-air collisions (MAC). The former represents how often two UAVs fly closer to each other than a certain thresholds, which is set to be 50 meters in most of the discussion in this dissertation, while the later describe the actual body-to-body collision between vehicles. The use of the Monte Carlo simulations is meant to overcome the limitation of available analytical methods in literature, by incorporating the effect of distributed CD&R system, as well as the heterogeneous condition setup for the airspace. The method, however, has rarely been preferred in the safety parameter derivation, due to its significantly time-consuming process to obtain any meaningful results. This problem is addressed in this research by simulating in high-density setups, of which results are scaled down latter on, to more realistic densities of an airspace.

Two CD&R protocols are modeled in the simulations, first one is the cooperative protocol, where each vehicle conduct avoidance that is implicitly coordinated by common rules-of-the-air, and the second one is the non-cooperative protocol, where each vehicle avoids with preferences that are randomly given. A certain target level of safety (TLS) is defined as well in research, to measured the collective performance of the CD&R systems, in which the frequency of NMACs and MACs should be lower than  $10^{-2}$  and  $10^{-7}$  per hour, respectively. Those values of TLS are proposed on the basis of the equivalent values in manned-flight history for the last decade.

As the results, while maintaining the TLS of the airspace, the distributed cooperative CD&R protocol is able to increase the maximum number of operating UAV in one flight level to almost ten times the number when no CD&R is applied. This would mean that for a city like Chicago that has an area of more than five-thousand kilometer-square, a total of 45 UAVs can operate independently in one altitude. It is also concluded that a much better results are obtained while using the cooperative protocol, which justifies the necessity of order in the airspace, which in this case is the implementation of the Right-of-way rules.

The usefulness of Monte Carlo simulations method is demonstrated in this research, testing various CD&R algorithms and protocols in a vast number of possible conditions, including those that are previously unpredicted. The downside of the method still appears, however, in which it cannot derive any meaningful results for the frequency of MACs within the number of samples tested, due to the rareness of MACs even in a high-

density setups. Hence, more samples are recommended for the future work, along with further extension to include aircraft dynamic model inside the simulations.

The fourth question is addressed in this research by introducing two novel CD&R algorithms which are adequate to fill in specific layers in the CD&R architecture explained before. The first algorithm is the Selective Velocity Obstacle (SVO) method, an extension of the Velocity Obstacle method (VO-method) with additional criteria for implicit coordination. This CD&R method is developed specifically for the Cooperative layer in the CD&R architecture, which is based on the unlikeliness of the future airspace to exist without some sort of order or coordination, such as the Right-of-way rules. The SVO is also used as the basis of the cooperative CD&R protocol in the previously explained NMAC frequency derivation using Monte Carlo simulations.

The second algorithm is the Three-dimensional Velocity Obstacle (3DVO) method that represent the VO-method in three-dimensional space, obtaining a much wider range of resolution possibilities. The three-dimensional resolution is performed in arbitrary avoidance planes, which number and direction can be set according to the UAV maneuverability. Furthermore, since it is designed to fill the Escape layer from the architecture, the 3DVO is equipped with Buffer Velocity Zones, an additional algorithm to anticipate adverse movements of uncoordinated obstacles. It is discovered, however, that the addition of the Buffer Velocity zones increases the algorithm performance more significantly than the number of Avoidance Planes available.

Both the SVO and 3DVO method have been validated by series of Monte Carlo simulations in a stressful heterogeneous airspace setup, in which they were able to significantly reduce the frequencies of NMACs and MACs, and hence are promising to support BVLOS operation in an integrated airspace. Both method, however, are lacking of vehicle dynamic model, which can significantly change the result, especially in the Escape layer, in which avoidance happen in a close range. Moreover, experiments to proof both concepts is also warranted for future works, especially in testing an actual BVLOS flight where the UAVs autonomously interact with the heterogeneous airspace. Furthermore, adequate algorithm to fill other layers in the architecture is also mandatory to support a complete BVLOS flight. This will further enrich the available CD&R approaches that can be selected for UAV operation in an integrated airspace.

Therefore, on the basis of the research performed in this dissertation, it is concluded that safe integration of UAVs into the airspace is very much feasible. The conclusion is supported by numerous simulations that have been conducted, demonstrating the possibility to reach the airspace TLS by resorting to an autonomous CD&R system, which is distributed and works independently in each vehicles. The low risk of UAV operations, even in a heterogeneous airspace conditions, is validated even more by the rarity of NMACs and MACs occurrences to the point that an artificially exaggerated setup, such as a super conflict or a high-density airspace, is required to measure the operational safety.

While many CD&R approaches for UAVs in literature have not been designed for a BVLOS flight in an integrated airspace, their algorithm can be adjusted to conform the proposed taxonomy. An example of such adjustment is presented in this dissertation by the extension of the VO-method into SVO method that fits the Cooperative approach,

and 3DVO that is designed for the Escape approach. With the large diversity of CD&R approach in literature, validation in a heterogeneous setup is a necessity, either by simulations or by actual flight experiments.

Compared to back in mid 2011 when this research was initiated, in this 2016 commercial use of UAVs are increasingly getting exposed to the general public. Regulations are being updated to define UAVs' airworthiness and widens their area of operations. Operator awareness of the regulations is also increasing as it is shown by the booming of registered number of drone owners. At the same time, drone advocacy groups are assembled to push regulatory policies to allow UAV operations, especially for BVLOS flight. These indicates that UAV integration into the airspace is inevitable, and that CD&R systems to support safety in such airspace is urgently needed. Therefore, at one point perhaps it is best for the authorities to simply start to accommodate the BVLOS flight in the airspace, allowing both UAVs and their CD&R system to mature based on experience they can gain in a real situation. As it has been shown in the history of manned-flight deregulation, this can create a competitive environment that pushes both manufacturer and operator to continuously strive for safety improvements in an integrated airspace system.



# CONTENTS

|   |            |
|---|------------|
| <b>Summary</b>  | <b>iii</b> |
| <b>1 Introduction</b>   | <b>1</b>   |
| 1.1 Unmanned Aerial Vehicles and the Airspace System . . . . .                | 1          |
| 1.2 Problem Definition . . . . .  | 4          |
| 1.2.1 Current Airspace Incompatibility . . . . .                              | 4          |
| 1.2.2 CD&R System Diversity . . . . .   | 5          |
| 1.2.3 UAV CD&R System Safety . . . . .  | 6          |
| 1.2.4 UAV Autonomous CD&R System Inadequacy . . . . .                         | 7          |
| 1.3 Research Objective . . . . .  | 7          |
| 1.4 Research Scope and Limitations . . . . .                                  | 8          |
| 1.5 Methodology and Dissertation Outline . . . . .                            | 10         |
| <b>2 Taxonomy and Architecture of CD&amp;R Approaches</b>                     | <b>13</b>  |
| 2.1 Introduction . . . . .  | 14         |
| 2.2 Inventory of Approaches for UAV CD&R System. . . . .                      | 16         |
| 2.2.1 Types of Airspace Surveillance . . . . .                                | 16         |
| 2.2.2 Types of Coordination . . . . .   | 18         |
| 2.2.3 Types of Avoidance Maneuver . . . . .                                   | 19         |
| 2.2.4 Types of Autonomy . . . . .   | 20         |
| 2.3 Taxonomy of Conflict Detection and Resolution Approaches for UAV. . . . . | 20         |
| 2.3.1 UAV Flight in the Future Integrated Airspace. . . . .                   | 21         |
| 2.3.2 Combination Process of CD&R Methods. . . . .                            | 23         |
| 2.3.3 Approaches Availability . . . . .                                       | 24         |
| 2.4 A Multi-layered Architecture . . . . .                                    | 26         |
| 2.4.1 Generic Approaches Arrangement . . . . .                                | 26         |
| 2.4.2 General Implementation. . . . .   | 27         |
| 2.5 Conclusion . . . . .  | 28         |
| <b>3 Safety Assessment of UAV CD&amp;R System</b>                             | <b>31</b>  |
| 3.1 Introduction . . . . .  | 32         |
| 3.2 Heterogeneous Airspace Model . . . . .                                    | 33         |
| 3.2.1 High Density Airspace with Periodic Boundary Condition . . . . .        | 34         |
| 3.2.2 The Uncertainty of Conflict Detection . . . . .                         | 36         |
| 3.2.3 The Variation of Conflict Resolution . . . . .                          | 36         |
| 3.2.4 Order in the Heterogeneous Airspace . . . . .                           | 38         |
| 3.3 Monte Carlo Simulations . . . . .   | 40         |
| 3.3.1 General Setup . . . . .   | 40         |
| 3.3.2 Output. . . . .   | 41         |
| 3.3.3 Convergence. . . . .  | 42         |

|          |  |           |
|----------|--|-----------|
| 3.4      | Result and Analysis . . . . .  | 42        |
| 3.4.1    | Visualization . . . . .  | 43        |
| 3.4.2    | NMAC and MAC Frequencies . . . . .                                       | 45        |
| 3.4.3    | Reaching the Target Level of Safety. . . . .                             | 47        |
| 3.4.4    | Severity of Intrusion . . . . .  | 49        |
| 3.5      | Conclusion . . . . .   | 49        |
| <b>4</b> | <b>Implicitly Coordinated Tactical Maneuver for Avoidance</b>            | <b>53</b> |
| 4.1      | Introduction . . . . .   | 54        |
| 4.2      | Selective Velocity Obstacle Method for UAV Collision Avoidance . . . . . | 54        |
| 4.2.1    | Original Concept of the Velocity Obstacle Method . . . . .               | 55        |
| 4.2.2    | Incorporating the Right-of-way Rules . . . . .                           | 56        |
| 4.2.3    | Avoidance Algorithm and the Minimum Avoidance Turning-rate . . . . .     | 57        |
| 4.3      | Implementation . . . . .   | 61        |
| 4.3.1    | Simulation Setup. . . . .  | 61        |
| 4.3.2    | Results . . . . .  | 61        |
| 4.3.3    | Validation . . . . .   | 64        |
| 4.4      | Conclusion . . . . .   | 67        |
| <b>5</b> | <b>Uncoordinated Escape Maneuver for Avoidance</b>                       | <b>69</b> |
| 5.1      | Introduction . . . . .   | 70        |
| 5.2      | The Three-dimensional Velocity Obstacle Method . . . . .                 | 71        |
| 5.2.1    | 3DVO method's Velocity Obstacle Cone . . . . .                           | 73        |
| 5.2.2    | Handling Maneuvering Obstacles: The Buffer Velocity Set . . . . .        | 75        |
| 5.2.3    | Avoidance Planes . . . . .   | 76        |
| 5.3      | Strategy for a Three-dimensional Avoidance . . . . .                     | 81        |
| 5.3.1    | Avoidance Algorithm. . . . .   | 81        |
| 5.3.2    | Choosing an Avoidance Plane . . . . .                                    | 82        |
| 5.3.3    | Avoidance Turning Rate . . . . .   | 84        |
| 5.4      | Implementation . . . . .   | 86        |
| 5.4.1    | Two Vehicles Converging. . . . .   | 86        |
| 5.4.2    | Multiple Heterogeneous Conflicts . . . . .                               | 90        |
| 5.4.3    | 3DVO method Validation. . . . .  | 91        |
| 5.5      | Conclusions. . . . .   | 93        |
| <b>6</b> | <b>Discussion, Conclusion, and Recommendation</b>                        | <b>95</b> |
| 6.1      | Discussion . . . . .   | 96        |
| 6.1.1    | On Airspace Incompatibility . . . . .                                    | 96        |
| 6.1.2    | On UAV CD&R System Diversity . . . . .                                   | 97        |
| 6.1.3    | On UAV CD&R System Safety. . . . .                                       | 98        |
| 6.1.4    | On Autonomous CD&R System Inadequacy . . . . .                           | 99        |
| 6.1.5    | On Research Methodology . . . . .  | 101       |
| 6.2      | Final Conclusion . . . . .   | 103       |
| 6.3      | Future Works . . . . .   | 105       |

---

|                             |            |
|-----------------------------|------------|
| <b>References</b>           | <b>107</b> |
| <b>Samenvatting</b>         | <b>119</b> |
| <b>Acknowledgement</b>      | <b>125</b> |
| <b>Curriculum Vitæ</b>      | <b>127</b> |
| <b>List of Publications</b> | <b>129</b> |



# 1

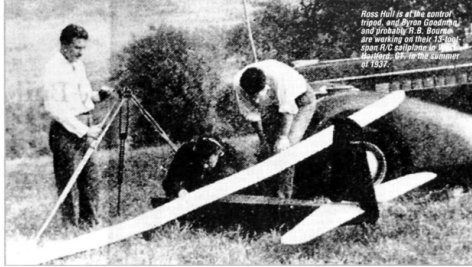
## INTRODUCTION

### 1.1. UNMANNED AERIAL VEHICLES AND THE AIRSPACE SYSTEM

**U**NMANNED Aerial Vehicles (UAV), also known as Uninhabited Aerial Vehicles, or Unpiloted Aerial Vehicles, or Unmanned Aircraft, or Remotely Piloted Aerial Vehicles, or Aerial Drones, or many other names, are defined as devices that are capable of sustainable flights in the atmosphere that do not require to have a human (pilot) on-board. With this definition, the technological history of UAVs can be stretched back as far as in March 1917, when A.M. Low's Ruston Proctor AT (Aerial Target/Aerial Torpedo) was launched using compressed air from a back of a lorry near Salisbury Plain, shown in Figure 1.1-a. Separately in March 1918, the first Curtiss-Sperry remote controlled 'Flying Bomb' was launched (see Figure 1.1-b) from the top of a Marmon automobile driving along the Long Island Motor Parkway, New York. Afterwards, the technology of remote controlled flight grew rapidly throughout the period of the First World War, particularly for those two purposes, as an Aerial Target (later known as target drones) and a Flying Bomb (later known as guided missiles). The first recorded UAV usage outside the military ground was demonstrated and documented in 1937 by Ross Hull and Clinton B. DeSoto, who flew their remote controlled 15-foot-span model plane shown in Figure 1.1-c [1, 2]. The military, however, continues to be the center of advancement for UAVs, expanding their (re)usability for intelligence, surveillance, target-acquisition, and reconnaissance.



(a)



(c)



(b)

Figure 1.1: The pioneers of Unmanned Aerial Vehicle Technology [1, 2] (a) A.M. Low's Ruston Proctor AT, (b) Curtiss-Sperry 'Flying Bomb', and (c) Ross Hull and Clinton B. DeSoto remote controlled model plane.

Not until recently have the commercial values of UAVs for civil purposes become widely recognized, thanks to the advancement of technology in materials, sensors, computation, and telemetry. As UAVs are becoming cheaper and more user-friendly, many companies are motivated to incorporate them in their everyday business. DeGarmo [3], back in 2004, introduced seven examples of prospective UAVs for civil applications, as illustrated in Figure 1.2. A decade latter, however, many unexpected types of civil UAV emerge abruptly. Retail companies, for example, have started to propose a UAV-based delivery service to their customers<sup>1</sup>, media has already used UAV to obtain immediate aerial footage of an incident<sup>2</sup>, and Information Technology companies have developed a high-altitude imagery UAVs to update their online map services<sup>3</sup>.

All of those prospective applications can be achieved once UAVs are fully integrated into the airspace system, which, however, is not yet the case. UAV operations, in most part of the world, are strictly regulated to fly only within the visual line of sight (VLOS) of the ground pilot. In the United States, for example, it is generally forbidden to fly an unmanned vehicle beyond the visual line of sight (BVLOS), while flying within visual line of sight (VLOS) can only be conducted when there is daylight. Furthermore, the UAV needs to weigh less than 25 kg, with maximum ground speed of 45 meters/second, and remain below 120 meters above ground level [4]. The same rules apply in the Nether-

<sup>1</sup>Gershgorn, D., "We now know where Amazon will be testing their delivery drones", 2016, accessed June 2016, <http://www.popsci.com/we-now-know-where-amazon-will-be-testing-their-delivery-drones>

<sup>2</sup>Goldman, D., "CNN cleared to test drones for reporting", 2015, accessed June 2016, <http://money.cnn.com/2015/01/12/technology/cnn-drone/>

<sup>3</sup>Barr, A., and Albergotti, R., "Google to Buy Titan Aerospace as Web Giants Battle for Air Superiority", 2014, accessed June 2016, <http://www.wsj.com/news/articles/SB10001424052702304117904579501701702936522>



Figure 1.2: Prospective commercial applications of UAVs, adapted from the work of [3] with several additions.

lands, with a maximum weight of 150 kg, and the possibility for an extended visual line of sight (E-VLOS) [5]. The newest regulation in the United Kingdom [6], on the other hand, already accommodates a BVLOS UAV flight. This, however, requires tedious work to obtain an approval for the method of aerial separation and collision avoidance, which should comply with the rules in manned-flight.

One main reason for such strict regulations is the apprehension about the safety of UAV operations, which are likely to be heterogeneous. Unlike manned-flight, UAV technology is increasingly accessible to the public, such that in just a few years, nearly everyone will be able to build and fly one to do any mission they could think of. Consequently, there will be a large and diverse collection of UAVs in the airspace, each with their own preference on how to interact with others, as well as with the current (manned) air traffic. For a BVLOS flight in particular, these interactions most likely involve some level of autonomy, which may also vary among the unmanned vehicles. All of this heterogeneity

will add to the complexity of the airspace management, especially in the mitigation of mid-air conflicts and collisions.

Therefore, the problem of safe UAV integration into the airspace is the selected topic for this research, as it has been one of the major topics in UAV research for the last decade, especially in the development of Conflict Detection and Resolution (CD&R) systems. This particular system describes any strategies and devices for vehicles to mitigate potential mid-air conflicts and collisions, from detection until resolution. For a UAV, this system needs to consider a wide range of obstacles it might encounter, starting from a static unmoving object to other vehicles with completely different characteristics. Moreover, there can be interactions between a fast fixed wing UAV and a hovering quad-rotor, or between two UAVs with different levels of CD&R system awareness, or between a UAV and a much larger manned aircraft. Hence, only when their CD&R systems, both strategies and devices, are fully defined and regulated to handle such diverse scenarios, can UAVs be fully integrated into the airspace.

## 1.2. PROBLEM DEFINITION

Any integration problem can be traced back to the level of readiness of the involved parties for such integration, which in this case are the manned-flight (and their systems) in the current airspace and the (future) UAVs. Safe integration can be achieved if both domains are compatible with each other. This is not yet the case, since they have been advancing separately in their research and practice of mitigating conflicts and maintaining safety: one has gathered experiences in real flight situations with a long history of both incidents and accidents, while the other has most commonly tested inside laboratories with isolated encounter scenarios. This creates a chicken and egg situation: UAV CD&R systems are not matured yet since they cannot fly along with the manned-flight in an integrated airspace situation, while at the same time, authorities do not allow UAVs to join the air traffic in the airspace since the CD&R system is not considered mature enough. These underlying problem are elaborated in four challenges, resulting in the formulation of four research questions, in the following subsections.

### 1.2.1. CURRENT AIRSPACE INCOMPATIBILITY

The airspace is currently dominated by manned-flights, starting from the vehicles, navigation systems, traffic managements, until the regulations. Considering this, to smoothen the process, it seems logical to put most of the effort for integration to UAVs as the newcomer. The process, therefore, should consist of UAVs adapting to what manned-flight has done in managing the airspace, especially in ensuring safety using CD&R systems. Necessary adjustments to the current system may be warranted, but disturbances should be kept as small as possible.

Manned-flight CD&R systems are managed in a fail-safe configuration, stacked in a multi-layered structure, commonly known as the Layers of Safety, as it can be observed in Figure 1.3 [7]. This structure was not formed instantly; rather, it was built and iterated throughout history, where most of its components exist as the result of evaluations of accidents [8]. Each layer is regulated and therefore mandatory for every commercial flight, with only a few exceptions.

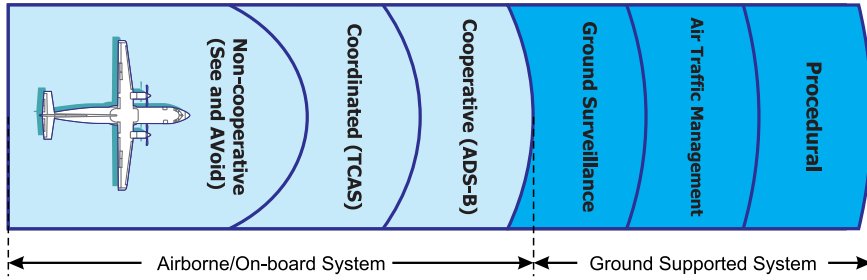


Figure 1.3: Manned flight Conflict Detection and Resolution Architecture (Layers of Safety)

Adapting this CD&R structure for UAVs, however, cannot be straightforward, since it neglects several key characteristics of UAV flights. For instance, the first three layers require centralized surveillance systems such as a primary RADAR, which has difficulty in detecting small objects built from non-metal materials such as most UAVs. The on-board sensors for the surveillance system, which are used primarily and extensively in unmanned vehicles, are not accommodated enough, and are only represented by the innermost ‘See and Avoid’ layer. These problems lead to a need to design a new CD&R structure for UAVs that is compatible with the current used in manned-flight. The challenge can be formulated as follows:

### Research Question 1

What structure can be defined to manage the Conflict Detection and Resolution system for UAVs operating in an integrated airspace?

### 1.2.2. CD&R SYSTEM DIVERSITY

Unlike the manned-flight CD&R system, UAV collision avoidance systems are not regulated, which results in every different UAV having its own unique method for avoidance, motivated by the type, the mission, and the developer discretion. This diversity adds even more complexity to the heterogeneous integrated airspace. This situation actually stimulates the rapid development of various methods of obstacle detection and conflict resolution, but at the same time creates confusion for authorities to decide which method should be the standard in an integrated airspace scheme. UAV research in obstacle detection mainly focuses on on-board sensors, either passive ones such as cameras [9], microphones [10] and acoustic-vector microphones [11], or active ones, such as, laser range-finders [12] and RADAR [13]. On the other hand, research in conflict resolution ranges from deterministic methods such as Global and Local path planning [14, 15], Behavior Tree algorithms [16], Evolutionary algorithms [17], to reactive methods such as the Potential Field method [18–20], Optical Flow method [21], and Velocity Obstacle method [22–26].

While a multi-layered CD&R structure, such as presented in Figure 1.3, might be realized by exploiting the diversity in approaches, each layer cannot be filled directly due

to the lack of categorization standard. It is difficult to identify the role of each available approach in an exhaustive multi-layered structure which should also be compatible with the already established manned-flight. Furthermore, there is also an issue of many terminology mismatches, for example, the term ‘Conflict Detection and Resolution system’ is not a common term in UAV domain, which prefers the term ‘Collision Avoidance System’.

Therefore, a comprehensive categorization on the diverse CD&R approaches is required as the first step in designing their structure for UAV operations. This categorization also can be used to identify redundancy of the approaches, as well as areas that might be lacking representative approach, in the literature. A taxonomy of CD&R approaches that is suitable for UAV operations in an integrated airspace can be produced from the categorization, as it is formulated in the second research question:

#### Research Question 2

How can the diverse UAV CD&R approaches be classified into a comprehensive taxonomy that is compatible with the current airspace?

### 1.2.3. UAV CD&R SYSTEM SAFETY

For a full UAV integration to happen, the doubts of its operational safety for both authorities and the public needs to be removed, which means that the overall operation can maintain a certain Target Level of Safety (TLS) [7]. One parameter of this TLS is the frequency of Mid-Air Collision (MAC), which, if strictly taken, needs to be less than one occurrence out of ten million hours, or  $10^{-7}$  per hour. The number is taken from the manned-flight domain, commonly derived either analytically using a gas model for the air traffic [27–29], or synthetically using the vast data of mid-air conflicts that is available for manned-flight [8]. The former method commonly assesses the air traffic safety where the speed and heading of each vehicle is constant, while the latter is used for a more dynamic airspace, which includes the performance of CD&R systems.

Assessing the TLS fulfillment of a CD&R protocol in UAV operations, however, is more difficult since similarly vast mid-air conflict data to those of manned-flight does not exist. To fill the lack of data, an extensive series of simulation of a comprehensive airspace model can be conducted. However, obtaining safety parameters via simulations is hardly advisable, since, in a realistic airspace situation, collisions are actually so rare that it will take a considerably large amount of time and computational power to obtain meaningful results. Therefore, a new way to assess the safety of the integrated airspace under the effect of a CD&R protocol is necessary, formulated as the third research question:

#### Research Question 3

How can the safety parameters of the integrated airspace, under influence of a heterogeneous CD&R approaches, can be determined?

#### 1.2.4. UAV AUTONOMOUS CD&R SYSTEM INADEQUACY

While many CD&R approaches for UAVs have been proposed and demonstrated, they are not practical yet for current airspace operations, especially in a BVLOS flight. Being developed exclusively by each developer, these approaches rarely see the vehicles as part of global air traffic, in which they have to deal with airspace problems such as heterogeneity, enforced rules, and unpredictable dynamics of the airspace. Heterogeneity in an integrated airspace is inevitable and as a consequence, some level of rules will most likely be required, restricting the maneuvers a UAV can take. At the same time, the resolution maneuver needs to take into account the adverse dynamics that can result from the different ways other UAVs react to a conflict.

Therefore, an extension of the available (or even a completely new) CD&R approach is required to include the integrated airspace characteristics. Since the heterogeneous airspace is most likely to be managed with a structure such as shown in Figure 1.3, more than one new approach maybe warranted. Lastly, to support BVLOS flights, the CD&R systems in focus are those that perform autonomously. This challenge is formulated in last research question:

##### Research Question 4

How can an autonomous CD&R system for UAVs be defined to handle potential conflicts, seeing the vehicle as part of the integrated traffic in the airspace?

### 1.3. RESEARCH OBJECTIVE

Based on the research questions, the main objective of this research is formulated as follows:

**To define and evaluate systems for detecting and resolving possible mid-air conflicts of Unmanned Aerial Vehicles, specifically to support safe beyond visual line-of-sight operations in an integrated airspace.**

This main objective is achieved by answering the interconnected research questions defined in the previous section. The structure to manage UAV CD&R systems in the first question requires the taxonomy definition that is compatible with the current airspace from the second question. Safety analysis of the heterogeneous airspace is conducted to answer the third research question, as well as to test the CD&R structure resulted from the first question. Finally, novel approaches for UAV CD&R are developed in order to match the requirements of the structure proposed in the result of the first question.

The research questions are answered throughout the dissertation within the scope that is presented in section 1.4, using the methodology that is explained, along with the dissertation outline, in section 1.5.

## 1.4. RESEARCH SCOPE AND LIMITATIONS

The objectives are achieved under several assumptions, in order to focus on the objective and reduce the complexity of the research. The following paragraphs formulate those assumptions using the scope and limitations of the main keywords in this research.

**Unmanned Aerial Vehicle:** The term 'Unmanned Aerial Vehicles', abbreviated as UAV, refers to the definition set by the Federal Aviation Administration (FAA) of the United States in [4], which is written as: *Unmanned aircraft means an aircraft operated without the possibility of direct human intervention from within or on the aircraft.* The word aircraft is interpreted further as a device that is capable of sustainable flight, which differentiates the UAV from projectiles (e.g. ballistic missiles) or buoyancy flying vehicle (e.g. weather balloons). While UAV history is explained in Section 1.1 starting from the flight of the first Aerial Target and Flying Bomb, those two devices are actually excluded in the latter discussion in this dissertation that focuses more on reusable vehicles.

The choice of word in this dissertation is 'UAV' instead of the Unmanned Aerial System (UAS), or Unmanned Aircraft (UA) that is used in most regulations, since it is the most popular keyword to refer such vehicle, and it emphasize more the airborne vehicle separately from the support systems, e.g., ground stations and airports. Finally, this research limits the discussion to UAVs that are designed for civil purposes. The UAV prospective that is presented in the work of DeGarmo et.al. [3], shown in Figure 1.2, fits in most of the discussion.

**Airspace System:** The word 'Airspace' refers to the portion of the atmosphere above the territory of a country, and hence controlled by that particular country. 'Airspace System', on the other hand, includes the navigation facilities and infrastructures, such as air traffic, satellites and airports. All the discussion focuses mostly in the civil airspace system, excluding the military parts. The civil airspace is managed in a way specified in the Federal Aviation Regulation (FAR), especially in part 71 [30], of the Federal Aviation Administration (FAA). Most countries have adopted this management method, with several slight difference that are neglected throughout this research.

For the purpose of demonstration, the traffic complexity in the airspace is mostly exaggerated from the current condition, which is in line with the view of the Next Generation Air Transportation System (NextGen) [31] and the Single European Sky initiative [32], which aim for an increase of air traffic volume, doubled by the year 2020. The concept of unmanaged airspace, also known as User Preferred Routing, or Free Flight, is especially used to describe the traffic, for both manned and unmanned flight, throughout this dissertation.

**Encounter, Conflict, and Collision:** These three terms are used in this dissertation to describe the situation of a vehicle in relation to other vehicles in the proximity, in the order of severity. 'Encounter' refers to a situation where the distance between two moving vehicles decreases through time. 'Conflict' describes an encounter where the vehicles are predicted to come close together until a specific threshold is violated. The threshold can be a separation distance, e.g. 50 meter from the center of a vehicle, or the effective dimension of a vehicle, such as the wing span. Such threshold is also dubbed as

**Protected Zone** in several part in this dissertation. Lastly, 'collision' is the moment when a vehicle violates the effective dimension of another vehicle, such that a body contact has occurred.

**Beyond the Visual Line of Sight:** Abbreviated as BVLOS, this term is used to describe a UAV flight of which the pilot has no visual references of the vehicle. The UAV in this case operates in a distance where it is not possible for the operator on-ground to observe the vehicle and its proximity to assist any collision avoidance directly, or with any other method to extend the visual observation. On the other end is the Visual Line of Sight (VLOS) flight, where a direct unaided visual contact can be maintained. The VLOS flights are commonly limited within 500 meter horizontally and 120 meter vertically from the operator. A middle ground between the two is the Extended Visual Line of Sight (EVLOS) in which UAV operates further than the limit of VLOS, but the visual observation can be achieved through other method or procedures such as a separate observer.

Consequently, the BVLOS flight requires some level of automation, as oppose to the VLOS flight, where the UAV is more of a Remotely Piloted Aircraft (RPA). Every recreational UAV is currently intended for VLOS flight, while most of the prospective UAVs in Figure 1.2 are intended for BVLOS flight. Most of the discussions in this dissertation are using the BVLOS assumption, where the conflict detection and resolution is achieved autonomously.

**Safe Integration:** The term 'integration' in this dissertation is used to describe the process of merging the potential civil UAV traffic, mostly BVLOS flights, into the current traffic in the civil airspace system, creating a new integrated airspace system. Therefore, the result of the integration is a heterogeneous intermixing of civil manned and unmanned flight in the same airspace with possibly shared infrastructures.

The work of Dalamagkidis et. al. [7] classified the possible issues in this integration into five part, i.e., safety, security, air traffic, regulation, and socio-economy. In this dissertation, discussion is mostly on the safety issues, especially in the mitigation of mid-air conflicts and collisions. The discussion includes the CD&R system to achieve a safe integration, as well as the required air traffic management and regulations.

**Conflict Detection and Resolution System:** Conflict Detection and Resolution (CD&R) system refers to the on-board and off-board systems that mitigate any mid-air conflict or collision. While this is a general term for any vehicle and traffic type, this dissertation uses it specifically for aircraft and air traffic. The system includes both software, (procedures, algorithms, and rules), and hardware (sensors, computers, actuators, and human operators). The discussion in this dissertation, however, will mostly focus on software. The definition of CD&R system, also commonly known as the collision avoidance system, focuses more on those that are autonomous, in order to support UAV BVLOS operations in an integrated airspace.

**Regulations:** In the beginning of this research in 2011, no airspace regulations allowed a civil UAV to fly, except in a permitted secluded space within the visual line-of-

sight of the operator. While the regulations itself are not the focus, the non-integrated flight situation is taken as the background of this research. At the end of the research, however, several new regulations have been produced, especially in the United States and Europe, which allow some exceptions for BVLOS operations in the airspace [4–6]. These new regulations are excluded in most of the discussions in this dissertation.

## 1.5. METHODOLOGY AND DISSERTATION OUTLINE

This section presents the methodology used to solve the research questions, along with the corresponding chapter in this dissertation where each of the questions is elaborated. The first two research questions are answered by the first chapter after the introduction, the third is solved by the following Chapter 3, while the fourth is dealt with by the remaining chapters. An overview of the relations between chapters and research questions can be observed in the schematic representation of the dissertation outline in Figure 1.4.

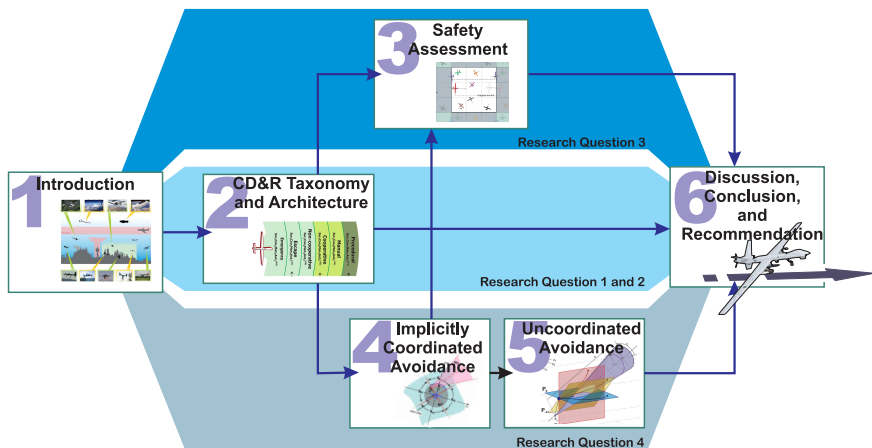


Figure 1.4: Structure of the chapters in the dissertation and their correlation with the research questions

**Chapter 2**, after this introduction, lays out a novel UAV CD&R taxonomy upon which all discussions in other chapters are based. This taxonomy consist of several 'generic approaches' that are suitable for operations in an integrated airspace, differentiated by their types of surveillance, coordination, maneuver, and autonomy. The generic approaches are then attributed to each method in the literature to determine whether the method is complementary or interchangeable with others. The resulting taxonomy also shows areas that are not sufficiently covered yet in literature, which will be the subject of Chapter 4 and Chapter 5. An example of a CD&R structure, or architecture, is then proposed by stacking the generic approaches as layers of safety, which ensures safe operation of UAVs in an integrated civil airspace.

**Chapter 3** evaluates the safety of UAV operations by running series of Monte Carlo simulations, in setups that mimic the situation of an integrated airspace. The effect of different CD&R protocols is included as well, by modeling the system independently in

each vehicle using the algorithm of the Velocity Obstacle method (VO-method). Heterogeneity in the simulations is induced by randomization of the speeds and headings across vehicles, as well as randomization of each CD&R parameter. To reduce the number of simulations required, a high density airspace setup is used, where each simulation is conducted with a minimum four vehicles per kilometer-square. This setup creates as many conflict as possible in the airspace, allowing the safety parameter to rapidly converge. The results are then scaled up for a realistic density to evaluate how well a CD&R protocol performs to fulfill the Target Level of Safety (TLS).

**Chapter 4** proposes a novel algorithm for UAV CD&R system called the Selective Velocity Obstacle (SVO) method, which reactively generates conflict resolutions based on the instantaneous encounter geometry. The SVO method, an extension from the original VO-method, accommodates the use of the right-of-way rules, which result in an implicitly coordinated resolution. While being reactive, the SVO in each UAV is able to handle obstacles with different speed and agility in two-dimensional space, as it is later demonstrated via a series of Monte Carlo simulations. This chapter, hence, presents SVO as a novel method that tackles a part of the CD&R taxonomy from Chapter 2, i.e. an autonomous, implicitly coordinated, tactical maneuver for BVLOS operation in an integrated airspace. As shown in Figure 1.4, this chapter influences other chapters in this dissertation: The proposed SVO method is used to model one of the CD&R protocols tested in Chapter 3, while the VO-method setup for UAVs in the chapter is used as the basis for another novel method in Chapter 5.

**Chapter 5** proposes another modification of the VO-method, referred to as the Three-dimensional VO-method (3DVO). This new CD&R method is designed to conduct an escape maneuver aggressively by exploiting the three-dimensional space. The method also drops the coordinated assumption in the SVO of Chapter 4, and add an extra algorithm to take into account the adverse maneuvers of the counterparts. Heterogeneity of the airspace is modeled the same way as in the previous chapter with an additional dimension. This chapter, therefore, presents 3DVO as a novel method that handles a part of the CD&R taxonomy from Chapter 2, i.e. an autonomous, uncoordinated, escape maneuver for BVLOS operation in an integrated airspace. The method is demonstrated using simulations of several three-dimensional conflicts, including a super-conflict where eight UAVs, initialized at the virtual corners of a cube, are heading to a single collision point. Validation of the method is also derived using Monte Carlo simulations, which show the method is advantageous compared to other methods in literature.

**Chapter 6** summarizes all the chapters into an overview of the overall results, inter-chapter discussions, and conclusions. The chapter also provides some recommendations for further research, especially towards integration of UAVs into the airspace system.

With the exception of the first and the last, all chapters in this dissertation are based on publications in journals that were written independently and, therefore, can be read separately. Each chapter is preceded by an introductory paragraph that explains how the chapter is related to the overall research. A list of publications of the research in this dissertation, either in posters, conference papers, or journal articles, can be found after the Appendices that follow the last Chapter.



# 2

## TAXONOMY AND ARCHITECTURE OF CD&R APPROACHES

*This paper is going to  
make you famous...*

Prof. Jacco M. Hoekstra

*The first step to achieve the goal of this dissertation is to define a novel UAV CD&R taxonomy upon which all discussions in other chapters are based. The development of such taxonomy is elaborated in three parts. In the first part (Section 2.2), an inventory of CD&R approaches, based on the types of surveillance, coordination, maneuver, and autonomy, is presented to see how large and diverse CD&R technology are in literature. The following part in Section 2.3 presents the taxonomy of UAV CD&R, consisting generic approaches, which are derived through a process of method combination and selective elimination. The availability of these generic approaches in the literature is also tabulated. In the third part (Section 2.4), an example of a multi-layered architecture for UAV CD&R is presented, along with a general implementation of the architecture. The chapter ends with conclusions and suggestions for future work.*

---

|                     |   |
|---------------------|---|
| <b>Paper Title</b>  | Taxonomy of Conflict Detection and Resolution Approaches in an Integrated Airspace for Unmanned Aerial Vehicles in Civil Airspace |
| <b>Authors</b>      | Yazdi I. Jenie, Erik-Jan van Kampen, Joost Ellerbroek, and Jacco M. Hoekstra  |
| <b>Published in</b> | IEEE Transactions of Intelligent Transportation System, 2016  |

*This paper proposes a taxonomy of Conflict Detection and Resolution (CD&R) approaches for Unmanned Aerial Vehicles (UAV) operation in an integrated airspace. Possible approaches for UAVs are surveyed and broken down based on their types of surveillance, coordination, maneuver, and autonomy. The factors are combined back selectively, with regard to their feasibility for operation in an integrated airspace, into several 'generic approaches' that form the CD&R taxonomy. These generic approaches are then attributed to a number of available methods in the literature to determine their position in the overall CD&R scheme. The attribution shows that many proposed methods are actually unsuitable for operation in an integrated airspace. Furthermore, some part of the taxonomy does not have an adequate representative in the literature, suggesting the need to concentrate UAV CD&R research more in those particular parts. Finally, a multi-layered CD&R architecture is built from the taxonomy, implementing the concept of defense-in-depth to ensure UAVs safe operation in an integrated civil airspace.*

## 2.1. INTRODUCTION

PROSPECTIVE civil applications of Unmanned Aerial Vehicles (UAVs) have motivated many to commercially fly them in the civil airspace [3]. One of the biggest concerns for these flights is ensuring their safety in the integrated airspace, which includes avoiding conflicts and collisions amongst themselves, as well as with the existing manned air traffic. A vast variation of approaches [8–10, 12, 14–18, 20, 21, 33–79], in both hardware and software concepts, have been proposed to handle that particular problem. These approaches are defined as Conflict Detection and Resolution (CD&R) systems.

Although many of these CD&R studies show promising results, the huge variety of approaches available adversely raises confusion on the integrated airspace management. Considering the rapidly increasing number of developers and users, a large variety of CD&R approaches is inevitable and therefore it is difficult for an authority to enforce a single standardized approach. Furthermore, the worthiness of each of the approaches to support an operation in an integrated airspace is still questionable since UAV CD&R systems are rarely demonstrated handling heterogeneous environments, where vehicles have different preferences in resolving conflicts and interacting with each other. This is one of the reasons why civil-UAVs are yet to be allowed to fly beyond the operator visual line-of-sight (BVLOS)<sup>1</sup>. [80, 81]

Perhaps what is lacking here is a versatile general architecture that defines the implementation of the variation of UAV CD&R in an integrated airspace. For comparison, manned-flight has managed to establish a standardized multi-layered CD&R architecture, commonly presented as 'layers of safety' [7] as shown in Figure 2.1. This architecture implements a defense-in-depth concept, that is, rather than having a single complex CD&R system to handle all types of conflicts, it incorporates several simpler subsystems where each of them are assigned to handle one particular type of conflict. Hence, the safety is managed from the procedural layer that eliminates unnecessary encounters simply by scheduling, up to avoiding any close-encounter obstacles in the 'See and Avoid' layer using the pilot's discretion.

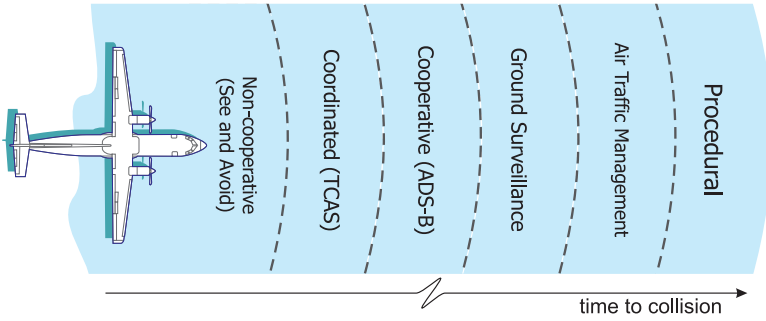


Figure 2.1: Multi-layered architecture of Manned-flight CD&R (Layers of Safety)

Taking example from the manned-flight, UAVs can also incorporate a multi-layered architecture that combines several approaches in a complementary manner. Adopting such architecture would also enable UAVs to act and respond as manned aircraft do, a key requirement in safely integrating into a non-segregated airspace[81]. The multi-layered architecture can also be viewed as a fail-safe system that will not directly leave a UAV vulnerable whenever a failure occurs. It is possible to realize this architecture by exploiting the large creativity of CD&R approaches available in the literature. A categorization of these approaches is therefore needed to identify redundancy in the available methods, as well as to identify areas that are not covered yet.

This paper, therefore, proposes a taxonomy of CD&R approaches aiming to define their positions in the overall safety management of UAV operations in an integrated airspace. The available approaches in the literature are broken down to create a taxonomy based on the type of (1) surveillance, (2) coordination, (3) maneuver, and (4) autonomy. The factors are then combined back, selectively with regard to their feasibility for operation in an integrated airspace, into several *generic approaches*. These can be attributed to each available CD&R approach in the literature to determine whether it is complementary or interchangeable with another. An example of an exhaustive multi-layered architecture based on the taxonomy is also proposed, along with the general implementation for UAV operation in an integrated airspace.

This paper is an extension of the work originally reported in [82] by the same authors. The current paper contributes to this study by providing an improved categorization of the existing UAV CD&R methods in a comprehensive taxonomy with bigger literature to identify important future avenues of research in UAV CD&R systems.

The research in this paper is presented as follows. After the introduction, Section II will present an inventory of CD&R approaches, based on the four factors explained before. Section III presents the taxonomy of UAV CD&R, consisting generic approaches which are derived through a process of method combination and selective elimination. The availability of these generic approaches in the literature is also tabulated. In Section IV, an example of a multi-layered architecture for UAV CD&R is presented, along with a general implementation of the architecture. Section V concludes the paper and provides suggestions for future work.

## 2.2. INVENTORY OF APPROACHES FOR UAV CD&R SYSTEM

The three factors that distinguish the layers of safety in the manned-flight CD&R are the type of surveillance, coordination, and maneuver, as shown in Figure 2.2. These three are the factors that directly affect the airspace management: surveillance and coordination require cooperation from other vehicles as well as the local authorities, while the length of maneuvers can affect the traffic globally. Hence, each of the manned-flight safety layers can be viewed as a generic approach that combines those three factors. For example, the Traffic Warning and Collision Avoidance System (TCAS) can be seen as a combination of *distributed dependent surveillance*, *explicit coordination*, and *escape maneuver*. Other types of CD&R categorizations can also be found in literature, such as in [83]. However, they focus more on the internal algorithms.

The UAV CD&R approaches in literature can also be broken down and viewed as combinations of those three factors. An additional factor of ‘autonomy’ is added in the taxonomy, differentiating whether an (human) operator is involved or not in the approach execution.

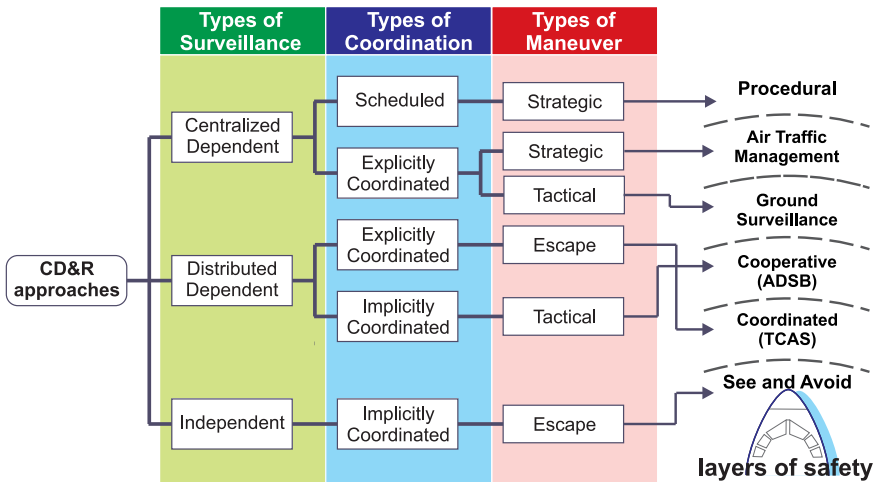


Figure 2.2: Taxonomy of CD&R approaches in manned flight

### 2.2.1. TYPES OF AIRSPACE SURVEILLANCE

Airspace surveillance is the detection step in the CD&R process. Here, three types of surveillance can be distinguished, as they are presented in Figure 2.3.

- **Sur<sub>1</sub>** : Centralized-dependent surveillance,
- **Sur<sub>2</sub>** : Distributed-dependent surveillance, and
- **Sur<sub>3</sub>** : Independent surveillance.

A centralized-dependent-surveillance system obtains data from a common station, or a station-network, and can be available even before the flight is conducted, e.g., a map of static obstacles. In manned-flight, this part is included in the first three safety layers. An aircraft can retrieve data about the traffic, terrain, and weather in the area

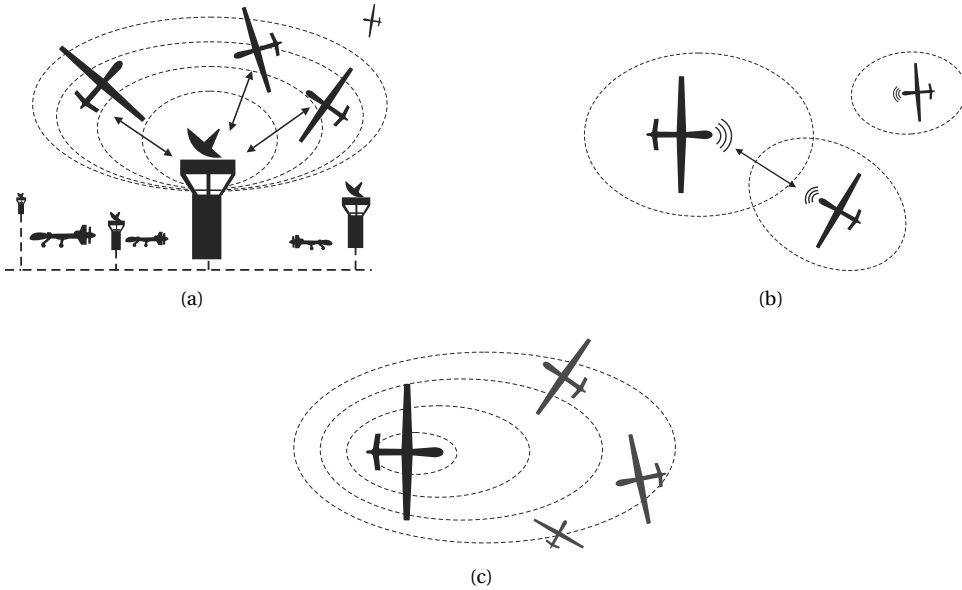


Figure 2.3: Airspace Surveillance for UAVs: (a) Centralized-dependent, (b) Distributed-dependent, and (c) Independent

from ground centers such as the Air Traffic Control (ATC) or the Aviation Weather Center (AWC). UAV operators might also employ this data to plan each flight and reduce any unnecessary conflicts. An example of this practice is demonstrated in [17] and [84]. In contrast to manned-flight, centralized-surveillance for UAVs might only be suitable before flight, since most UAVs, being small and manufactured with non-metal materials, are difficult to detect using conventional (primary) RADAR on ground.

A distributed-dependent-surveillance system obtains data from the traffic itself. This surveillance method, therefore, requires every vehicle to cooperatively broadcast their flight data. In manned-flight, this practice is conducted by using the Automatic Dependent Surveillance Broadcast (ADS-B) [85] system, using the Secondary Surveillance RADAR (SSR), or using the TCAS. Applications for UAVs, which is also known as collaborative sensing, such as presented in [58] and [54]. CD&R approaches that does not mention a particular surveillance method are considered to be using a distributed dependent surveillance system.

The third method of surveillance obtains airspace data independently using an on-board sensor system. In manned-flight, this type of surveillance is only present through (human) visual confirmation, used in the last layer of safety, the 'see and avoid' procedure [86]. While this type is the primordial system for avoidance in manned-flight, in the UAV domain it dominates most of the research. On-board sensors are the most popular way to provide surveillance, or sensing, in UAV studies, which includes cameras (visual light and infra-red) [9], acoustic sensors [10], acoustic-vector sensors [11], and even miniaturized versions of active-sensors like the laser-range-finder [12] or RADAR [13].

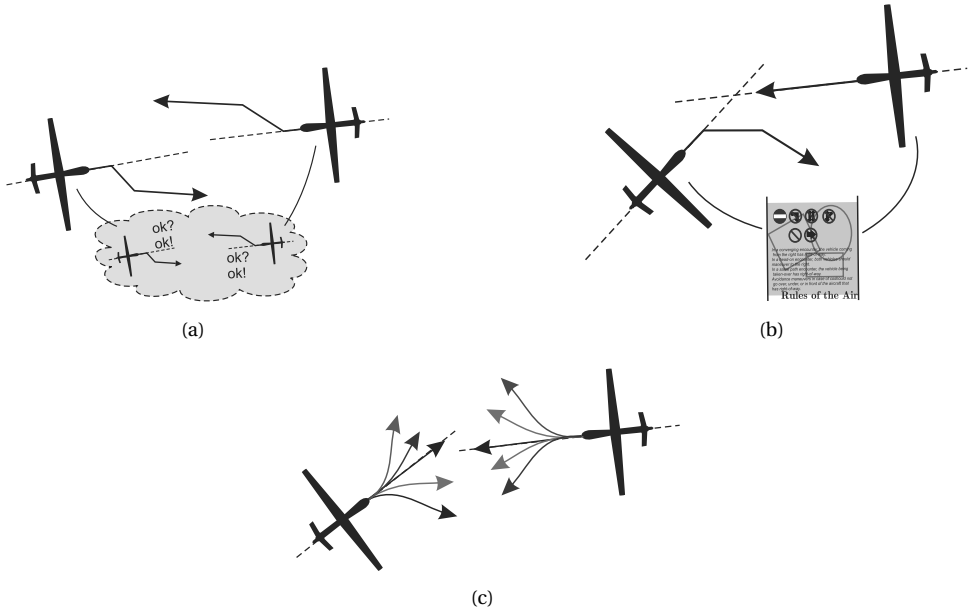


Figure 2.4: Types of Coordination: (a) Explicitly Coordinated, (b) Implicitly Coordinated, and (c) Uncoordinated

### 2.2.2. TYPES OF COORDINATION

In order to simplify the resolution, many studies assume some level of coordination between vehicles. This research differentiates the levels into three types of coordination, as listed below, and as depicted in Figure 2.4. The scheduled coordination, in the Procedural layer shown in the Figure 2.2, is omitted from the list since it can be viewed as an implicit (rule-based) coordination.

- **Coo<sub>1</sub>** : Explicitly coordinated avoidance,
- **Coo<sub>2</sub>** : Implicitly coordinated avoidance, and
- **Coo<sub>3</sub>** : Uncoordinated avoidance.

Avoidance is said to be explicitly coordinated if an explicit communication exists among the involved vehicles. Hence, a specific resolution, often using a common algorithm, can be produced, such as TCAS that gives a pair of aircraft a confirmed advisory to avoid conflict. In the UAV domain, the ACAS Xu[8], a part of the next generation of TCAS, shows an example of this coordination. This paper also includes methods that only avoid static obstacles, as an explicitly-coordinated avoidance.

An avoidance is implicitly coordinated if each involved vehicle maneuvers according to a common set of rules or strategies. This ensures a level of coordination without a direct communication for resolution. Being partially limited by the rules, the vehicles can simplify the resolution by limiting the maneuver choice, or by setting up priorities based on vehicle types. An example of this type of coordination in manned-flight is the use of right-of-way rules in the 'see and avoid' procedure[86]. The 'Free-flight' concept introduced in [36, 39, 53, 87], also employs an implicitly coordinated method for avoid-

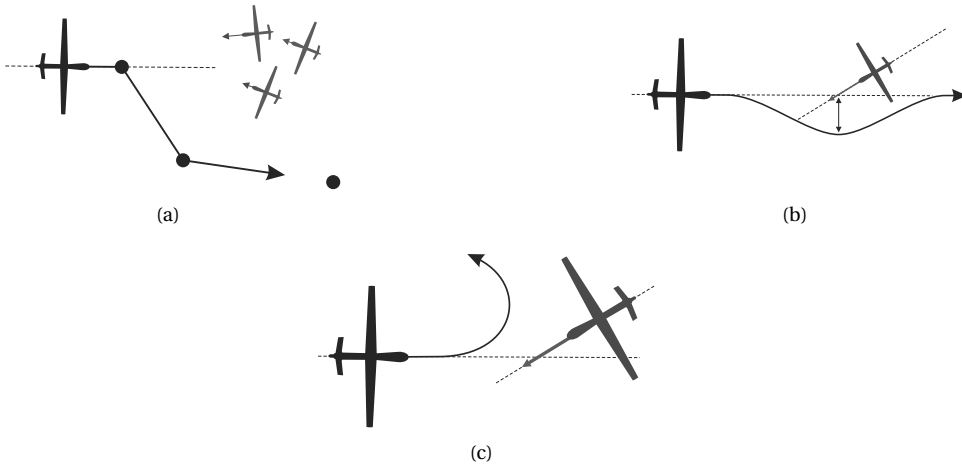


Figure 2.5: Types of Maneuver: (a) Strategic maneuver, (b) Tactical maneuver, and (c) Escape maneuver

ance. The work in [47] and [75] presents an example of this type of coordination for UAV applications. This paper also includes methods that only avoid obstacle with known and constant trajectory, as an implicitly-coordinated avoidance.

When the avoidance is uncoordinated, each involved vehicle has its own preference for resolution based on the conflict situation, and therefore can create a complex situation. The ownership in this case can assume that the obstacle is rogue and may conduct unexpected maneuvers. This makes the resolution calculation more difficult since it has to take into account every possible movement and collision risks induced by an obstacle. In manned flight, this avoidance is not implemented unless it is an emergency, which highly depend on the pilot judgment. In UAVs, some examples exist for an agile UAV, such as presented in [45]. Some work, such as in [33], applies this type by using a predefined set of actions for an aggressive sure-escape, avoiding the entire portion of the risk at once.

### 2.2.3. TYPES OF AVOIDANCE MANEUVER

As airborne vehicles, UAVs are able to perform many kinds of maneuvers in the 3-Dimensional space. This research differentiates between three types of maneuvers, as presented in Figure 2.5.

- **Man<sub>1</sub>** : Strategic maneuver,
- **Man<sub>2</sub>** : Tactical maneuver, and
- **Man<sub>3</sub>** : Escape maneuver.

A strategic maneuver is a long-range action that changes the initial flight-path significantly, in the attempt to avoid unnecessary encounters. The maneuver commonly generates several new waypoints, which can be both in vertical and horizontal direction. The flight-planning in both manned and unmanned flight[17, 50], is included in this type of maneuver.

A tactical maneuver is a mid-range action that changes a small part of the flight path while aiming to keep the deviation as small as possible. This type of maneuver focuses on ensuring a certain separation threshold during an encounter with other vehicles. An example of this method in manned-flight is the airborne separation system presented in [64]. Most of the advanced methods for UAVs are using this maneuver to limit the path deviation as small as possible by using, for instance, geometric guidance[66] or optimization of a cost function[67]. Several papers mention this type of maneuver as a deconflict maneuver[75, 88].

The last approach is to escape any potential collision all together with a maneuver that solely brings the vehicle to safety. This escape maneuver should be aggressive and conducted immediately, commonly using an open-loop command, driven by the maximum performance limit of the vehicle. In manned-flight, this type of maneuver is applied in the 'see and avoid' layer, in the way that they ignore any optimization, and focus only on safety. The way the TCAS and the ACAS X[8] works where a maneuver is conducted in a relatively short distance, is also included as an escape maneuver. In UAV domain, several examples use this maneuver type, including the work in [56] and in [21].

#### 2.2.4. TYPES OF AUTONOMY

Based on the type of autonomy, a UAV can conduct avoidance based in two different ways:

- **Aut<sub>1</sub>** : Manually, or
- **Aut<sub>2</sub>** : Autonomously

In this research, these are differentiated more on the involvement of a human operator in the final decision for avoidance, and not on the calculation process. For instance, if a conflict situation is processed on-board, but then the results is send for the ground operator to decide, it is still considered to be manual avoidance. Manual avoidance is preferable by most of the current regulations, which limits UAV operation to within line-of-sight of the operator[80].

Beyond the visual line-of-sight (BVLOS), however, the effectiveness of manual avoidance is greatly reduced, as the situational awareness of the operator becomes low[47]. The final decision for avoidance, hence, should be given to the on-board autonomous system. Currently, even though many studies proposed various autonomous methods, such as in [77], this is not applicable in a commercial manned-flight due to safety reasons. In the UAV domain, on the other hand, research has been focused mostly on the autonomous avoidance ability.

### 2.3. TAXONOMY OF CONFLICT DETECTION AND RESOLUTION APPROACHES FOR UAV

By direct combination from the approach inventory in the previous section, there can be 54 possible generic approaches to form the taxonomy, resulting from 3 types-of-surveillance  $\times$  3 types-of-coordination  $\times$  3 types-of-maneuver  $\times$  2 types-of-autonomy. Several of these combinations, however, might not be suitable for a UAV flight in an integrated airspace, and therefore can be removed from the final structure of the taxonomy. This section presents the taxonomy by first elaborating the characteristics of prospective

UAV flights in the integrated airspace.

**2.3.1. UAV FLIGHT IN THE FUTURE INTEGRATED AIRSPACE**

The taxonomy is built under the assumption that UAVs are already integrated in the airspace system, as depicted in Figure 2.6. Each of these prospective UAVs is listed in Table 2.1, along with the references.

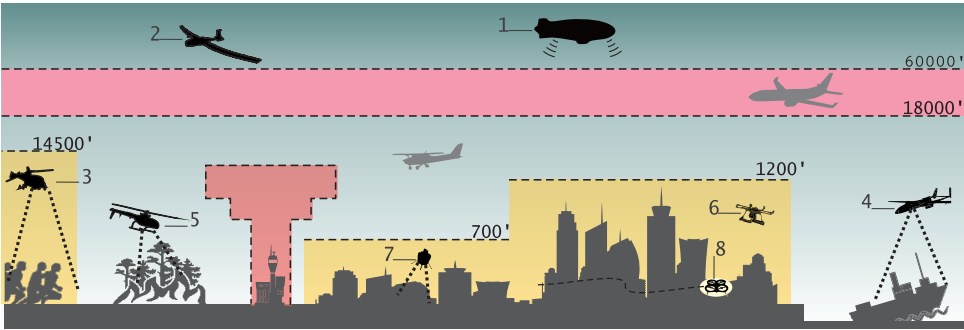


Figure 2.6: Prospective use of UAVs in Civil Airspace, adapted from [3]. The UAV numbers refer to Table 2.1.

Table 2.1: Prospective UAVs operation in the civil airspace[3]

| Mission                               | Operational Weight | Cruising Altitude |
|---------------------------------------|--------------------|-------------------|
| 1. Telecommunication [3, 89, 90]      | ± 20 ton           | 20 km             |
| 2. High-Altitude Imagery [3, 91]      | ± 800 kg           | 18 km             |
| 3. Border Patrol[3, 92]               | < 25 kg            | < 6 km            |
| 4. Maritime Surveillance[3, 93]       | < 20 kg            | < 6 km            |
| 5. Environmental Sensing[3, 94]       | < 25 kg            | < 6 km            |
| 6. Media and Traffic Reporting[3, 95] | < 10 kg            | <1.5 km           |
| 7. Law Enforcement[3, 96]             | < 25 kg            | < 120 m           |
| 8. Delivery Service[97]               | <25 kg             | < 120 m           |

Observing the future integrated airspace prospectives, a few characteristics can be defined, along with the improbability in implementing some combinations of the CD&R methods. The superscripts following each improbable combination are codes used for building the taxonomy in the next subsections.

DETECTABILITY

Observing Table 2.1, most of the prospective UAV examples are small vehicles that are below 25 kilograms, operating at low altitude, and manufactured mostly using non-metal materials. Consequently, they are hard to detect by a centralized surveillance system

such as a conventional primary RADAR. Therefore, any centralized surveillance in the future might only be able to support UAVs before their flight, as a center for traffic, terrain, or weather information. This is the implementation of a strategic maneuver coupled with an implicit-coordination, which happens manually before flight. Hence, the improbable combinations caused by this characteristics are:  $[\mathbf{Sur}_1 + \mathbf{Coo}_1]^{(1a)}$ ,  $[\mathbf{Sur}_1 + \mathbf{Coo}_3]^{(1b)}$ ,  $[\mathbf{Sur}_1 + \mathbf{Man}_2]^{(1c)}$ ,  $[\mathbf{Sur}_1 + \mathbf{Man}_3]^{(1d)}$ , and  $[\mathbf{Sur}_1 + \mathbf{Aut}_2]^{(1e)}$ .

#### COOPERATION

As shown in Figure 2.6, there can exist different types of UAV carrying out various missions in the same part of the airspace. To ensure safety while embracing this heterogeneity, the authorities might require each UAV to cooperatively broadcast its states and/or intents to the surrounding vehicles, hence utilizing a distributed-dependent surveillance. This surveillance, however, is not reliable for a strategical maneuver, since the broadcast range is limited. Furthermore, the update rate of the broadcast system is commonly inadequate for a close distance escape maneuver, e.g., the ADS-B, which only broadcast once per second. Therefore, the improbable combinations caused by this characteristic are:  $[\mathbf{Sur}_2 + \mathbf{Man}_1]^{(2a)}$ , and  $[\mathbf{Sur}_2 + \mathbf{Man}_3]^{(2b)}$ .

#### SENSE AND AVOID

Currently, all examples of UAVs listed in Table 2.1 utilize an on-board sensor system to independently (hence, independent-surveillance) provide the required data in high sampling rate. The data is then used to generate an avoidance maneuver, which completes the process commonly known as Sense and Avoid. This is likely to be preserved in the future integrated airspace as a last resort maneuver to resolve conflicts when other methods fail. Sense and Avoid, however, can only be a tactical or an escape maneuver, due to the relatively short detection range of its surveillance system. This range limitation also warrants an autonomous system to provide a fast response in avoidance. Hence, the improbable combinations caused by this characteristics are:  $[\mathbf{Sur}_3 + \mathbf{Man}_1]^{(3a)}$ , and  $[\mathbf{Sur}_3 + \mathbf{Aut}_1]^{(3b)}$ .

#### COORDINATION

The heterogeneity of the future integrated airspace will also trigger the heterogeneity of CD&R protocols. Therefore, enforcing an explicit-coordination among these UAVs is inherently difficult regardless of the surveillance and maneuver methods. Hence, the authorities might only impose some sort of implicit-coordination such as a right-of-way rules[86]. The possibility of rogue obstacles in the airspace, however, would still require the UAVs to also consider an uncoordinated avoidance scheme. Therefore, the improbable combinations caused by the heterogeneity are:  $[\mathbf{Coo}_1 + \mathbf{Sur}_1]^{(4a)}$ ,  $[\mathbf{Coo}_1 + \mathbf{Sur}_2]^{(4b)}$ ,  $[\mathbf{Coo}_1 + \mathbf{Sur}_3]^{(4c)}$ ,  $[\mathbf{Coo}_1 + \mathbf{Man}_1]^{(4d)}$ ,  $[\mathbf{Coo}_1 + \mathbf{Man}_2]^{(4e)}$ , and  $[\mathbf{Coo}_1 + \mathbf{Man}_3]^{(4f)}$ .

#### AUTONOMY

Perhaps only the Media and Traffic reporting mission, from the list in Table 2.1, has the UAV operating within the line-of-sight of the operator. All other missions are conducted beyond the visual line-of-sight (BVLOS), which reduce the operator ability to manually mitigate conflicts due to the lack of situational awareness[47]. Therefore, autonomous operation is needed for the BVLOS escape maneuver. Hence, this characteristic makes the  $[\mathbf{Aut}_1 + \mathbf{Man}_3]^{(5a)}$  combination improbable.

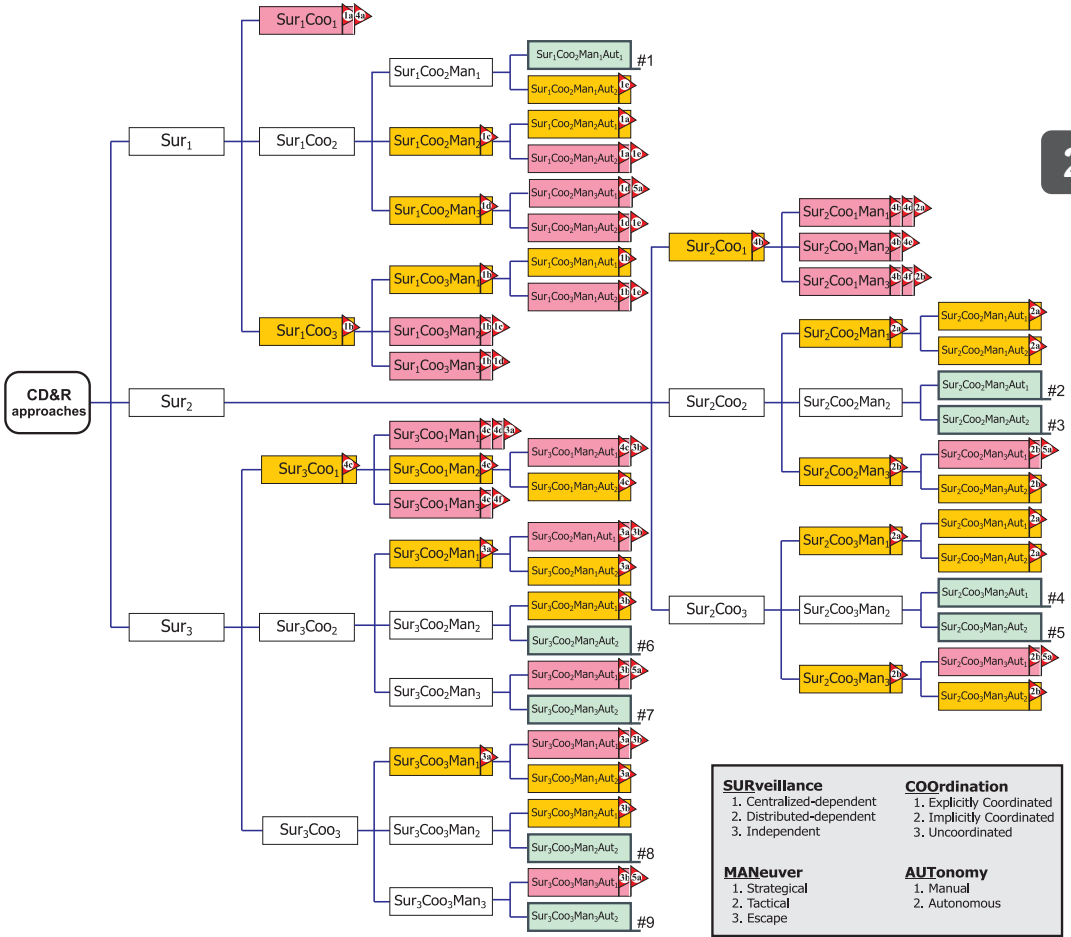


Figure 2.7: Derivation of the CD&R approaches Taxonomy for UAVs flight. The flag's number refer to the improbable combination code (see section III.A). The combinations that do not raise any flag until the end are numbered form #1 to #9.

**2.3.2. COMBINATION PROCESS OF CD&R METHODS**

The combining process is conducted in succession, instead of using direct permutation of the four methods, to remove any infeasible combination early, as shown in Figure 2.7. This paper selects a combination order that starts from the type of surveillance and ends with the type of autonomy, based on the factors' influences to the airspace authorities, air-traffic, and operators.

In every step, each combination is reviewed against the integrated airspace characteristic, as explained and coded in the previous subsection. If a combination is suitable, the process is continued until all four methods are combined as one 'generic approach'. When a combination is improbable, it is marked with an improbability flag. The combination process is still continued for this case, since, while it is difficult, it is not entirely

impossible. Only when a particular combination generates more than one flag, then the process is discontinued, as it is shown in Figure 2.7. Note that some combinations can raise more than one flag at once, e.g., **Sur<sub>1</sub>Coo<sub>1</sub>**.

Ultimately, nine combinations emerge as generic approaches that do not raise any improbability flags throughout the process. These nine are the final approaches of the proposed taxonomy for the UAV CD&R. Although some of them already are popular with a lot of supporting studies, other flagged combinations are rendered as less probable to be applied in the future integrated airspace. This is discussed more in the next subsection.

### 2.3.3. APPROACHES AVAILABILITY

Table 2.2 listed a total of 64 previous studies on a CD&R system, along with each of their method combination attribution. The matches and mismatches of the CD&R approaches in the literature with the proposed taxonomy are also shown, where the rows of the nine generic approaches in the taxonomy are shadowed. This table omits combinations that are both flagged and do not have representative in the literature. It should be noted that the classification of approaches is strictly based on the demonstration shown in each reference, either by simulations or by real experiments.

Evidently, the high number of mismatches indicates that most research on CD&R are not ready to facilitate UAV integration into the airspace. The lack of representative methods on some parts of the taxonomy suggests that the research needs to change its focus to the parts that handle the characteristics of the future integrated airspace.

The first three rows of Table 2.2 consist of the combination of centralized-dependent surveillance (**Sur<sub>1</sub>**) and the explicit coordination (**Coo<sub>1</sub>**). This combination, however, is immediately marked with two improbability flags, considering the detectability and the coordination of UAVs. These improbabilities do not apply in manned-flight, which is predominance in these first three rows.

The **Sur<sub>1</sub>Coo<sub>2</sub>Man<sub>1</sub>Aut<sub>1</sub>** combination, the first generic approach of the taxonomy, is very similar to the Procedural layer of manned-flight (see Figure 2.1). Hence, the CD&R examples include methods for flight traffic management, which is not yet being considered in UAV domains. Local path planning studies, such as in [14] and [15] (**Sur<sub>1</sub>Coo<sub>2</sub>Man<sub>1</sub>Aut<sub>2</sub>**), can actually fill this particular position if they are modified to a global path planning, which is conducted before each flights.

Many examples match the second and the third generic approach in the taxonomy (**Sur<sub>2</sub>Coo<sub>2</sub>Man<sub>2</sub>Aut<sub>1</sub>** and **Sur<sub>2</sub>Coo<sub>2</sub>Man<sub>2</sub>Aut<sub>2</sub>**). These two approaches are popular since most studies are focused on developing the best avoidance method in terms of fuel or time efficiency, which is a trait specifically owned by the tactical maneuver (**Man<sub>2</sub>**). The assumption of distributed-dependent surveillance (**Sur<sub>2</sub>**), furthermore, reduces the possible uncertainties in the surveillance system and allows the studies to focus more on maneuver optimization. An example of this is presented in [75] that uses the Velocity Obstacle method to generate a deconflicting path with a minimum Closest Point of Approach.

In contrast, the fourth and fifth generic approach (**Sur<sub>2</sub>Coo<sub>3</sub>Man<sub>2</sub>Aut<sub>1</sub>** and **Sur<sub>2</sub>Coo<sub>3</sub>Man<sub>2</sub>Aut<sub>2</sub>**) do not have any representative method at all. The only difference from the previous two approaches is that the avoidance here is uncoordinated (**Coo<sub>3</sub>**). One reason

Table 2.2: Existing and/or suitable combinations of methods for UAVs in an integrated airspace. Combinations that are included in the proposed taxonomy are highlighted and numbered (see figure 2.7)

| Combination   | Flags | Examples   | No.       |
|---|-------|--|-----------|
| <b>Sur<sub>1</sub>Coo<sub>1</sub>Man<sub>1</sub>Aut<sub>1</sub></b> | ≥ 2   | Prandini <sup>†</sup> [34], Nikolos <sup>†</sup> [17], Visintini <sup>‡</sup> [49], Borrelli[50], and Vela <sup>‡</sup> [59]   |           |
| <b>Sur<sub>1</sub>Coo<sub>1</sub>Man<sub>2</sub>Aut<sub>1</sub></b> | ≥ 2   | Mao <sup>‡</sup> [53], and Treleven <sup>‡</sup> [57]  |           |
| <b>Sur<sub>1</sub>Coo<sub>1</sub>Man<sub>2</sub>Aut<sub>2</sub></b> | ≥ 2   | Huang <sup>‡</sup> [77]  |           |
| <b>Sur<sub>1</sub>Coo<sub>2</sub>Man<sub>1</sub>Aut<sub>1</sub></b> | 0     | -  | <b>#1</b> |
| <b>Sur<sub>1</sub>Coo<sub>2</sub>Man<sub>1</sub>Aut<sub>2</sub></b> | 1     | Beard[14], and Duan[15]  |           |
| <b>Sur<sub>1</sub>Coo<sub>3</sub>Man<sub>3</sub>Aut<sub>2</sub></b> | ≥ 2   | Teo[45]  |           |
| <b>Sur<sub>2</sub>Coo<sub>1</sub>Man<sub>2</sub>Aut<sub>1</sub></b> | ≥ 2   | Mao <sup>‡</sup> [53], and Velasco <sup>‡</sup> [79]   |           |
| <b>Sur<sub>2</sub>Coo<sub>1</sub>Man<sub>2</sub>Aut<sub>2</sub></b> | ≥ 2   | Richards[42], Sislak <sup>‡</sup> [61], Chipalkatty <sup>‡</sup> [69], and Hurley <sup>†</sup> [73]  |           |
| <b>Sur<sub>2</sub>Coo<sub>2</sub>Man<sub>1</sub>Aut<sub>2</sub></b> | 1     | Beard[14], Duan <sup>†</sup> [15], and Devasia <sup>‡</sup> [62]   |           |
| <b>Sur<sub>2</sub>Coo<sub>2</sub>Man<sub>2</sub>Aut<sub>1</sub></b> | 0     | Hoekstra <sup>†</sup> [39], Hoekstra <sup>‡</sup> [35], Peng <sup>‡</sup> [60], Lupu <sup>‡</sup> [63], Ellerbroek <sup>‡</sup> [64], and Ellerbroek <sup>‡</sup> [74]                                     | <b>#2</b> |
| <b>Sur<sub>2</sub>Coo<sub>2</sub>Man<sub>2</sub>Aut<sub>2</sub></b> | 0     | Bicchi <sup>‡</sup> [36], Tomlin <sup>‡</sup> [37], Mao <sup>‡</sup> [38], Pallottino <sup>‡</sup> [40], Paielli[43], Richards[46], Christodoulou <sup>‡</sup> [51], Park[58], Mujumdar[66], and Jenie[75] | <b>#3</b> |
| <b>Sur<sub>2</sub>Coo<sub>2</sub>Man<sub>3</sub>Aut<sub>1</sub></b> | 2     | LeTallec[47], Zeitlin[54], and Kochenderfer <sup>†</sup> [8]   |           |
| <b>Sur<sub>2</sub>Coo<sub>3</sub>Man<sub>2</sub>Aut<sub>1</sub></b> | 0     | -  | <b>#4</b> |
| <b>Sur<sub>2</sub>Coo<sub>3</sub>Man<sub>2</sub>Aut<sub>2</sub></b> | 0     | -  | <b>#5</b> |
| <b>Sur<sub>2</sub>Coo<sub>3</sub>Man<sub>3</sub>Aut<sub>1</sub></b> | 2     | Winder[33]   |           |
| <b>Sur<sub>3</sub>Coo<sub>1</sub>Man<sub>1</sub>Aut<sub>2</sub></b> | ≥ 3   | Kelly <sup>†</sup> [52], Langelaan <sup>†</sup> [55], Obermeyer <sup>†</sup> [71], and Chowdhary <sup>†</sup> [70]   |           |
| <b>Sur<sub>3</sub>Coo<sub>1</sub>Man<sub>2</sub>Aut<sub>2</sub></b> | 1     | Netter <sup>†</sup> [98], Nikolos <sup>†</sup> [17], Yang <sup>†</sup> [44], McGee <sup>†</sup> [48], Patel <sup>†</sup> [67], Hrabar <sup>†</sup> [12], and Jung <sup>†</sup> [76]                        |           |
| <b>Sur<sub>3</sub>Coo<sub>1</sub>Man<sub>3</sub>Aut<sub>2</sub></b> | ≥ 2   | Beyeler <sup>†</sup> [21], Bouabdallah <sup>†</sup> [56], deCroon <sup>†</sup> [65], deCroon <sup>†</sup> [72], and Muller <sup>†</sup> [10]   |           |
| <b>Sur<sub>3</sub>Coo<sub>2</sub>Man<sub>2</sub>Aut<sub>2</sub></b> | 0     | Kitamura[18], Fasano[9], Prevost[68], Klaus[16], and Schmitt[78]   | <b>#6</b> |
| <b>Sur<sub>3</sub>Coo<sub>2</sub>Man<sub>3</sub>Aut<sub>1</sub></b> | 2     | Lam <sup>†</sup> [19], and Lam <sup>†</sup> [20]   |           |
| <b>Sur<sub>3</sub>Coo<sub>2</sub>Man<sub>3</sub>Aut<sub>2</sub></b> | 0     | -  | <b>#7</b> |
| <b>Sur<sub>3</sub>Coo<sub>3</sub>Man<sub>2</sub>Aut<sub>2</sub></b> | 0     | Rathbun[41]  | <b>#8</b> |
| <b>Sur<sub>3</sub>Coo<sub>3</sub>Man<sub>3</sub>Aut<sub>2</sub></b> | 0     | -  | <b>#9</b> |

<sup>†</sup> Indoor application, against static obstacles.

<sup>‡</sup> Manned-flight applications

for the lack of representative is the contradiction fact: although the UAVs cooperatively broadcasting their states with a distributed-dependent surveillance (**Sur**<sub>2</sub>), the avoidance conducted is rogue without some sort of coordination. Therefore, while suitable for a UAV operation in an integrated airspace, these two particular approaches are actually improbable to be implemented.

The combination of independent surveillance (**Sur**<sub>3</sub>) and autonomous final decision (**Aut**<sub>2</sub>) dominates the UAV avoidance research. However, many of those studies fall into neither of the remaining generic approaches, since they demonstrate avoidance only between homogeneous vehicles or static obstacles, and therefore regarded as applying an explicitly coordinated avoidance (**Coo**<sub>1</sub>). The work in [33], [19], and [20], on the other hand, are considered improbable since they relies on manual operation, which is difficult to be applied in a BVLOS operation.

From the remaining generic approaches in the taxonomy, the sixth combination have the most examples, where the other three almost have none. Here the popularity of a tactical maneuver (**Man**<sub>2</sub>) still applies, but with a more advance algorithm that compensates errors in an independent surveillance system (**Sur**<sub>3</sub>).

Although examples for the seventh and ninth approach in the taxonomy (**Sur**<sub>3</sub>**Coo**<sub>2</sub>**Man**<sub>3</sub>**Aut**<sub>2</sub> and **Sur**<sub>3</sub>**Coo**<sub>3</sub>**Man**<sub>3</sub>**Aut**<sub>2</sub>) are not found in the surveyed literature, many studies actually use the open-loop input concept to autonomously generate an escape maneuver. These studies, however, only involve static obstacles and hence they are included as an explicit coordinated avoidance, resided in the row of **Sur**<sub>3</sub>**Coo**<sub>1</sub>**Man**<sub>3</sub>**Aut**<sub>2</sub>. Another case is the work in [45], with its Emergency Escape Maneuver, that comes close to the seventh and ninth approaches. However, it is only demonstrated under the support of a centralized dependent surveillance **Sur**<sub>1</sub> from the ground.

Most of CD&R studies, apparently avoid the coupling between an independent surveillance and an uncoordinated avoidance (**Coo**<sub>3</sub>) that is featured in the eighth and ninth approach of the taxonomy. The main reason is because the combination would double the amount of uncertainties compared to if those factors are used separately. The example in [41], in this case, stands out from the literature as being the only example of the **Sur**<sub>3</sub>**Coo**<sub>3</sub> combination.

## 2.4. A MULTI-LAYERED ARCHITECTURE

Figure 2.8 presents an example of a multi-layered architecture for a UAV CD&R system when operating in an integrated airspace, along with the comparison with the one of manned-flight. The new architecture is built using six generic approaches taken from the proposed taxonomy. The arrangement and general implementation are discussed in the following subsections.

### 2.4.1. GENERIC APPROACHES ARRANGEMENT

As presented in Figure 2.1, the order of layers in the manned-flight CD&R architecture corresponds to each approach's distance thresholds, which depends on the range of the surveillance and the total length of the maneuver. This particular order is also used in the elaboration of the types of surveillance and maneuver (see Section II), which makes the numbering of generic approaches in the taxonomy are already in order.

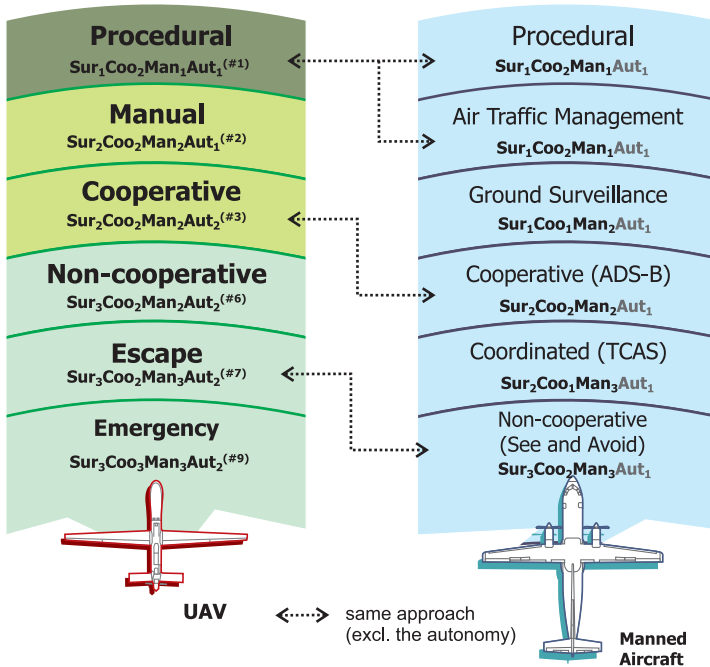


Figure 2.8: Example of a multi-layered CD&R architecture for UAVs, presented as layers of safety comparable with the manned-flight's[7]

By those arrangement, six generic approaches are taken from the taxonomy to build a multi-layered architecture as shown in Figure 2.8. The fourth and fifth approach are left out, due to the improbability reason explained in Section II.C. The eighth approach ( $Sur_3Coo_3Man_2Aut_2$ ) is also removed, since applying its tactical maneuver after the use of escape in the seventh approach would be pointless.

Figure 2.8 compares the proposed UAV CD&R architecture with the one of manned-flight. Each of the proposed layers can be designated with a name that represent its most stand-out characteristics, i.e., (1) the Procedural, (2) the Manual, (3) the Cooperative, (4) the Non-cooperative, (5) the Escape, and (6) the Emergency layer.

### 2.4.2. GENERAL IMPLEMENTATION

The implementation of the multi-layered architecture depends closely on the type of mission. In one particular mission some layers might become less necessary, while in others they might be important. This subsection presents a general implementation in a mission where it is possible to deploy all six layers.

First, before a flight is even conducted, the UAV operator seeks approval for the mission flight-plan and collect traffic data. This activity is represented by the Procedural Layer ( $Sur_1Coo_2Man_1Aut_1$ ). The aim is to avoid unnecessary conflict with other traffic, static obstacles, or bad weather. This is done with a centralized surveillance such as an Air Traffic Control (ATC) station.

In the transition airspace after departure, the UAV relies first on its dependent surveillance system, which can be either the ADS-B, or Flight-Alarm (FLARM)<sup>1</sup>. The system detects other vehicles early enough to send the updated traffic data to the ground, and conducts a tactical maneuver manually, i.e., the Manual layer (**Sur<sub>2</sub>Coo<sub>2</sub>Man<sub>2</sub>Aut<sub>1</sub>**). The implicit coordination in this layer can be a simple rule like, for example, not to bother the existing traffic (first-come-first-served). These first two layers (Procedural and Manual) apply also in the landing phase.

In the en-route phase, which is mostly BVLOS, the UAV can switch to the Cooperative Layer (**Sur<sub>2</sub>Coo<sub>2</sub>Man<sub>2</sub>Aut<sub>2</sub>**). The avoidance in this layer uses a shorter tactical range and is conducted autonomously. Implicit rules, such as an adaptation of the manned-flight Visual Flight Rules (VFR)[86], are applied to simplify the resolution. At this point, all conflicts with normal manned-aircraft are resolved.

The Non-cooperative Layer (**Sur<sub>3</sub>Coo<sub>2</sub>Man<sub>2</sub>Aut<sub>2</sub>**) intends to avoid obstacles that are not detected using previous distributed-dependent surveillance. On-board sensors, such as camera, can be used to generate an autonomous tactical maneuver. In this layer, every conflict with normal aircraft, manned or unmanned, is resolved.

The Escape Layer (**Sur<sub>3</sub>Coo<sub>2</sub>Man<sub>3</sub>Aut<sub>2</sub>**) aims to avoid any remaining non-cooperative obstacles that are hard to detect within sufficient range for a tactical maneuver, and are possibly not cooperative. To escape to a safety zone as soon as possible, the ownship's maneuverability should be the deciding factor in determining the layer threshold. The implicit-rules in avoiding, however, are still obeyed by the ownship, expecting that the obstacles do not intentionally make the conflicts .

Due to various unexpected situations, penetrations through all the five previous layers are still possible. For example, a cooperative UAV that has failure in its control system, rogue objects without any means of avoidance, or even a hostile UAV aiming to take the ownship down. In these situations, the Emergency layer (**Sur<sub>3</sub>Coo<sub>3</sub>Man<sub>3</sub>Aut<sub>2</sub>**) is implemented, where the UAV can disregard the rule and conduct necessary maneuver using its maximum capability to ensure safety.

## 2.5. CONCLUSION

The paper has proposed a taxonomy of Conflict Detection and Resolution (CD&R) approaches for Unmanned Aerial Vehicles (UAV), which consist of generic approaches that have been reviewed with regard to their feasibility for operation in an integrated airspace. The taxonomy has then been used to attribute a total of 64 proposed CD&R methods in literature, in order to determine their positions in an overall CD&R function of UAVs. This attribution has shown that many of the available methods fall outside the taxonomy, and suggests the need to concentrate the CD&R research more to parts where representative methods are lacking.

An example of an exhaustive multi-layered architecture for UAV CD&R systems has also been elaborated in this paper, consisting of six layers of generic approaches taken from the proposed taxonomy. Although its general implementation has been discussed, the multi-layered architecture is still lacking physical thresholds between the layers, such

<sup>1</sup>—, "FLARM Technology, System Design and Compatibility", August 2015, retrieved June 2016 from <https://flarm.com/wp-content/uploads/2015/08/FLARM-System-Design-and-Compatibility.pdf>

as distances or time-to-collision. Improvement is warranted for future works, nevertheless, it has been shown that the proposed taxonomy and architecture can be a guideline for the authorities, operators, and developers, to facilitate the UAV integration into the civil airspace.



# 3

## SAFETY ASSESSMENT OF UAV CD&R SYSTEM

*A robot must protect its own existence  
as long as such protection does not conflict  
with the First or Second Laws*

**Third Law of Robotics,**  
Isaac Asimov

*This Chapter evaluates the safety of UAV operations by running Monte Carlo simulations setups that mimic situations in an integrated airspace. The safety is evaluated in two CD&R protocols, which corresponds to the Cooperative and the Non-cooperative layers from the architecture proposed previously in Chapter 2. The Chapter starts (Section 3.2) with the discussion on a heterogeneous airspace model, consisting of four main elements, i.e. (1) the high density airspace, (2) the uncertainties of detection, and (3) the variety of resolutions and (4) order in a heterogeneous airspace. Afterwards in Section 3.3, the outputs of the Monte Carlo simulations are presented. Section 3.4 elaborates the overall result and analysis of the outputs, including a recommendation in reaching the airspace Target Level of Safety. The methodology in this Chapter is used as the basis to validate the performance of the method developed in Chapter 4 and 5.*

---

|                     |   |
|---------------------|---|
| <b>Paper Title</b>  | Safety Assessment of UAV CD&R System in a High Density Airspace using Monte Carlo Simulations |
| <b>Authors</b>      | Yazdi I. Jenie, Erik-Jan van Kampen, Joost Ellerbroek, and Jacco M. Hoekstra                  |
| <b>Submitted in</b> | The IEEE Transactions of Intelligent Transportation System 2016                               |

*This paper presents a safety assessment method for Unmanned Aerial Vehicle (UAV) operations, including the effect of a distributed Conflict Detection and Resolution (CD&R) system, in a high density airspace environment. Here, the expected conflicts occurrence and chances for each CD&R system to perform are sufficiently high to extract two parameters of safety, i.e., the frequency of Near Mid-air Collision (NMAC) and the frequency of Mid-air Collision (MAC), by series of Monte Carlo simulations. The results are then used to derive the safety parameters in a more realistic, less dense airspace. Two cases of distributed CD&R protocols are assessed and compared, i.e., (1) uncoordinated protocol where each vehicle has its own avoidance preferences, and (2) implicitly coordinated protocol where each vehicle, while still independent from each other, apply simple common rules. Using those CD&R protocols, the result shows a reduction of more than 94% of possible NMAC. More over, while maintaining the Target Level of Safety in the airspace, the maximum number of UAVs under an implicitly coordinated CD&R protocol can be at least ten times more than cases when no CD&R is applied.*

### 3.1. INTRODUCTION

INTEGRATING Unmanned Aerial Vehicles (UAVs) into the airspace presents new challenges for the airspace management, especially in ensuring operational safety by detecting and resolving any possible mid-air conflicts with each other, as well as with the existing air traffic. The challenge becomes more complicated with inevitable heterogeneity of the UAV Conflict Detection and Resolution (CD&R) system due to the potentially large range of UAV developers, types, and missions. Current airspace authorities cannot yet accommodate UAV integration since, firstly, regulations are aimed at managing the much more homogeneous manned-flight traffic, and secondly, there is no standard measure of the airworthiness of the CD&R system in each UAV. Taking safe measures, the airspace authority restricts all UAV operation in the airspace, especially those that fly beyond the operator line of sight, until a certain target level of safety (TLS) can be assured [7].

Several analytical methods have been proposed to assess the TLS by deriving two main parameters of safety, i.e., the frequency of Near Mid-air Collision (NMAC) and the frequency of Mid-Air Collision (MAC). The NMAC is defined as the moment when a vehicle separation, a threshold distance or time-to-collide from the vehicle center, is violated by another vehicle. The MAC, on the other hand, expresses the event when body contact between vehicles occur, hence, an actual collision. Ref.[99], [28], [100] and [101] derive the parameters based on the possibility of intruders existed in each aircraft's effective volume, while flying in a uniformly populated airspace. This concept is known as the gas model, since it uses the same concept as that of molecular gas collision probability. In [102], the concept is used to calculate an airspace safety when UAVs are flying near several manned aircraft. Other methods, such as in [27], use probabilistic functions instead, as a way to include error in detection and properly design a flight plan. The results of all these methods, however, are highly conservative since they assume that no conflict resolution (collision avoidance) maneuver is taken.

Incorporating the effect of CD&R systems in a safety assessment is difficult without an extensive method of modeling and simulation of the vehicle dynamics, such as by performing Monte Carlo simulations[103], or by using dynamic programming[8]. Safety parameters are drawn statistically from numerous simulations of airspace samples, each with different combinations of aircraft states. Hence, various conflicts can be generated to test CD&R systems in every possible situation. These methods, however, are seldom desirable since, in a realistic airspace density, conflicts and collisions are so rare that it will take a considerably large amount of time and number of samples to obtain a significant result, such as presented in [104] and [75].

The current paper presents a safety assessment method for UAVs, including their distributed CD&R system performances, using Monte Carlo simulations in high density airspaces, instead of a realistic situation, to overcome the drawbacks of the method. In such airspace, the expected value of conflict, as well as chances for each CD&R system to perform, are sufficient to conclude the expected value for NMAC and MAC frequencies. Moreover, the area of interest is enclosed with a periodic boundary condition, which wraps the movement of the vehicles and eliminates unavailing samples, such as when some vehicles leave the area before encountering others. The results are then used to derive the safety parameters in a realistic, less dense airspace, by assuming the applicability of the gas model.

The contribution of the research in this paper is threefold. First, a novel method for safety assessment, which includes the effect of the collective performance of the CD&R system in each vehicle, is introduced. Secondly, the method is versatile enough to also test and compare two cases of distributed CD&R protocols: (1) an uncoordinated system, and (2) an implicitly coordinated system that applies the Right of way rules[86]. These two protocols are also compared with the cases where no CD&R system is activated, which case should correspond to the cases described in the gas model. Thus, the last contribution is the validation of the gas model in various initial conditions in a high density airspace.

This paper is structured as follows. After this introduction, Section II discusses the heterogeneous airspace model, which consists of four main elements, i.e. (1) the high density airspace, (2) the uncertainties of detection, and (3) the variety of resolutions and (4) order in a heterogeneous airspace. Section III presents the results and the target outputs of the Monte Carlo simulations based on the model. A brief discussion of the output convergence is also given in the end of this section. Overall result and analysis on the safety parameters are presented in Section IV, which includes a recommendation in reaching the airspace Target Level of Safety. Section V concludes the paper and provides suggestions for future work.

### 3.2. HETEROGENEOUS AIRSPACE MODEL

A simulator capable of simulating numerous independent vehicles is built, where the performance of each vehicle, as well as how it detects and reacts to a conflict, can be varied independently. The simulator models the vehicles as point masses, to focus on the performance of a CD&R protocol in a randomized airspace. Since it is designed to perform numerous simulations in a Monte Carlo setup, the model uses a discrete equation of motion, in which the time-step,  $\Delta t$ , is fixed.

### 3.2.1. HIGH DENSITY AIRSPACE WITH PERIODIC BOUNDARY CONDITION

The model initializes vehicles in a high density airspace setup, where numerous UAVs are uniformly packed in square area of interest in an upright or a diagonal square-lattice configuration, as shown in Figure 3.1. The number of vehicle for these configuration, however, can only be taken from the set  $N_V = \{4, 5, 8, 9, 13, \underline{16}, 18, \underline{25}, 32, \underline{36}, 41, \underline{49}, 50, 61, \underline{64}, 72, \underline{81}\}$ . The underlined numbers in the set are for the upright-square lattice, which is a quadratic sequence. From these orderly initializations, the headings  $\chi$  of each vehicle are uniformly randomized to produce various encounter situations required for the Monte Carlo analysis.

3

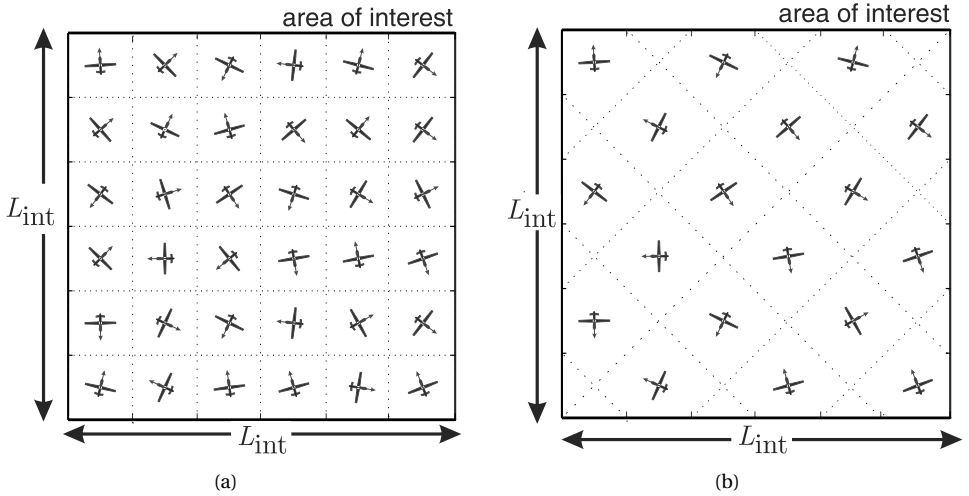


Figure 3.1: (a) upright, and (b) diagonal square lattice initialization of the UAVs in the area of interest

The simulation is conducted within the square boundary without any physical walls, where the density parameter is maintained by resorting to a two-dimensional Periodic Boundary Condition (PBC), as shown in Figure 3.2. This boundary condition assumes that the area of interest is a square unit cell, which is part of a large (infinite) uniform system. The square unit cell, therefore, has nine adjacent 'clone' cells. Whenever a vehicle crosses one of the edges of the area of interest, it gets replaced immediately by a new vehicle on the opposite edge with the same velocity vector. This setup eliminates unavailing cases where some vehicles directly leave the area of interest without having the chance to perform any avoidance.

Equations (3.1) and (3.2) present the modification of a discrete equation of motion in which the vehicle global position,  $\vec{X}$ , is updated each time-step  $\Delta t$ , by both current ownship velocity  $\vec{V}$  and the PBC transformation matrix. The PBC setup is also a part of the reason why the vehicles are packed in a square area of interest, since this provide simplicity in defining the wrap-around effect. Other shapes, such as a hexagonal configuration, can actually pack the vehicles in a more dense way, but have a higher complexity in applying the PBC.

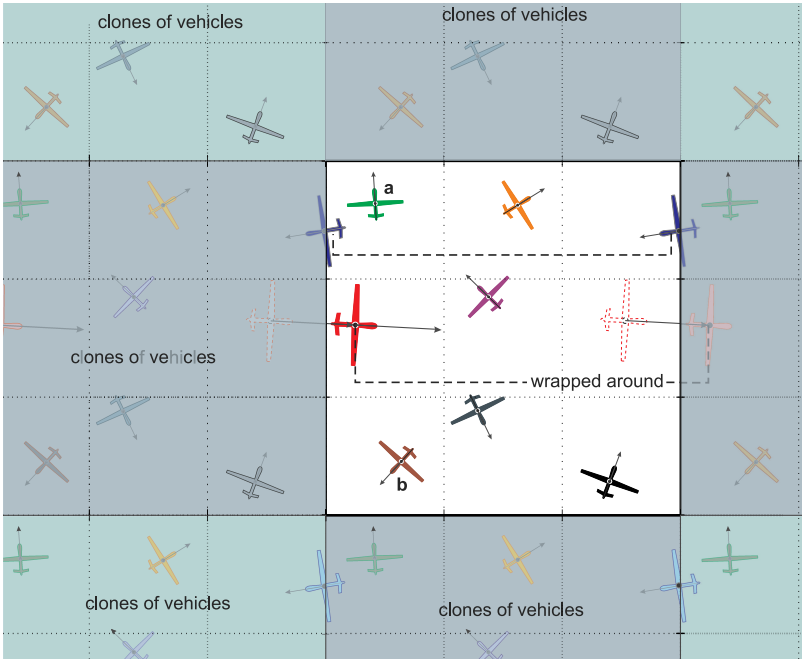


Figure 3.2: Simulation with periodic boundary condition

$$\vec{X}(k+1) = \vec{X}(k) + \vec{V}(k)\Delta t + \begin{bmatrix} \sigma_x & 0 \\ 0 & \sigma_y \end{bmatrix} \tag{3.1}$$

with,

$$\begin{cases} \sigma_{x,y} = -L_{int}, & \text{if } (X_{x,y}(k) + V_{x,y}(k)\Delta t) > \frac{1}{2}L_{int} \\ \sigma_{x,y} = L_{int}, & \text{if } (X_{x,y}(k) + V_{x,y}(k)\Delta t) < -\frac{1}{2}L_{int} \\ \sigma_{x,y} = 0, & \text{otherwise} \end{cases} \tag{3.2}$$

where,

- $\vec{X}$  Vehicle position in the area of interest,
- $\vec{V}$  Vehicle velocity,
- $L_{int}$  Length of the Area of interest,

In implementing the PBC, the wrap-around effect needs to be considered in the conflict detection and resolution generation. This is illustrated in Figure 3.2, where UAV **a** and UAV **b** need to detect and avoid each other, while their positions are actually on the opposite sides of the area. Therefore, while the 'clone' motions are only copied and not computed, their existence should still be considered in the CD&R method.

In cases where body-to-body collisions, or an MAC, occurred due to failure in avoidance, the density of the area cannot be maintained, since all involved vehicles are removed immediately. However, these cases only have small chance to occur, even with-

out any CD&R system, and therefore the effects are neglected in the overall analysis. Loss of separation without actual collision, or an NMAC occurrence, does not remove the involved vehicles from the simulation, and therefore each vehicle might lose its separation more than once.

### 3.2.2. THE UNCERTAINTY OF CONFLICT DETECTION

The entire CD&R process begins with the detection of obstacles in proximity. In order to decide whether an obstacle is in a conflicting course or not, both detection methods require at the very least two states, i.e., position and velocity vectors of the obstacle, as well as of the ownship. One of the conflict detection methods that exploits these two states is the Velocity Obstacle method[22, 75], which is used in the overall airspace model in this research, explained in detail in the next subsection.

The uncertainty of detection in the airspace model is represented, therefore, by adding a specified error of the position and velocity vector measurements of the obstacle, denoted as  $\epsilon_x$  and  $\epsilon_v$ , respectively. Equation (3.3) and (3.4) present the measurements of the obstacle position and velocity,  $\vec{X}_i^*$  and  $\vec{V}_i^*$ , under the influence of the errors. These errors are randomized with Gaussian (normal) distribution through time and are not affected by previous values or by any other states in the detection process.

$$\vec{X}_i^* = \begin{bmatrix} x_i^* \\ y_i^* \end{bmatrix} = \begin{bmatrix} x_i + \epsilon_x \\ y_i + \epsilon_x \end{bmatrix} \quad (3.3)$$

$$\vec{V}_i^* = \begin{bmatrix} v_{x_i}^* \\ v_{y_i}^* \end{bmatrix} = \begin{bmatrix} v_{x_i} + \epsilon_v \\ v_{y_i} + \epsilon_v \end{bmatrix} \quad (3.4)$$

where,

$\vec{X}_i^*$  Measured position of obstacle- $i$  from ownship,

$\vec{V}_i^*$  Measured velocity of obstacle- $i$  from ownship,

$\epsilon_x$  Measurement error of position,

$\epsilon_v$  Measurement error of velocity.

Although it should also be covered by the heterogeneous assumption, variation in detection systems are not considered in this research, and is only represented by the difference in errors of measurements for each UAV independently. Other variations in measurements, such as on ranges, frequencies, or accuracies, are included together as the variation in resolutions.

### 3.2.3. THE VARIATION OF CONFLICT RESOLUTION

A vast collection conflict resolution algorithms can be found in the literature, many of them are reviewed and classified in Ref. [83] and [82]. This research uses a method called the Velocity Obstacle method (VO-method)[22, 75] that can generate a variety of resolutions by giving each vehicle different thresholds for two of the VO-method variables: the avoidance distance ( $d_{avo}$ ) and the radius of protected zone  $r_{pz}$ . Since the VO-method generates resolutions reactively based on the instantaneous geometry of a conflict, no predetermined plan or any dynamic predictions are involved in the airspace model.

The concept of the VO-method is explained using Figure 3.3, in which for every encounter case, a collision cone  $\mathbf{CC}_i$  can be drawn by collecting the extensions of relative

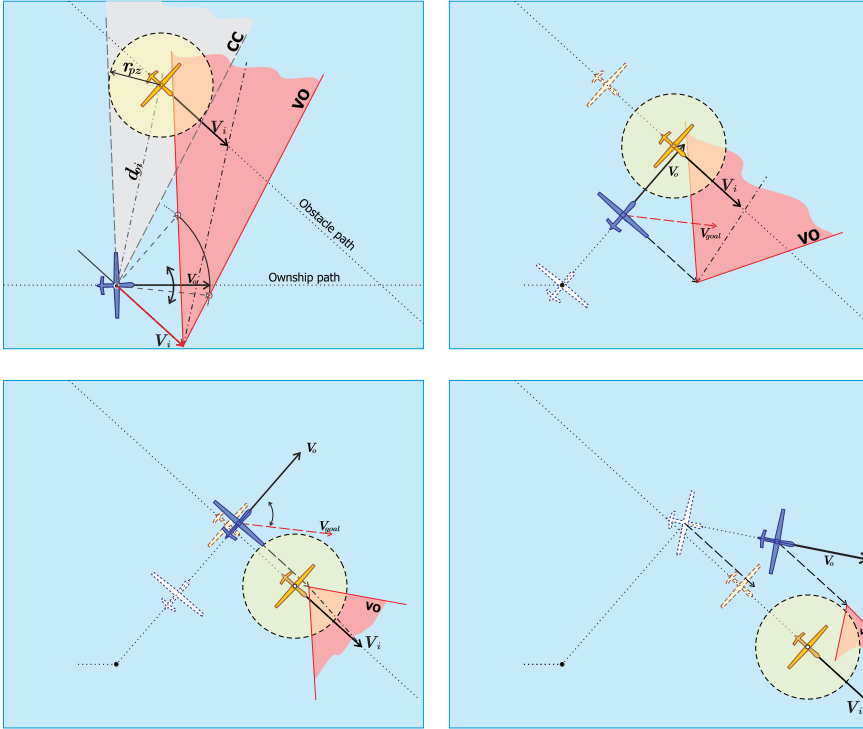


Figure 3.3: The Velocity Obstacle method for case of two-dimensional encounter

velocity vectors of an ownship that intersect a specified protected zone ( $S_{pz}$ ). The protected zone is a threshold area around the obstacle that should be avoided. The edge of  $S_{pz}$  also represents the preferred Closest Point of Approach (CPA) for each vehicle. The VO-method uses the absolute velocity vector representation of the  $CC_i$  set, the  $VO_i$  set, as depicted in the Figure 3.3, where  $CC_i$  is translated along  $V_i$  to create the  $VO_i$  set. Hence, every ownship velocity that is included in the  $VO_i$  set will eventually lead to an intrusion into the protected zone.

Equation (3.5) is used to determine if the ownship velocity,  $\vec{V}$ , is included in the  $VO_i$  set after the conflict is imminent, i.e., the measured distance between the two vehicles,  $d_i^* = |X_i^*|$ , is smaller than a specified avoidance starting point  $d_{avo}$ . It should be noted that all equations in this subsection refer to the ownship body-axis frame of reference, and therefore, the ownship velocity,  $\vec{V}$ , will always lie on the horizontal axis. The asterisk (\*) superscript is used on the measured obstacle variables, to indicate that their values include the measurement errors.

$$\vec{V} \in VO_i \iff \left\{ 0 < \frac{|\vec{V} - \vec{V}_i^*|}{|\vec{V} - \vec{V}_i^*|} \cdot \frac{\bar{X}_i^*}{\sqrt{(d_i^*)^2 - r_{pz}^2}} < 1 \wedge d_i^* < d_{avo} \right\} \quad (3.5)$$

where,

|                 |                                      |
|-----------------|--------------------------------------|
| $\mathbf{VO}_i$ | Velocity Obstacle set,               |
| $\vec{V}$       | Velocity of ownship vehicle,         |
| $r_{pz}$        | Radius of the protected zone,        |
| $d_i^*$         | Measured distance of obstacle- $i$ , |
| $d_{avo}$       | avoidance starting distance,         |

Hence, to avoid violating the  $S_{pz}$ , the ownship needs to change its velocity vector to any reachable point outside the  $\mathbf{VO}_i$  set immediately after the criteria in (3.5) is fulfilled. The simplest way to do this is by applying a predefined avoidance turning rate,  $\omega_{avo}$ , rotating  $\vec{V}$  until it can get out of the corresponding  $\mathbf{VO}_i$  set, as presented in Figure 3.3, formulated in (3.6). Afterward, the velocity vector is maintained for a while to suppress any oscillating motion. Only when the distance between vehicles is larger than the avoidance starting distance,  $d_i^* \leq d_{avo}$ , can the ownship turn its velocity vector back to the original goal. A more detailed explanation of this particular turning-only avoidance using the VO-method can be found in [104] and [75].

$$\vec{V}(k+1) = \vec{V}(k) \begin{bmatrix} \cos \omega_{avo} \Delta t & -\sin \omega_{avo} \Delta t \\ \sin \omega_{avo} \Delta t & \cos \omega_{avo} \Delta t \end{bmatrix} \quad (3.6)$$

where,

|                |                         |
|----------------|-------------------------|
| $\omega_{avo}$ | Avoidance turning rate, |
| $\Delta t$     | Simulation time-step,   |

The variation in avoidance methods across the vehicles, which induces the heterogeneity of the airspace, is achieved by assigning different avoidance distances ( $d_{avo}$ ), and different radii of the protected zone ( $r_{pz}$ ). The former parameter affects the aggressiveness of the resolution: the closer the avoidance starting point to the obstacle, the more aggressive the maneuver needs to be. The radius of the protected zone, on the other hand, results in the preferred closest point of approach (CPA) between the vehicles. This heterogeneity is increased even more by the randomization of the turning direction, whether to go to the right or to the left. Examples of variation in conflict resolutions can be observed in Figure 3.4.

### 3.2.4. ORDER IN THE HETEROGENEOUS AIRSPACE

While heterogeneity of the future integrated airspace is inevitable, authorities can still facilitate each UAV with a more predictable environment, such as by enforcing rules of the air. Examples of these common rules are the Right of Way rules (RoW) used in the manned aircraft [86], which have been incorporated into the VO-method in [75], by introducing the Selective Velocity Obstacle (SVO) Method. The RoW implementation creates an implicitly coordinated situation, which is resolved according to the following list:

1. On converging encounter, the one on the right hand has the right of way
2. On head-on encounter, both aircraft should move to the right side
3. On same-path encounter, the one that is about to be taken over has the right of way
4. Avoidance should not go over or under, or in front of other aircraft that have right of way.

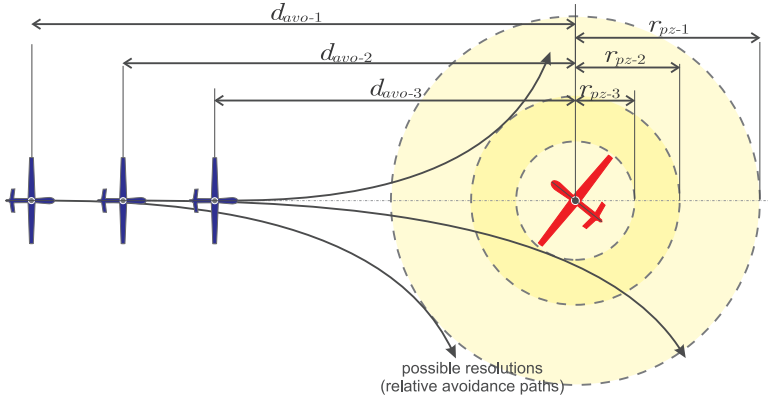


Figure 3.4: Examples of resolution varieties due to different preferences of avoidance starting distance ( $d_{avo}$ ) and radius of protected zone ( $r_{pz}$ )

The encounters, the situation in which collision are imminent, are differentiated as either converging, head-on, and taking over, based on the bearing angle of the obstacle to an ownship. This research takes the example from [75] and used a 90 degree steps differentiation, as it can be observed in Figure 3.5. Here, the ownship is facing four potential intruders: two converging intruders (**b** and **d**), one same-path intruder (**a**), and one head-on intruder (**c**), from which the ownship only has the right of way over intruder-**b**. To fulfill the last rule item, every avoidance is always conducted to the right side of the ownship flight path.

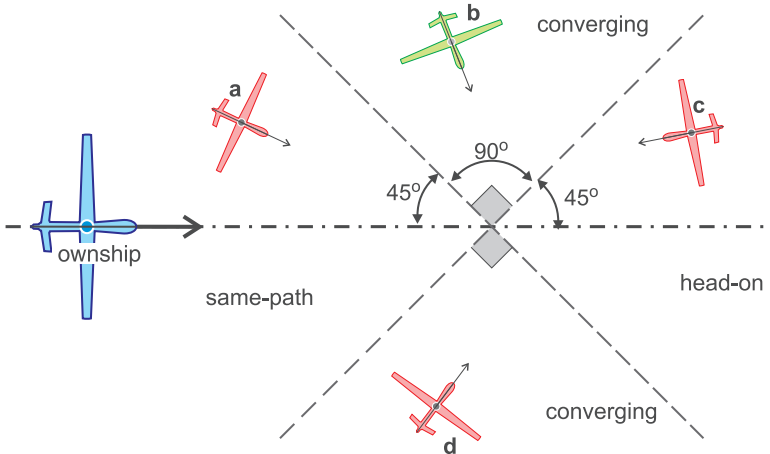


Figure 3.5: Encounter definition for Right-of-way rules implementation

Table 3.1: Tested cases in Monte Carlo simulation

| Case | CD&R | RoW | note                          |
|------|------|-----|-------------------------------|
| 1    | ×    | ×   | no CD&R                       |
| 2    | ✓    | ×   | uncoordinated (all maneuvers) |
| 3    | ✓    | ✓   | implicitly coordinated        |

## 3

### 3.3. MONTE CARLO SIMULATIONS

The Monte Carlo analysis is made by setting up and simulating numerous airspace samples, in which speeds and goals for every UAV are randomized. Three types of cases are assessed in this research to observe the effect of the distributed CD&R system implementation, as well as the RoW rule enforcement, as listed in Table 3.1.

#### 3.3.1. GENERAL SETUP

Table 3.2 lists the parameter setup for the Monte Carlo simulations in this research. For the entire simulation, the area of interest is kept the same at one kilometer-square. Sixteen different density points, configured by the number of vehicles in the area of interest ( $N_V = \{4, 5, 8, 9, 13, 16, 18, 25, 32, 36, 41, 49, 50, 61, 64, 72, 81\}$ ) are tested in a series of simulations with at least 250 samples.

Table 3.2: parameter ranges and randomization

| Parameters                             | Range                         | Randomization | Unit  |
|--|-------------------------------|---------------|-------|
| Number of vehicles, $N_V$              | (4, 100)                      | -             | [-]   |
| Total Simulation time, $T$             | 380                           | -             | [s]   |
| Simulation time step, $\Delta t$       | 0.1                           | -             | [s]   |
| Radius of separation, $r_n$            | 50                            | -             | [m]   |
| Radius of collision, $r_m$             | 1                             | -             | [m]   |
| Avoidance turning rate, $\omega_{avo}$ | $2\pi$                        | -             | [-/s] |
| Initial positions, $X$                 | $(-\frac{1}{2}, \frac{1}{2})$ | -             | [km]  |
| Initial headings, $\chi$               | $(0, 2\pi)$                   | uniform       | [-]   |
| Speed, $ V $                           | (15 – 25)                     | uniform       | [m/s] |
| Error in position, $\epsilon_x$        | (-2, 2)                       | normal        | [m]   |
| Error in velocity, $\epsilon_v$        | (-0.2, 0.2)                   | normal        | [m/s] |
| Avoidance distance, $d_{avo}$          | (300, 400)                    | uniform       | [m]   |
| Protected zone radius, $r_{pz}$        | (55, 60)                      | uniform       | [m]   |

Each of the simulations is run for a time that is needed for the slowest vehicle ( $V = 15$  m/s) to cross the diagonal of the area four times, to cover the wrap-around effect for the four edges of the area,  $T = \frac{4\sqrt{2}}{|V_{min}|} = 377.12 \approx 380$  seconds. The time-step, on the other

hand, is fixed at 0.1 second. The radius of separation  $r_n$  and the radius of collision  $r_m$  are the threshold of the NMAC and MAC, respectively, such that one NMAC or MAC is recorded every instant there are two vehicles with distance closer than  $r_n$  or  $r_m$ .

The initial headings are uniformly randomized within the range of  $0 - 2\pi$ , which represents the different goals of each vehicle. The speeds are uniformly randomized as well, from 15 - 25 meter/second, which represents the variation of UAVs in the integrated airspace. Since every resolution from a conflict is conducted by turning only, the speeds in each UAVs are constant throughout the simulation. The avoidance turning rate itself is set to be the same across the vehicles, at 360 degree per second.

The ranges for the errors in detection,  $\epsilon_x$  and  $\epsilon_v$ , are chosen from the FAA ADS-B requirements for navigational accuracy, as presented in [105] and [106]. The research assumed that the errors are within the limits specified by **NACp-11** and **NACv-4**, which values are listed in Table 3.2. **NACp** and **NACv** stand for Navigation Accuracy Category for Position, and Velocity, respectively. The errors are generated randomly, using a Gaussian distribution, for each UAV for every time-step at the beginning of the simulation.

To generate the variation in resolution for each UAV, parameters  $d_{avo}$  and  $r_{pz}$  are different for each vehicle, randomly given at the beginning, and kept constant throughout the simulation. The range of those parameters is set to covers numerous possible maneuvers to avoid an NMAC radius ( $r_n$ ), which is set to be 50 meters for all simulations in this research. The avoidance distance is uniformly randomized from the avoidance distance of 6 to 8 times the radius of NMAC, to provide enough space for turning. The remaining distance until the  $r_n$  from the obstacle is left for the CPA choices, represented as the radius of protected zones ( $r_{pz}$ ), which is also uniformly randomized among the vehicles. Note that for the uncoordinated CD&R in case 2, the direction of avoidance, either to go to the left or to the right, is randomized as well for each vehicle, regardless the conflict geometry.

### 3.3.2. OUTPUT

The main parameters derived from the Monte Carlo simulation are the frequency of NMACs,  $f_{nmac}$ , and the frequency of MACs,  $f_{mac}$ , per hour in the area of interest of one kilometer-square. This parameter are derived from the recorded occurrences of NMAC and MAC during the entire Monte Carlo set of airspace samples-  $j = 1, 2, \dots, N_{MC}$ . The frequencies are then described as the expected value of the parameters, as it is presented in (3.7), along with the variance in (3.8). The precision of the estimation is determined using the central limit theory, collecting the final results that are within the range presented in (3.9), for the 95% confidence interval. The  $N_{mac}$  is derived in the same manner.

$$E[f_{nmac}] = \frac{1}{N_{MC}} \sum_{j=1}^{N_{MC}} \frac{N_{nmac}^j}{T} \quad (3.7)$$

$$\sigma_f^2 = \frac{1}{N_{MC} - 1} \sum_{j=1}^{N_{MC}} \left( \frac{N_{nmac}^j}{T} - E[f_{nmac}] \right)^2 \quad (3.8)$$

$$f_{nmac} = E[f_{nmac}] \pm \frac{1.96\sigma_f}{\sqrt{N_{MC}}} \quad (3.9)$$

where,

|               |   |
|---------------|---|
| $N_{nmac}^j$  | Number of NMAC occurrences in sample- $j$ , |
| $T$           | Simulation time,                            |
| $E[f_{nmac}]$ | Expected value of NMAC frequency,           |
| $N_{MC}$      | Number of Monte Carlo simulations,          |
| $\sigma_f^2$  | Variance in NMAC frequency,                 |
| $f_{nmac}$    | Frequency of NMAC.                          |

Besides the frequencies, the depth of intrusion into the NMAC radius,  $r_n$ , is also an important factor in safety assessment to determine the severity of the NMAC. For instance, an NMAC that happens in a short period, but intrudes deeper and closer to the other vehicle, is riskier than a shallow one over a longer period. Therefore, ten zones that divide the NMAC circle are defined. The frequency of exclusive intrusion into each of the zones is recorded as  $f_i$ , which range from  $f_{10}$  to  $f_{100}$ , where the subscript denotes the percentage of intrusion. The expected number of intrusions for the entire Monte Carlo simulation is derived in the same manner as the  $f_{nmac}$  in (3.7) to (3.9).

### 3.3.3. CONVERGENCE

Examples of the derivations of  $f_{nmac}$  and  $f_{mac}$ , along the number of Monte Carlo simulation runs  $N_{MC}$ , are shown in the convergence graph in Figure 3.6. The graphs also compare different results between the three tested cases. The shaded background represents the corresponding 95% confidence interval. Note that while there are a total of 17 density points, only three of them are shown in the figures for a distinguishable comparison.

For case 1, without any CD&R, the parameters are shown to converge after approximately 100 airspace samples. These results demonstrate the effectiveness of the high-density setup in generating sufficient samples of random conflicts encounters.

The convergence, however, is not featured in the other cases where a CD&R system is implemented, especially in low density. This demonstrates the difficulty in using the Monte Carlo simulation: the simulation would require much more samples to derive significant results. The result for case 2 and 3 cannot be shown in Figure 3.6 due to similar reason, that for the 250 sample tested, none of them shows MAC occurrences. This is true even for the highest density of the simulation setups. Nevertheless, it can also be said that the distributed CD&Rs implementation is able to reduce the frequencies of MAC, until the point where no collision is recorded for all the samples.

## 3.4. RESULT AND ANALYSIS

The safety parameters for each case and density point are extracted from each corresponding Monte Carlo simulation by taking the last expected values along with each range of confidence. All results are presented in Figure 3.8 and 3.9, and discussed throughout this section. The discussion is preceded with a brief simulation visualization of a few cases, to observe the general characteristics of UAVs flying in a high density and heterogeneous airspace model.

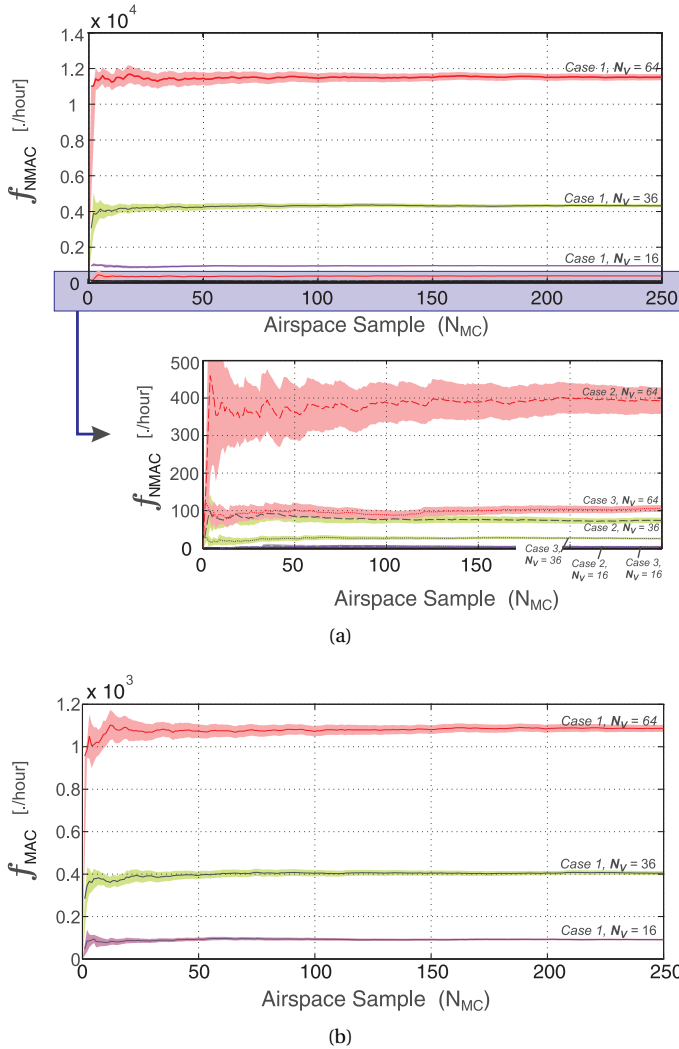


Figure 3.6: Monte Carlo simulation results against the number of samples ( $N_{MC}$ ) for frequency of (a) near mid-air collision (NMAC) and (b) mid-air collision (MAC)

### 3.4.1. VISUALIZATION

Figure 3.7 visualizes three samples of simulation for case 2, the particular case where vehicles have the most difficulty in maintaining safety due to the randomness of maneuvers. The simulations are shown for four different setups of  $N_V$ , where each UAV is represented by a point with an arrow extending from the center, depicting its velocity vector. The circle around each vehicle represents half of the radius of the NMAC separation zone, so that NMAC occurs when two circles overlap each other. To observe the characteristic of a flight path in the dense airspace, four center vehicles, shaded and

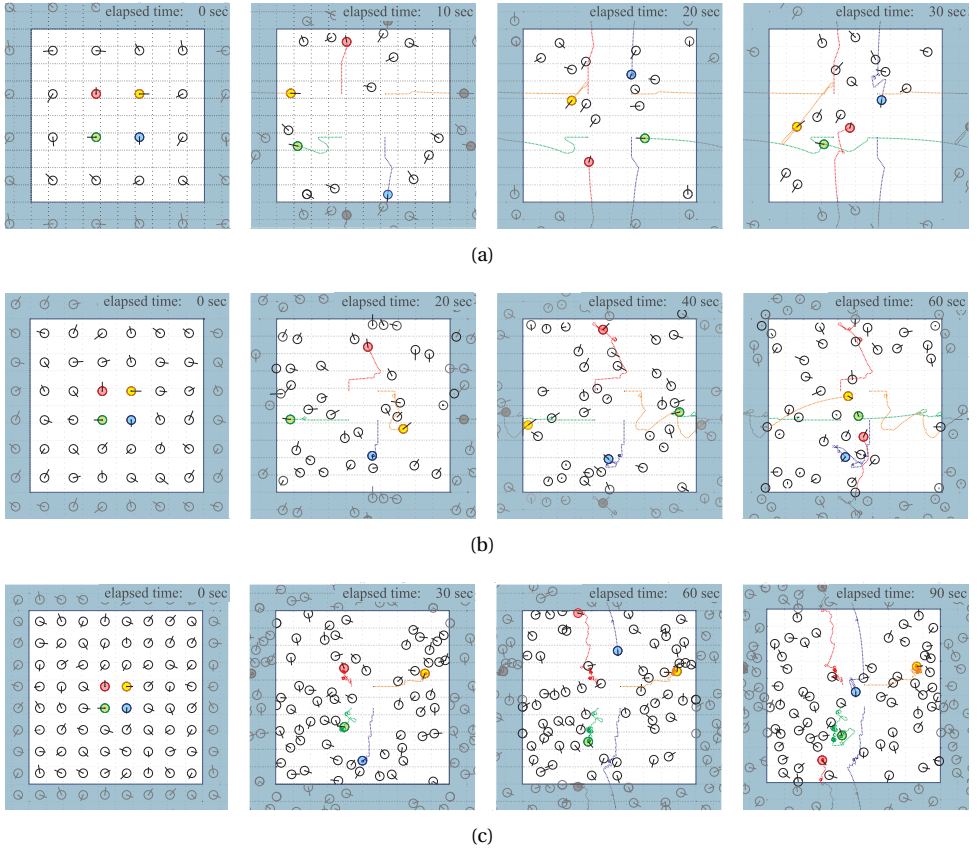
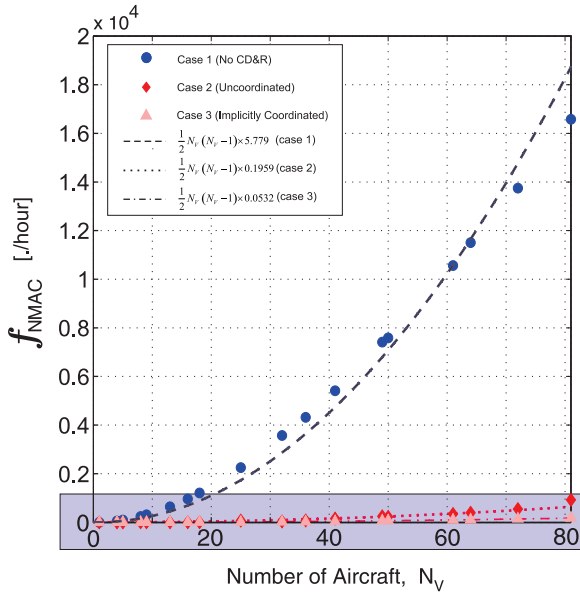


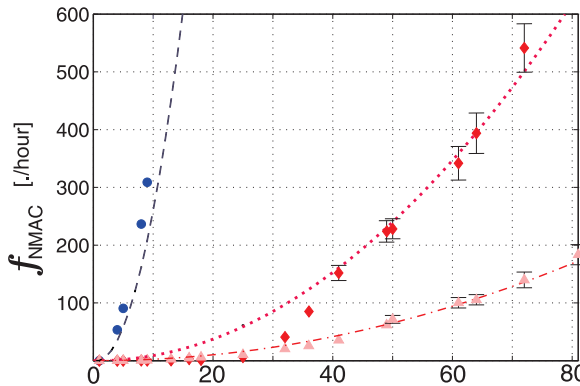
Figure 3.7: Example of the High-Density airspace simulation in one kilometer-square airspace with (a) 16 vehicles, (b) 36 vehicles, and (c) 64 vehicles

tracked, are given goals to complete a path to the respective area edges and reappear again on the other side. Note that this setup is used only for visualization, and not applied in the overall Monte Carlo simulations.

In the least dense airspace in Figure 3.7, the center-vehicles are able to complete their mission with only small occasional deviations, conforming the rare occurrences of conflicts in the airspace. In an example case with 36 vehicles, the encounters become more complex where most of the UAVs need to conduct many avoidances, resulting in a lot of zig-zag paths and round-about maneuvers. The later actually indicates that the CD&R is unable to find an escape path and instead making turns continuously until the conflict is resolved. In an extreme high density with 64 vehicles, it is apparent that the circular round-about motion dominates the vehicle path, preventing the four center vehicles from reaching any edges of the area.



(a)



(b)

Figure 3.8: (a) Monte Carlo simulation results for frequency of near mid-air collision (NMAC) for all density points. (b) Graph zoom-in for a clearer results of case 2 and 3

### 3.4.2. NMAC AND MAC FREQUENCIES

Confirming the visual observations, Figure 3.8 and 3.9 shows that both parameters increase with the airspace density in a quadratic manner. The curves confirm the reduction of collision occurrences just by limiting the number of vehicles in the airspace. In the case where no-CD&R is applied, the results for  $f_{nmac}$  and  $f_{mac}$  reach  $1.7 \times 10^4$  and  $1.6 \times 10^3$  per hour, respectively, in the highest density airspace.

In the cases where CD&R in each vehicle is activated, much lower  $f_{nmac}$  values are obtained. The NMAC frequency for case 2 reaches 923.5 per hour, which means that the

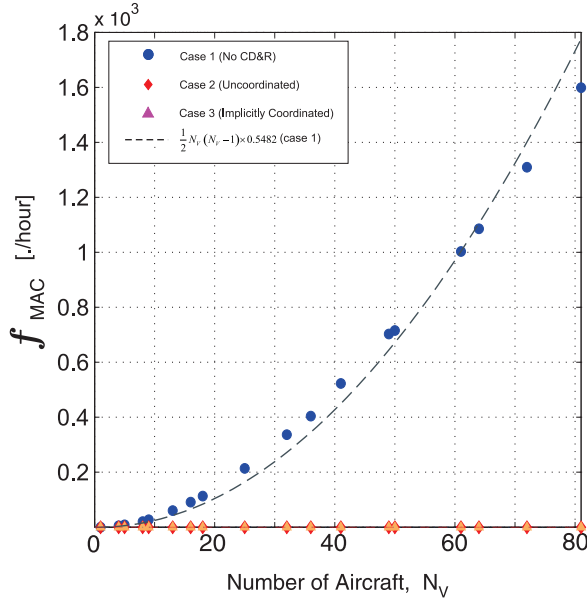


Figure 3.9: Monte Carlo simulation results for frequency of mid-air collision (MAC) for all density points.

distributed CD&R, without any rule implementation, are able to resolve more than 94.43 % of the conflicts at the densest airspace in this research. By incorporating the RoW rules, the NMAC is reduced even more up to 98.89 % with more accurate results with a narrower range of confidence, shown in Figure 3.8. The same conclusion, however, cannot be drawn for the MAC frequency since there are no MACs detected in case 2 and 3 throughout the entire Monte Carlo simulation.

The use of the gas model[28, 99–101], formulated in (3.10), is able to produce a good fit with the results of case 1, as shown in Figure 3.8 and in 3.9. This validates the gas model in high density airspace, even when the speeds vary for each vehicle. The  $\hat{p}_{n,m}$  component, however, has a different meaning in the setup of this research from the conventional gas model. Since it is possible for each vehicle here to encounter one another more than once, taking the factor of possible encounter combination, i.e.  $\frac{1}{2}N_V(N_V - 1)$ , from the frequencies does not translate into probabilities, such as presented in [100] and [101]. Therefore,  $\hat{p}_{n,m}$  in this research, where a hat is added to the symbol, is defined as the average expectation of NMAC or MAC of each vehicle to one another, per unit time. This parameter is described in (3.11), which summarized the average relative velocity of pairs of vehicles, the radius of NMAC or MAC, the width of the area of interest, which represent the airspace density, and an airspace constant.

$$f_{nmac,mac} = \frac{1}{2}N_V(N_V - 1)p_{n,m} \quad (3.10)$$

$$\hat{p}_{n,m} = \frac{c_{n,m} \cdot r_{n,m} \vec{V}_R}{A_{int}} \quad (3.11)$$

where,

- $\hat{p}_{n,m}$  average expectation of NMAC or MAC of each vehicle to one another,
- $|\bar{V}_R|$  Average relative velocity of pairs of vehicles,
- $c_{n,m}$  Airspace constant,
- $r_{n,m}$  Radius of NMAC or MAC,
- $A_{int}$  Area of interest.

The least-square curve fitting on the  $f_{nmac}$  results in the  $\hat{p}_n = 5.779$  per hour, and  $\hat{p}_m = 0.5582$  per hour. These values means that, in the preconditioned environment, in average a UAV can loss its separation to another with a specific heading more than five times per hour, and collide with that vehicle more than once every two hours. These values require the same value of airspace constant,  $c_n$  and  $c_m$ , which is approximately 0.6. This factor that may have come from the velocity randomization for a finite number of vehicle, as oppose to the homogeneous density assumption in the gas model. Note that the average  $\bar{V}_R$  is approximated by  $\frac{4|\bar{V}|}{\pi}$ , as presented in [100], where  $|\bar{V}|$  is the average speeds of all vehicles. The same curve fitting with the gas model is also conducted for the results in case 2 and 3, as it can be found in the legends of Figure 3.8 and in Table 3.3.

Table 3.3: NMAC and MAC average expectation

| case | $\hat{p}_n$ | $\hat{p}_m$ | unit     |
|------|-------------|-------------|----------|
| 1    | 5.779       | 0.0594      | [-/hour] |
| 2    | 0.1959      | -           | [-/hour] |
| 3    | 0.0532      | -           | [-/hour] |

### 3.4.3. REACHING THE TARGET LEVEL OF SAFETY

The frequencies of NMAC and MAC,  $f_{nmac}$  and  $f_{mac}$ , need to reach certain values of the Target Level of Safety (TLS), in order to safely integrate the UAVs operation into the airspace system. The equivalent values of in manned-flight, for a certain period, are commonly taken as the based in determining the UAV TLS. For example, [7] proposed a value  $f_m^{tls} = 10^{-7}$  to be the maximum MAC occurrences per hour in an airspace, which is determined from the NTSB analysis of manned aircraft in-flight collision between 1983 - 2006[7]. The NMAC frequency TLS,  $f_n^{tls}$  can be determined in the same way, by analyzing the NMAC occurrences in manned flight. Based on the FAA data for the last decade in the entire US airspace [107], the NMAC occur in manned flight at  $1.3 \times 10^{-2}$  per hour. Hence, the rate of  $f_n^{tls} = 10^{-2}$  per hour is proposed for UAV operations.

Using the determined  $f_n^{tls}$ , together with (3.10), (3.11), and the NMAC average expectation data in Table 3.3, the maximum number of UAV that can operate in a one kilometer-square area can be deduced. To scale this up to a realistic area, such as a city with area of  $A_{int}$ , the corresponding NMAC expected value per pair of UAV need to be redefined. Suppose an certain city with area  $A_{int}$  having a NMAC expectation of  $\hat{p}_{n_{int}}$ , based on equation (3.11) and the Monte Carlo simulation result,

$$\hat{p}_{n_{int}} : \hat{p}_n = \frac{1}{A_{int}} : \frac{1}{A} \Leftrightarrow \hat{p}_{n_{int}} = \hat{p}_n \frac{A}{A_{int}}. \quad (3.12)$$

Then, using the quadratic formula on equation (3.10), the following equation (3.13) can be used to determine the  $N_V^{tls}$ , the recommended maximum number of UAVs that can operate above  $A_{int}$  in one level of altitude. Note that in the equation,  $A_{int}$  are in kilometer-square unit, and hence  $A = 1$  is omitted.

$$N_V^{tls} = \frac{1 + \sqrt{1 + 8 \frac{f^{tls}}{\bar{p}_{int}}}}{2} = \frac{1 + \sqrt{1 + 8 \frac{A_{int} f^{tls}}{\bar{p}}}}{2} \quad (3.13)$$

Table 3.4 listed five examples of large cities in the world and the recommended maximum number (rounded down) of UAVs that can operate in one level of altitude above them, based on the NMAC requirement and the preconditioned environment explained in Section 3.3. It should be noted that the results are obtained from an assumption that the frequency curves, for cases under the effect of CD&R protocols, still follow the gas model in (3.10). As it can be observed in Figure 3.8-b, the assumption is not true for the lower density of case-2. Hence, a higher  $N_V^{tls}$  can actually be resulted if a fitter and less conservative model, such as the canonical quadratic function:  $aN_V^2 + bN_V + c$ , is used. Finding the physical parameters of such model, however, is beyond the scope of this research and left for future works.

Table 3.4: Maximum number of UAVs operating in one flight altitude of airspace, within the preconditioned environment explained in Section 3.3

| City               | Area<br>[km <sup>2</sup> ] | $N_V^{tls}$ |        |        |
|--------------------|----------------------------|-------------|--------|--------|
|                    |                            | case 1      | case 2 | case 3 |
| New York Metro, US | 8,683                      | 6           | 30     | 57     |
| Tokyo/Yokohama, JP | 6,993                      | 5           | 27     | 51     |
| Chicago, US        | 5,498                      | 4           | 24     | 45     |
| Jakarta, ID        | 661.5                      | 2           | 8      | 16     |
| Amsterdam, NL      | 219.32                     | 1           | 5      | 9      |

As the outcomes indicate, in the airspace of the largest city, New York, a maximum of 57 UAV can operate in one flight level at the same time. This is almost ten times more than in the cases without any CD&R. Evidently, the role of CD&R is strengthened with the implementation of an order in the airspace, via the RoW rule. The numbers, however, might still not be ideal for some high populated city. For instance, Jakarta is 1.7 times more dense in population than Chicago, which can be an indication of a high UAV demand. However, it can only harbor 16 UAVs per altitude, which is less than a third of the limit of Chicago. These results, however, only correspond to one level of altitude, such that if the airspace above the cities were to be divided into for example 16 layers, as in [101], then the number of UAVs above Jakarta can be up to 256, while in the New York sky can be up to 800 UAVs.

A better CD&R system might also be warranted, instead of the simple VO-method explained in Section II.C. Alternatively, controlling the heterogeneity of missions, or set more layers of flight level, such as presented in [101], will also enable more UAVs to be

operated. These are the possibilities that can be tested using the high density Monte Carlo setup in order to assess the safety parameter, as well as to produce a mature CD&R system.

#### 3.4.4. SEVERITY OF INTRUSION

Another way to determine the collective performance of the distributed CD&R is by looking at how severe the intrusion is in each occurrence of NMAC. Figure 3.10 presents the distribution of intrusion frequency,  $f_i$ , in each zone of severity, i.e., how deep an intrusion goes into the NMAC circle, from  $r_n = 50$  m. Note that the depth of intrusion is recorded at the point when it does not go any deeper. For instance, an intrusion to a point in the 40-50% zone of the separation is not recorded in all the previous zones of which the obstacle needs to go through before reaching that point.

It can be observed in the figures that, for cases without CD&R, the severity of intrusions are almost uniformly distributed, meaning that there are as many less-severe intrusions as there are severe. This result is similar for every density point.

The use of CD&R proposed, in case 2 and 3, is able to make intrusions less severe, even though it may not be guaranteed a 100% NMAC free operation. The implementation of RoW is evidently superior, as it shows not only a reduced number of intrusions, but each intrusion is also less severe than of the uncoordinated CD&R in case 2. The remaining area on the right side of the curves illustrates the spare zones in the NMAC circle that is left for any other emergency avoidance.

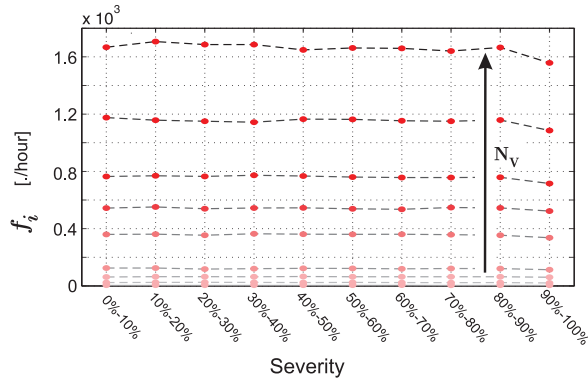
The severity graph in Figure 3.10 also indicates the ideal NMAC radius for the proposed CD&R in case 2 and 3. If the NMAC separation can be relaxed for UAVs, then using  $r_n = 25$  meter will reduce the NMAC to almost zero, and thus increases the number of UAVs that can be operated in the airspace.

### 3.5. CONCLUSION

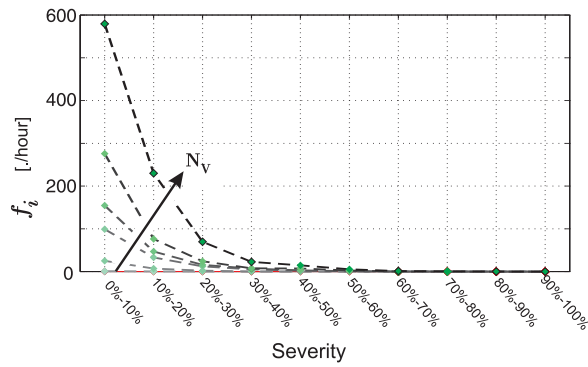
This research has evaluated the safety of Unmanned Aerial Vehicle (UAV) operations, within the preconditioned environment, using a series of Monte Carlo simulations. Two cases of distributed Conflict Detection and Resolution CD&R are tested in the simulation: (1) an uncoordinated CD&R where each vehicle has random avoidance preferences, and (2) an implicitly coordinated CD&R that incorporates the Right-of-way rules. From those two cases, two parameters of safety are drawn, i.e., the frequency of Near Mid-air Collision (NMAC) and the frequency of Mid-air Collision (MAC). In both cases of CD&R, a reduction of NMAC for more than 94% is demonstrated in the entire density points.

The results are then scaled to calculate the maximum number of UAVs that can be operated in a realistic density. It is suggested that by using the implicitly coordinated CD&R, it is safe to fly a little more than 50 UAVs in one level of altitude above the large city such as New York Metro or Tokyo. The application of layered airspace can increase the number up to 800 UAVs. The number can be even higher with a more advanced and mature CD&R system.

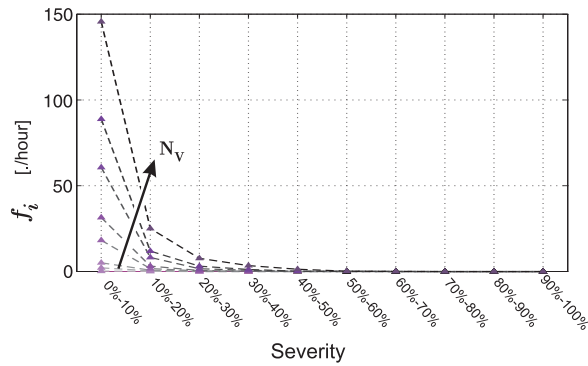
Many improvements of the high density Monte Carlo simulation can be conducted in future research. This includes extending the concept into three dimensions, adding more layers of flight level, or mixing the airspace with manned-flight that has higher pri-



(a)



(b)



(c)

Figure 3.10: Intrusion frequency for each zone of NMAC radius, (a) for no CD&R (case 1), (b) for uncoordinated CD&R (case 2), and (c) for implicitly coordinated CD&R (case 3)

ority. The frequency of actual mid-air collision, the MACs, under the influence of CD&R, which in the end cannot be determined by the simulations, is probably the main item to

be refine in this research safety assessment method. Nevertheless, the proposed method is a versatile method that can provide a solid safety parameter of various types CD&R system, which is essential in supporting UAVs integration into the airspace system.



# 4

## IMPLICITLY COORDINATED TACTICAL MANEUVER FOR AVOIDANCE

*The results reminds me of  
Feymann's research..*

Cornelis C. de Visser

*Starting from this chapter, the fourth research question is assessed, defining methods for UAV to handle potential conflicts autonomously, as part of traffic in the airspace system. This chapter present a novel method, named the Selective Velocity Obstacle method, that is designed to handle the encounter situation in the Cooperative Layer, a part of the architecture proposed in Chapter 2. In Section 4.2, after a brief introduction, the method framework for the encounter situations is presented. The performance of the method is demonstrated afterwards in section 4.3, along with a validation using the same methodology explained in Chapter 3 previously. Parts of this chapter's methodologies, such as the VO-method criteria extension, strategy, and critical turning-rate derivation, are also used in the following Chapter 5.*

---

|                     |  |
|---------------------|--|
| <b>Paper Title</b>  | Selective Velocity Obstacle Method for Deconflicting Maneuver Applied to Unmanned Aerial Vehicles  |
| <b>Authors</b>      | Yazdi I. Jenie, Erik-Jan van Kampen, Cornelis C de Visser, Joost Ellerbroek, and Jacco M. Hoekstra |
| <b>Published in</b> | The AIAA Journal of Guidance, Control, and Dynamics, 2015  |

## 4.1. INTRODUCTION

CURRENTLY, Unmanned Aerial Vehicle (UAV) technology is advancing into everyday applications and, as a result, concern has arisen on the safety of their operations in the civil airspace [7]. One of the main problems is the autonomous avoidance of mid-air collisions with other UAVs, which has driven many studies to develop various algorithms for a collision avoidance system.

For civil UAV avoidance, the Geometric Guidance algorithms are potentially best suited since they do not need to conduct extensive predictions and analyses, which require large computational resources on-board. Instead, they give solutions reactively based on the instantaneous geometry of an imminent conflict. Examples of Geometric Guidance include the Collision Cone [108, 109], the Velocity Obstacle Method (VO-method) [22–24, 26, 74, 110], the Minimum Effort Guidance (MEG) [111], and the Differential Geometric Guidance [112].

Most of those studies, however, neglect the situation in a controlled airspace where the UAVs are heterogeneous, each with its own mission and preference for avoidance. Furthermore, there might be various procedures and rules enforced by the authorities to manage the airspace. Several existing methods that consider those kinds of situations are commonly predictive methods, for instance the Airborne Collision Avoidance System X (ACAS X) [8], or the Jointly Optimal Conflict Avoidance (JOCA) [113].

This paper proposes a novel method for UAV-to-UAV autonomous collision avoidance called the Selective Velocity Obstacle method (SVO). The method is an extension of the former Velocity Obstacle method [22] that is designed to reactively generate an avoidance maneuver based on conflict geometry. The maneuver generated from the SVO is a deconflict maneuver, a tactical maneuver that aims to avoid obstacles while limiting the deviation from the original route. Following the avoidance system architecture presented in Ref. [88] and [103], the maneuver can start anywhere within a particular zone called the deconflict-zone, as shown in figure 4.1. The zones in the figure can also represent the layers of safety that use deconflict maneuvers in the architecture presented in Ref. [114]. The conflict cases for SVO are set to be heterogeneous, involving vehicles with different characteristics and missions. To comply with the vision of the European Commission for Unmanned Aerial System (UAS) [115], all of the avoidance in SVO is implicitly coordinated by incorporating the right-of-way rules [86], which also reduce the complexity of solution for heterogeneous conflicts.

Elaborated in Section II, the conflict situations in the airspace, which includes the heterogeneity and the rules based coordination, are modeled in the Velocity Obstacle framework. A few problems in the previous method are identified and solved throughout this section. Several simulations are presented in Section III to demonstrate the performance of the method, along with a validation using Monte Carlo simulations. This is then followed by the conclusions in Section IV.

## 4.2. SELECTIVE VELOCITY OBSTACLE METHOD FOR UAV COLLISION AVOIDANCE

Figure 4.2 shows an example of a two-dimensional encounter situation between two UAVs, referred to as the own-ship and the obstacle. The own-ship must first decide

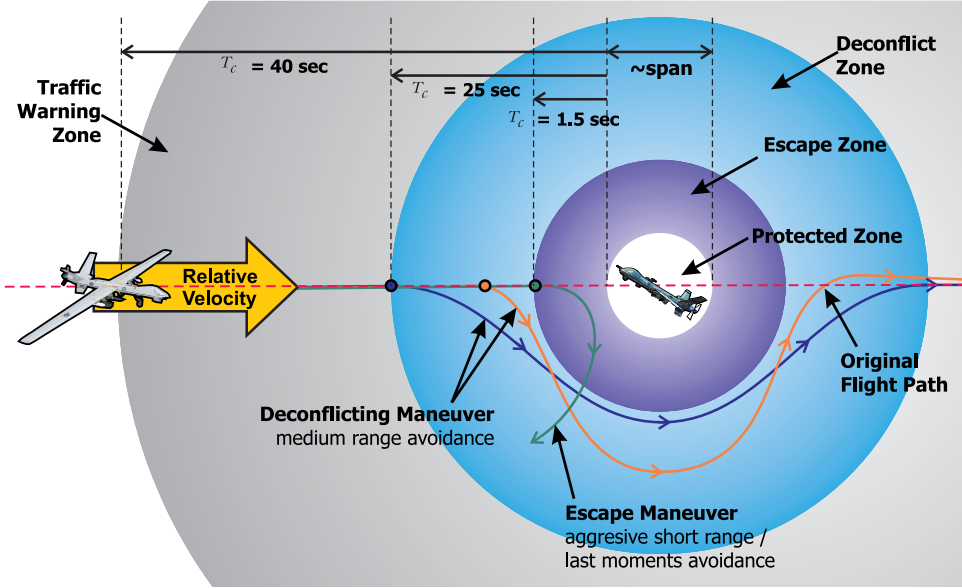


Figure 4.1: Architecture of collision avoidance for UAVs, adapted from Ref.[88] and [103].

whether or not a situation is a conflict and, if necessary, conduct any appropriate resolution maneuver. In this case, the conflict is defined when the own-ship is predicted to violate the escape-zone,  $S_{esc}$ , a circle with radius of  $r_{esc}$  from the center of the obstacle.

#### 4.2.1. ORIGINAL CONCEPT OF THE VELOCITY OBSTACLE METHOD

The concept of the original Velocity Obstacle method (OVO) presented in this section is adapted from Ref. [22]. In figure 4.2, the Collision-cone,  $CC_{oi}$ , is generated from an instantaneous situation by collecting relative velocity extensions,  $\lambda_{V_R}$ , that cut through the  $S_{esc}$ . The Velocity Obstacle set,  $VO_{oi}$ , is the translation of the  $CC_{oi}$  along the shadow of the obstacle velocity,  $V_i'$ . The OVO uses this  $VO_{oi}$  set to determine the conflict: The own-ship will violate the  $S_{esc}$  at some time in the future if and only if  $V_o \in VO_{oi}$ . The method also determines whether the two vehicles are diverging or not, with the use of the diverging set,  $DIV_{oi}$ : The own-ship is diverging the obstacle if and only if  $V_o \in DIV_{oi}$ . The two determinations are made under the assumption that both velocities  $V_o$  and  $V_i$  are constant.

An avoidance maneuver is conducted whenever  $V_o \in VO_{oi}$ , by updating the  $V_o$  to a new velocity that is outside the  $VO_{oi}$  set. The common strategy is to choose the closest point from the current  $V_o$  on one of the  $VO_{oi}$  edges. this point is marked with small circle  $V_{avo}$  in figure 4.2. As soon as the  $V_o$  is updated and falls outside the Velocity Obstacle set, i.e.,  $V_o \notin VO_{oi}$ , then the vehicle can be directed back to its original goal. The entire algorithm is started when an encounter is imminent, that is, when the distance of the obstacle is less than or equal to a predefined avoidance distance,  $d_{avo}$ .

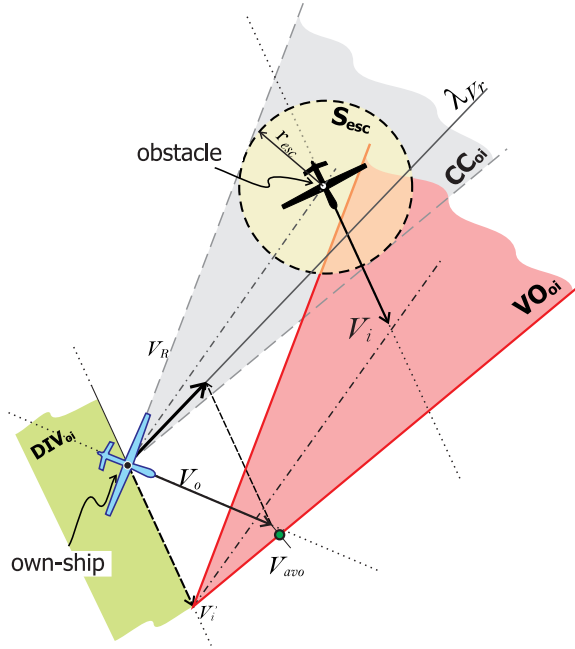


Figure 4.2: Velocity-obstacle set generation from an instantaneous encounter situation, adapted from Ref.[22].

In cases of multiple encounters, in which more than one encounter is imminent, the global velocity-obstacle set,  $VO_o$ , and the global diverging set,  $DIV_o$ , need to be derived. The  $VO_o$  is simply the union of all the  $VO_{oi}$  sets of each obstacle- $i$ , whereas the  $DIV_o$  is the intersection of all the  $DIV_{oi}$  sets.

#### 4.2.2. INCORPORATING THE RIGHT-OF-WAY RULES

If only one of the two conflicting vehicles is required to avoid, the OVO gives a good resolution with a small Closest Point of Approach (CPA) from the obstacle. However, in reciprocative cases where both vehicles are avoiding, several problems will arise, e.g., the reciprocating dance, as stated in Ref.[26].

In manned-flight, the reciprocative problems are prevented explicitly by coordinating the maneuvers using directives from an Air Traffic Control station, or implicitly by incorporating the right-of-way rules. The Selective Velocity Obstacle method (SVO) uses the latter approach and incorporates rules into its algorithm, which are the Visual Flight Rules[86], presented in figure 4.3. The SVO assumes that, in a conflict situation, all vehicles having the right-of-way will stay on their current path and all that do not will conduct an avoidance maneuver.

Thus, there are five ways an own-ship can encounter an obstacle, i.e., right-converging, left-converging, head-on, taking-over, or being taken over. The first and the last will make an own-ship obtain the right-of-way (**RoW**), while others will make it lose the right-of-way (**~RoW**). The type of encounter can be determined by checking the inclusion of the  $VO_{oi}$  origin in one of the five additional sets, shown in figure 4.4-b. The four

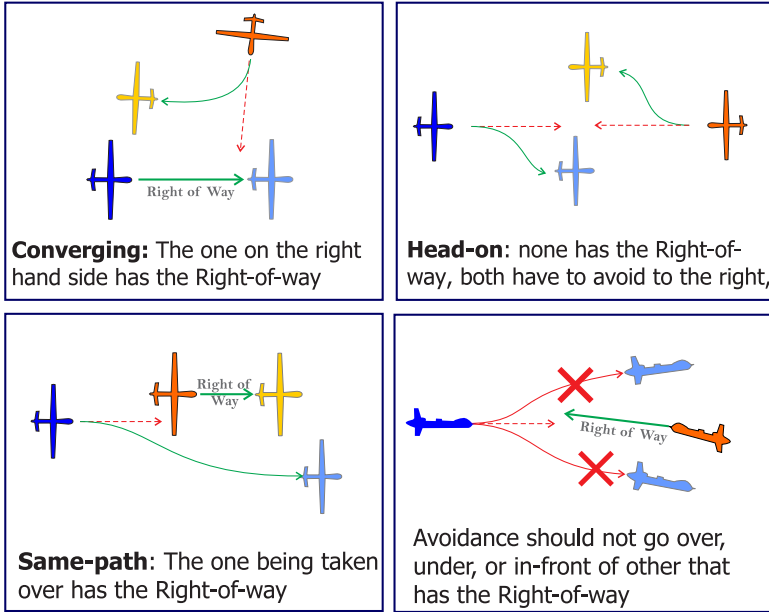


Figure 4.3: The right-of-way rules definitions, adapted from Ref.[86]

sectors,  $S_{R1}$ ,  $S_{R2}$ ,  $S_{R3}$ , and  $S_{R4}$ , are generated with regard to the own-ship's track, the  $X_w - Y_w$  axis, with offsets taken from Ref. [116], as shown in figure 4.4-a. The last set, the  $S_{V_o}$ , is a circle with radius of  $|V_o|$ . Lemma 1 elaborates how these sets are used.

**Lemma 1** *In an encounter situation between the own-ship and an obstacle- $i$ , if  $V_o \in VO_{oi}$ , then,*

1. *Whether the own-ship is in a conflict with the obstacle in the same path, converging from left, head-on, or converging from right, can be determined by the inclusion of the origin point of  $VO_{oi}$ , or the  $V'_i$ , within the set of  $S_{R1}$ ,  $S_{R2}$ ,  $S_{R3}$ , or  $S_{R4}$ , respectively.*
2. *In case of  $V'_i \in S_{R1}$ , whether the obstacle is taking-over or being taken-over by the own-ship can be determined by the inclusion or exclusion of the origin point of  $VO_{oi}$  from the  $S_{V_o}$  set.*

Ambiguous situations might occur if the  $V'_i$  lies exactly on an edge between sets. Hence, a convention is used that determines the types in the following order of priority: head-on, converging, and same-path.

### 4.2.3. AVOIDANCE ALGORITHM AND THE MINIMUM AVOIDANCE TURNING-RATE

Different from previous variations of the VO-method, the SVO algorithm uses three modes to generate the maneuver, i.e., turn, maintain, and mission, as shown in figure 4.5. The turn-mode is set to comply with the right-of-way rules that prefer lateral avoidance to

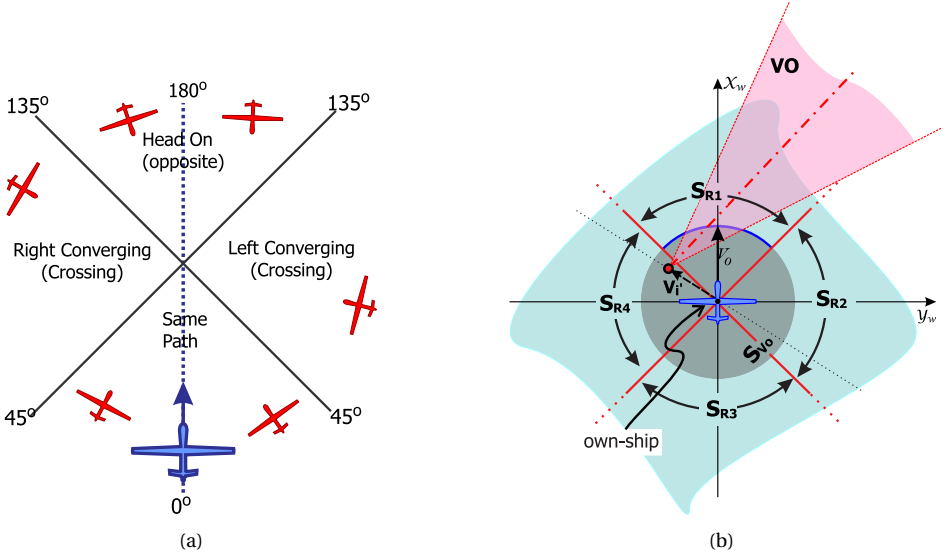


Figure 4.4: (a) Encounter type definitions, adopted from Ref.[116] (b) SVO additional set definitions

the right and, for simplification, it is limited to turn only without speed alteration. In this mode, the  $V_o$  is updated by applying the avoidance-turning-rate,  $\omega_{avo}$ , instead of point-to-point discrete updates used in the previous VO-methods. The maintain-mode is introduced to keep the own-ship at its current velocity when it has the right-of-way or when  $V_o \notin VO_{oi}$  even though the encounter is imminent. This mode is especially used to suppress the oscillation problem in OVO[26], that is, when the  $V_o$  changes frequently, going back and forth to outside and inside the  $VO_{oi}$ . The mission-mode is activated when the conflict is cleared, directing the vehicle back to the original goal. The state of the vehicle is initiated also from this mode.

Two parameters that need to be defined for the algorithm to work are the avoidance distance,  $d_{avo}$ , and the avoidance-turning-rate,  $\omega_{avo}$ . To model the heterogeneous situation, each involved vehicle can freely choose their own preference for those parameters. The minimum limit of  $\omega_{avo}$  is defined in order to ensure safety. Denoted as  $\omega_{a.min}$ , the minimum limit of the avoidance-turning-rate is a function of the variables of the encounter-geometry. In the SVO method framework, the geometry includes the speeds ( $|V_o|$ ,  $|V_i|$ ), the initial headings ( $\psi_o$ ,  $\psi_i$ ), and the avoidance starting point ( $d_{avo}$ ), as shown in figure 4.6. The kinematic equations for the own-ship, by setting the obstacle relative position as the fixed origin, are described in the relative velocity  $V_{R_x}(t)$  and  $V_{R_y}(t)$ , and their integrals within an interval of time,  $X_R(t)$  and  $Y_R(t)$ , in equation (4.1) and (4.2).

$$\begin{aligned} V_{R_x}(t) &= |V_o| \cos(\psi_o + \omega_{avo}t) - |V_i| \cos(\psi_i) \\ V_{R_y}(t) &= |V_o| \sin(\psi_o + \omega_{avo}t) - |V_i| \sin(\psi_i) \end{aligned} \quad (4.1)$$

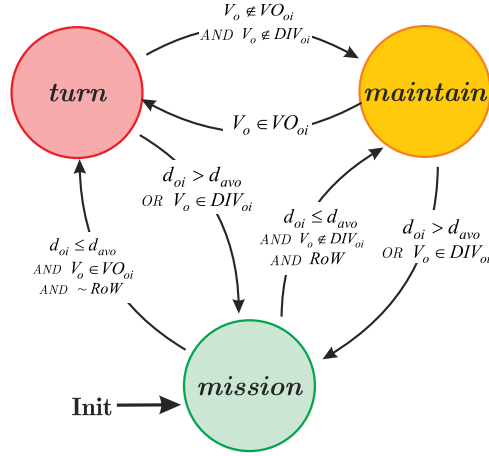


Figure 4.5: State diagram of the Selective Velocity Obstacle algorithm

$$\begin{aligned} x_R(t) &= \frac{|V_o|}{\omega_{avo}} \sin(\psi_o + \omega_{avo}t) - |V_i|t \cos(\psi_i) - d_{avo} \\ y_R(t) &= -\frac{|V_o|}{\omega_{avo}} \cos(\psi_o + \omega_{avo}t) - |V_i|t \sin(\psi_i) \end{aligned} \quad (4.2)$$

Applying a turning rate,  $\omega_{avo}$ , from  $t = 0$ , or point-1 in figure 4.6, will change the direction of  $V_o$ , without changing the  $V_i$ . It can be observed that the own-ship is using the minimum turning rate  $\omega_{a.min}$ , if it avoids by grazing the edge of the  $S_{esc}$ , as shown at point-2 in the figure. The boundary conditions for this kind of avoidance are described in equation (4.3) and (4.4). The former is the relative distance that should be equal to the  $r_{esc}$ . The latter describes the grazing situation in which the vector of the relative velocity is equal to the tangent line of  $S_{esc}$  at the point where the own-ship touches. Hence, the vector of the relative velocity should be perpendicular to the line from the origin to point-2.

$$\sqrt{x_R(t)^2 + y_R(t)^2} = r_{sep} \quad (4.3)$$

$$\left| \frac{V_{Ry}(t)}{V_{Rx}(t)} \right| = \left| -\frac{x_R(t)}{y_R(t)} \right| \quad (4.4)$$

In this paper,  $\omega_{a.min}$  is derived by iterating the value of  $\omega_{avo}$  in the relative position equation (4.2), with a random sample of the initial conditions  $|V_o|$ ,  $|V_i|$ ,  $\psi_o$ ,  $\psi_i$ , and  $d_{avo}$ . Starting with a small value of  $\omega_{avo} = 0.01$  degrees/second, the relative positions are solved discretely from  $t_0 = 0$ , until the own-ship violates the  $S_{esc}$  or until the right side of equation (4.4) is greater than the left. The process is repeated with increased value of  $\omega_{avo}$  by 0.01 degrees/second. The iteration continues until no violation occurs when equation (4.4) is fulfilled. Hence the  $\omega_{avo}$  at the end of the iteration is the minimum turning rate,  $\omega_{a.min}$ , for the particular sample.

The  $\omega_{a.min}$  value is derived in this research for a thousand randomly selected sets of conflicting initial conditions, ranging in speed from 8 to 13 meters/second, and in

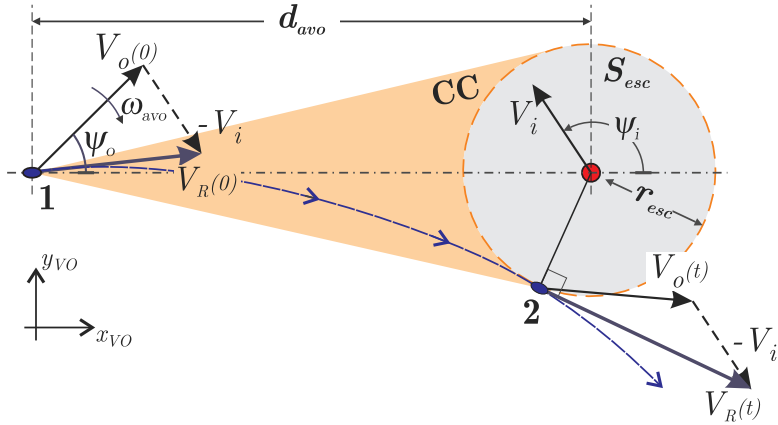


Figure 4.6: An example of a deconflict maneuver with minimum avoidance turning rate.

avoidance distance from 50 to 700 meters. These are the ranges for UAVs in category I, the Small-slow UAVs, described in Ref.[103]. Figure 4.7 maps these results along the corresponding  $d_{avo}$ . The map shows a clear boundary of the safe  $\omega_{a,min}$  for any encounter geometry at a particular  $d_{avo}$ . This boundary is defined as the recommended minimum turning rate, denoted in this paper as  $\omega_{a,min}^*$ . It should be noted that different ranges of initial conditions will result in different maps of  $\omega_{avo}$  and  $\omega_{avo}^*$ .

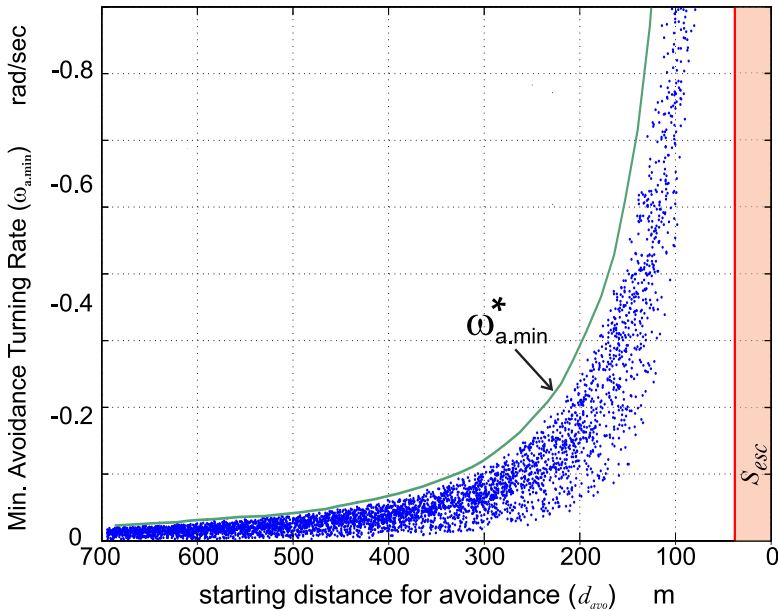


Figure 4.7: Map of  $\omega_{a,min}$  from sets of initial conditions, along the corresponding  $d_{avo}$

Table 4.1: Ranges of parameters for UAVs in category I (Small-Slow UAV)[103].

| Parameter                     | Range                  | Unit    |
|-------------------------------|------------------------|---------|
| Speed, $ V $                  | 8 - 13                 | [ m/s ] |
| Turning rates, $\omega_{avo}$ | $\omega_{a.min}^* - 5$ | [deg/s] |
| Distance to avoid             | 50 - 700               | [m]     |

### 4.3. IMPLEMENTATION

To evaluate the SVO method, a MATLAB program has been developed. It simulates multiple vehicles, each embedded with an avoidance system that is based on the SVO-method algorithm. The simulated vehicles are assumed to exchange their flight-data among each other, such as by using the Automatic Dependent Surveillance Broadcast (ADS-B), without delays or losses. The simulation limits both conflict and motion of the vehicle in the 2-dimensional plane.

#### 4.3.1. SIMULATION SETUP

The simulation presented in this section shows encounters of UAVs from category I; the Small-slow UAVs, which is based on the work in Ref. [103]. The value of speeds, turning rates and distances to start avoidance, are randomized within the ranges specified in table 4.1. The avoidance maneuver thus starts at an arbitrary point of  $d_{avo}$ , which is within the deconflicting-zone, 50 to 700 meters from the obstacle. The objective of the avoidance is to prevent violation into the escape-zone  $S_{esc}$ , which is a circle of radius  $r_{esc} = 50$  meters centered on the obstacle.

Simulations are conducted for the converging, head-on, and same-path encounters. In all cases, the initial parameters are varied randomly within the ranges listed in table 4.1. The results are presented using time-captures from a top-down point-of-view, as shown in figure 4.8 and figures 4.12 - 4.14. Each circle in those figures represents the half-radius of the  $S_{esc}$ . The used half-radius for the circle conserves the visualization of the separation, such that when two circles touch, the vehicles are on the edge of each other's escape-zone.

#### 4.3.2. RESULTS

Figure 4.8 depicts a simple converging case of two homogeneous agents. This first simulation shows a deconflict maneuver from a randomly chosen starting point, by applying an avoidance-turning-rate of 5 degrees/second, well above the  $\omega_{a.min}^*$  recommended for that distance (refer to figure 4.7). Figure 4.9 shows the comparison of avoidance path profiles between three values of  $\omega_{avo}$ , i.e.,  $5^\circ/s$ , the recommended minimum avoidance turning rate  $\omega_{a.min}^* = 1.71^\circ/s$ , and the true minimum avoidance turning rate  $\omega_{a.min} = 0.292^\circ/s$ . The path profiles for using OVO with  $\omega_{avo} = 5^\circ/s$  is shown as well for comparison. Figure 4.10 shows the comparison of the distance between vehicles showing that the deviation and the CPA are reduced as the turning rate gets slower. The use of the  $\omega_{a.min} = 0.292^\circ/s$ , specifically derived for the initial condition of the case, results in the subtlest deconflict maneuver in SVO, resulting zero distance of CPA. The short

maintain-mode line in the heading profile in figure 4.11 indicates that the  $V_o$  escapes the  $VO_{oi}$  set only at the last moment before violation. The fact that this line is not zero, however, indicates a delay in restoring to the mission-mode.

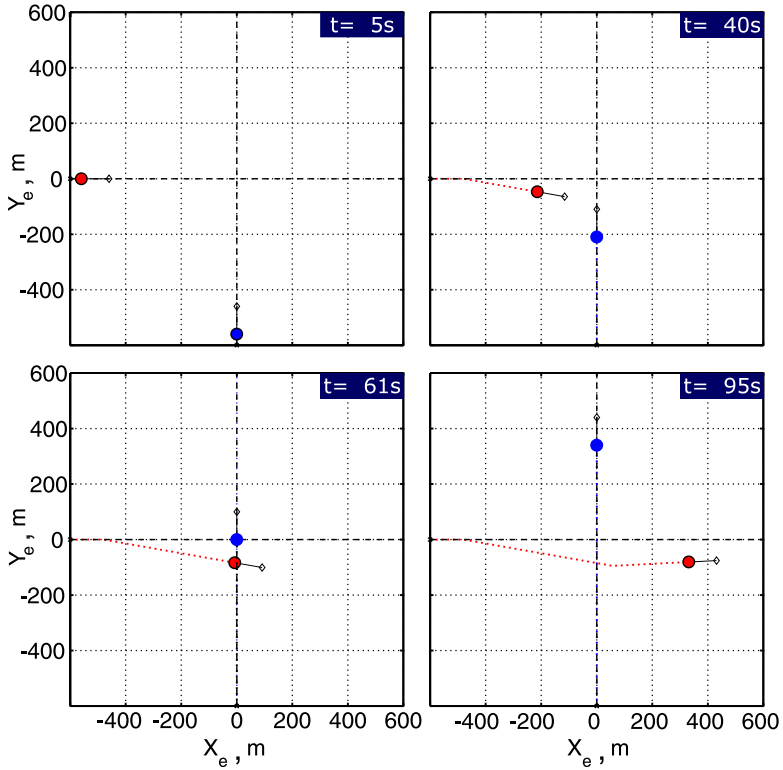


Figure 4.8: Simulation of converging encounters and the avoidance solutions using SVO

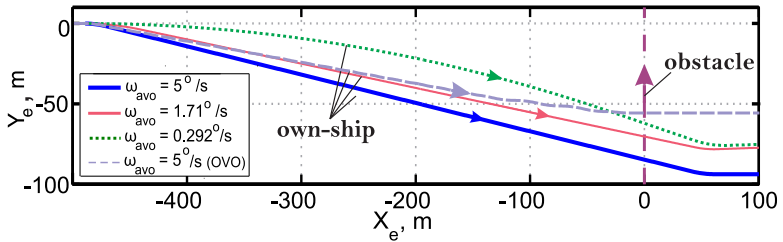


Figure 4.9: Comparison of deconflict paths resulting from different  $\omega_{avo}$ , for the case shown in Figure 4.8.

Figure 4.9, 4.10, and 4.11 also show the results of using OVO with  $\omega_{avo} = 5^\circ/s$ . The  $V_o$  tendency to oscillate in OVO is shown clearly in figure 4.11, which affected the path of the own-ship. This oscillation can enforced large avoidance turning rate to avoid with

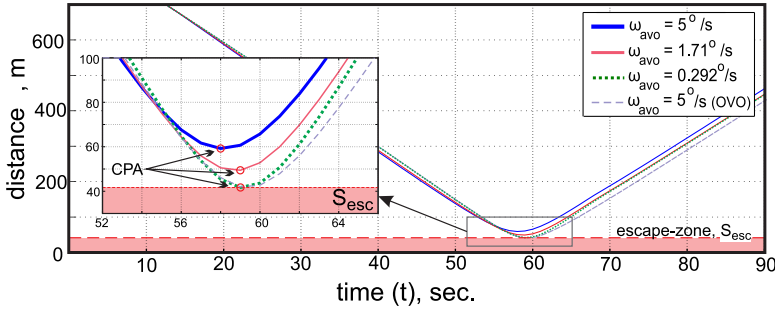


Figure 4.10: Comparison of distances between the pair of vehicles resulting from different  $\omega_{avo}$ , for the case shown in Figure 4.8.

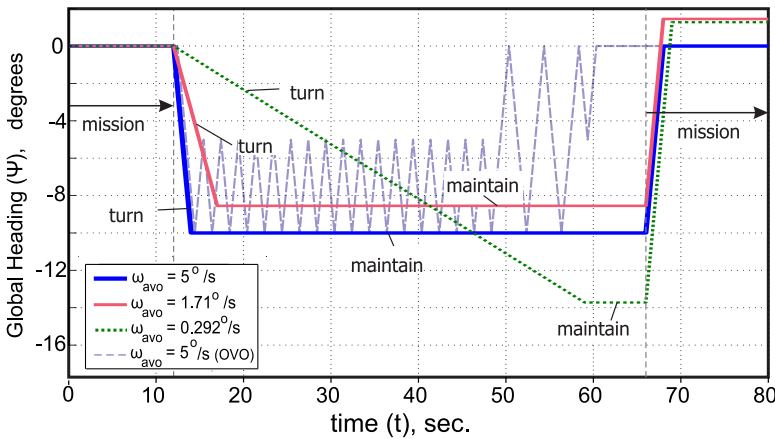


Figure 4.11: Comparison of Heading time-responses resulting from different  $\omega_{avo}$ , for the case shown in Figure 4.8.

zero distance of CPA, but the avoidance will be inefficient since the heading changes frequently. Figure 4.9 shows that the SVO can almost match the flight path of OVO using  $\omega_{a.min}^*$ , without any oscillation. The total path deviation using SVO, however, is larger since the own-ship has to wait in maintain-mode for a while for extra safety, that is, until the  $V_o$  is diverging or until the encounter is not imminent anymore.

Figure 4.12 shows a case of heterogeneous multiple encounters. The use of SVO results in different magnitudes of deviation from the corresponding original path. Two of the vehicles even stay exactly on their original path. This simulation also shows the problem with delay in switching to mission-mode in the algorithm that keeps vehicles from restoring their path, even after the CPA is passed. This problem comes from the definition of the  $DIV_{oi}$  set, which collects diverging velocities from the entire obstacle flight-path, including the part that has been passed. For instance, as shown in figure 4.12, the last path  $A_5$  has to cross belongs to  $A_7$ , instead of  $A_8$ , the last vehicle it cleared. Redefinition of the diverging set is required to eliminate this problem.

Figure 4.13 and 4.14 also show successful deconflict maneuvers in head-on and same-

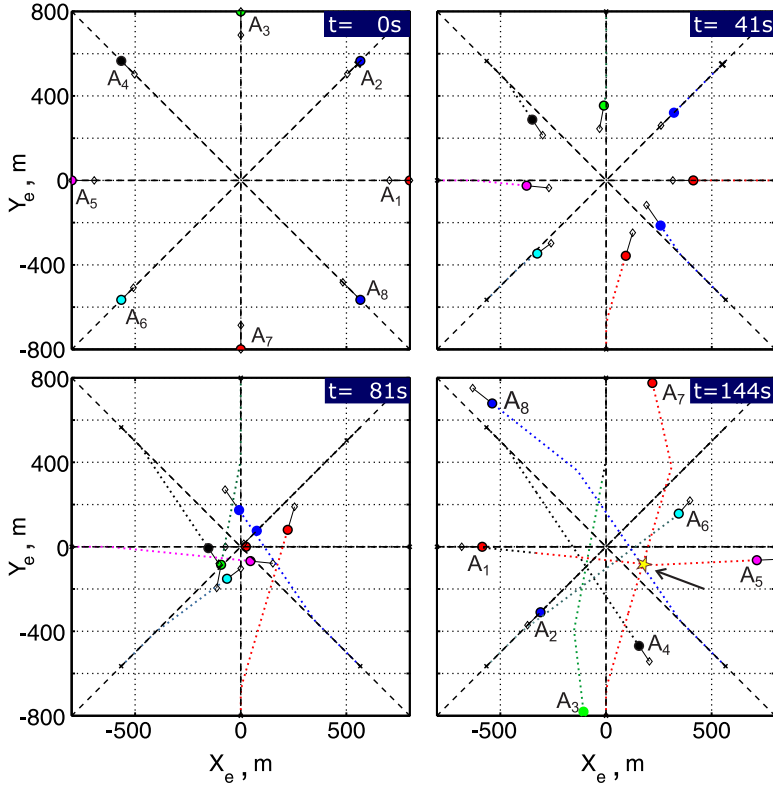


Figure 4.12: Simulation of converging encounters and the avoidance solutions using SVO

path encounters. The entire avoidance maneuver complies with the right-of-way rules. The result in figure 4.13 reveals that multiple head-on encounters will always be mixed with same-path encounters, since the vehicles on the right side are in a same-path situation first. In this case,  $A_3$  tries to take over  $A_2$  first before it starts to avoid  $A_1$ .  $A_2$  tries to avoid a head-on collision with  $A_1$  early, while  $A_4$  waits until almost the last moment.  $A_4$  deviation becomes large since it has to avoid  $A_3$  as well, before it can restore its path.

#### 4.3.3. VALIDATION

The SVO-method is validated using Monte Carlo simulations with random initial condition setup across the simulation, within the ranges specified in table 4.1. The simulations involve two to five vehicles that are randomly directed and positioned. Initially, all vehicles are positioned outside each other's deconflict-zone, within a square area that is proportional to the number of vehicles, i.e.,  $(N \times 1000)^2$  meter-square. These random scenario generations act as replacements for the lack of operational data and models, the two sources of scenarios that are commonly used in TCAS validation[8]. The violation probability,  $P_{vio}$ , is defined in equation (4.5), i.e.,

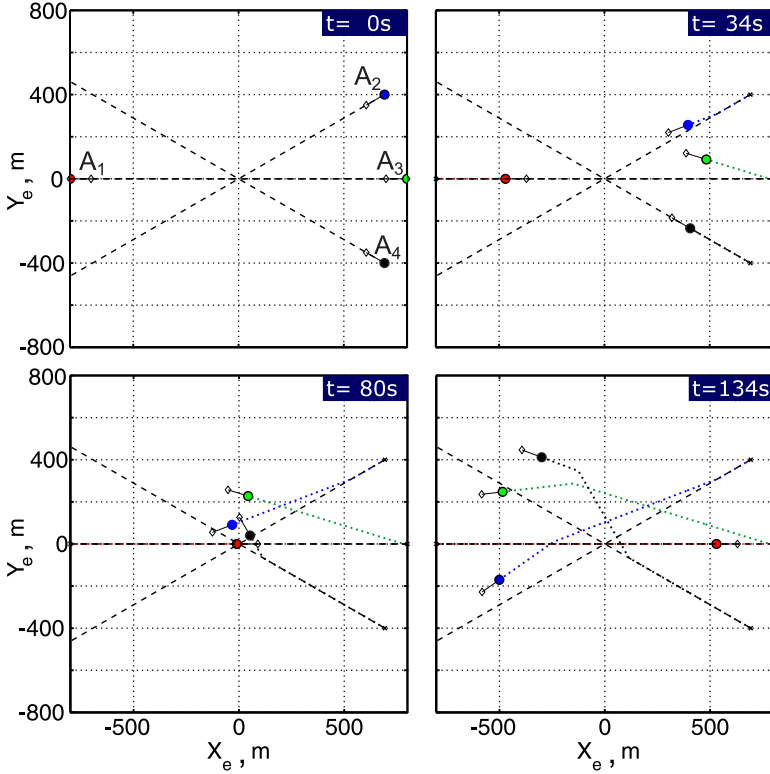


Figure 4.13: Simulation of head-on encounters and the avoidance solutions using SVO

$$P_{vio} = \frac{N_{vio}}{N_{MC}} \quad (4.5)$$

The  $N_{vio}$  is the number of violation occurred and  $N_{MC}$  is the number of the total Monte Carlo samples, which is at least  $10^6$  samples. For comparison, this probability is derived for cases without avoidance, with OVO avoidance, and with SVO avoidance, as shown in table 5.2. The OVO in this case uses a large turning rate of  $5^\circ/s$  with a randomly generated direction, i.e., to the left or to the right.

From the result for cases without any avoidance, it can be concluded that the probability of conflict will always exist and gets higher with the number of vehicles involved, even if the area of interest is widened proportionally. The OVO is able to suppress the number of violations into almost one-hundred time smaller. Some failed avoidances, however, still occur mainly contributed to the oscillation and the reciprocating dance problem[26]. The SVO is demonstrated to be able to resolve conflicts and avoidance problems, with zero violations in all samples of initial condition.

An interesting note is that all the conflicts across the samples are pairwise, i.e., only between two vehicles. In fact, it is hard to find a multiple-encounter situation, such as shown in figure 4.12, in a random setup, which suggest that the SVO only needs to

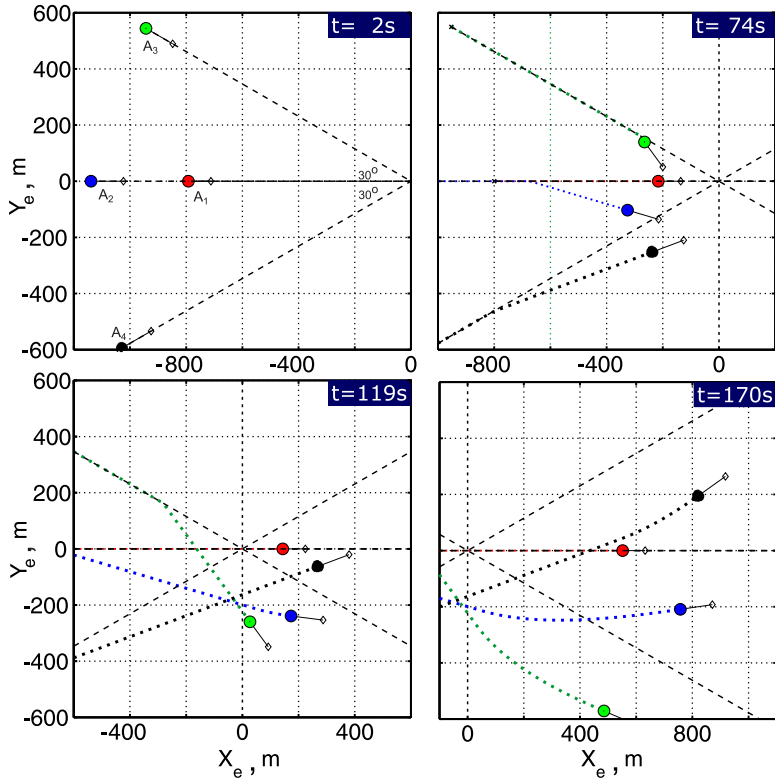


Figure 4.14: Simulation of same-path encounters and the avoidance solutions using SVO

resolve conflicts in a one-by-one manner. Therefore, the validation result is limited to single-encounters. Further analysis is required to determine the SVO validity in more stressful multiple-encounter condition.

Table 4.2: Violation probability in cases without avoidance, using the OVO, and using the SVO.

| Number of Vehicles | Probability of Violation |           |           |
|--------------------|--------------------------|-----------|-----------|
|                    | No Avoidance             | Using OVO | Using SVO |
| 2                  | 1.033 %                  | 0.01 %    | 0 %       |
| 3                  | 2.366 %                  | 0.029 %   | 0 %       |
| 4                  | 3.838 %                  | 0.046 %   | 0 %       |
| 5                  | 5.353 %                  | 0.056 %   | 0 %       |

#### 4.4. CONCLUSION

This paper elaborates the novel Selective Velocity Obstacle Method (SVO) that supports Unmanned Aerial Vehicle (UAV) autonomous collision avoidance. The SVO is shown to be able to generate deconflict maneuvers separately to resolve heterogeneous situations, while obeying the right-of-way rules, using a distance-based prescribed turning rate. Problems in the original Velocity Obstacle method (OVO) are resolved in SVO and validated through a Monte Carlo simulations procedure. The procedure also reveals that, in a random situation setup, multiple-encounters are very unlikely to happen and, hence, the SVO only needs to resolve conflicts in one-by-one manner. Several challenges in the method are noted, such as the late onset in restoring to the mission-mode. The method also does not consider a wide range of vehicle types, possible uncertainties in the exchanged data, and three-dimensional conflicts. The results, however, show that the SVO is a suitable method to reduce the risk of collision and, hence, increase the safety of UAV operations in the airspace system.



# 5

## UNCOORDINATED ESCAPE MANEUVER FOR AVOIDANCE

*He didn't even use 3D software,  
the drawing is actually 2D and  
the 3D is in his head ..*

Erik-jan van Kampen

*This chapter present the novel Three-Dimensional Velocity Obstacle method, designed to handle the encounter condition in the Escape Layer, one of the six layers of safety in the architecture proposed in Chapter 2. The method autonomously generate an escape maneuver without any coordination with the counterpart, exploiting the limited space left for a UAV in three-dimensional manner. Section 6.2 of this chapter presents the method framework for the three-dimensional encounter situations. The avoidance strategy is elaborated next in section 6.3, by introducing the concept of avoidance planes. Afterwards, several simulations are presented for validation, along with a validation of 3DVO performance using Monte Carlo simulation in a super-conflict situation.*

---

|                     |  |
|---------------------|--|
| <b>Paper Title</b>  | Three-Dimensional Velocity Obstacle Method for Uncoordinated Avoidance Maneuvers of Unmanned Aerial Vehicles |
| <b>Authors</b>      | Yazdi I. Jenie, Erik-Jan van Kampen, Cornelis C. de Visser, Joost Ellerbroek, and Jacco M. Hoekstra          |
| <b>Published in</b> | The AIAA Journal of Guidance, Control, and Dynamics, 2016  |

*This paper proposes a novel avoidance method called the Three-Dimensional Velocity Obstacle (3DVO) method. The method is designed for Unmanned Aerial Vehicle (UAV) applications, in particular to autonomously handle uncoordinated multiple encounters in an integrated airspace, by exploiting the limited space in a three-dimensional manner. The method is a three-dimensional extension of the Velocity Obstacle method that can reactively generate an avoidance maneuver by changing the vehicle velocity vector based on the encounter geometry. Adverse maneuvers of the obstacle are anticipated by introducing the concept of a buffer velocity set, which ensures that the ownship will diverge with sufficient space in case of sudden imminence. A three-dimensional resolution is generated by choosing the right plane for avoidance, in which the UAV conducts a pure turning maneuver. Implementation of the 3DVO method is tested in several simulations that demonstrate its capability to resolve various three-dimensional conflicts. A validation using Monte Carlo simulations is also conducted in stressful super-conflict scenarios, which results in zero collisions occurrences for the entire 25,000 samples.*

## 5

## 5.1. INTRODUCTION

FOR UNMANNED Aerial Vehicles (UAV) to be integrated into the airspace system, they are required to have an autonomous Conflict Detection and Resolution (CD&R) system that can demonstrate an adequate level of safety during its operation [7]. In this context, a UAV will encounter dynamic obstacles, such as manned aircraft and other UAVs, that can be negligent in avoidance, move in an unpredictable way, or actually seek a collision (hostile). These kinds of situations can only be detected independently by relying on sensors on-board, since the counterparts do not cooperatively broadcast their flight data and intention. As a result, the space for avoidance will be limited by the sensor range of detection. The resolution maneuver, therefore, needs to fully exploit the remaining space left, while anticipating the possible movement of those counterparts. To be able to reach safety as fast as possible, a resolution maneuver has to be aggressively conducted with the maximum performance of the UAV, comprehend several obstacles in the traffic at once, and neglect any original mission or trajectory. Ref.[114] describes this type of avoidance situation and resolution as an Escape CD&R approach

Reactive collision-avoidance methods are potentially the most suitable to support an escape maneuver autonomously. These methods rely on the instantaneous situation detection to quickly calculate the avoidance maneuver, instead of depending on predetermined data or extensive iteration that might be optimized, but processed slower, such as in Local Path Planning methods [17, 50] or Dynamic Programming [8]. Several reactive avoidance methods can be found in the literature, including the Potential Field method [34, 117–119], and Geometric guidance methods such as the Collision Cone [108, 120] or the Velocity Obstacle method [22–26, 64, 74, 75, 121–124]. Since they are less computationally intensive, these reactive methods are promising in providing a fast avoidance solution in a dynamic environment.

Most of those methods, however, include several simplifying assumptions that limit their practical use for an escape situation. Those assumptions include one or more of

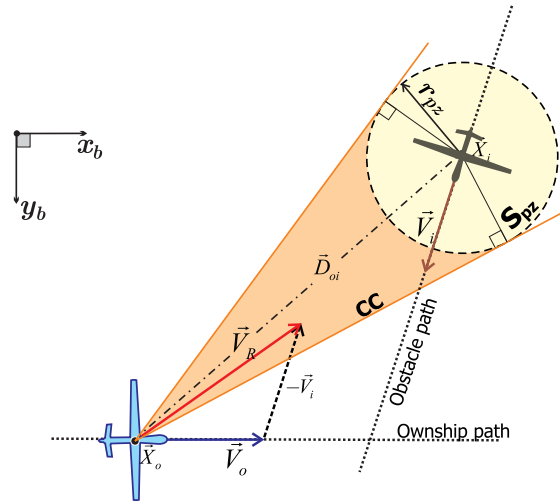
the following: generates resolutions only in two-dimensional space, involves only homogeneous vehicles, non-maneuvering obstacles, and only for a coordinated avoidance. The methods demonstrated in [120] and [125] are among the few that provide both encounter handling and resolution generation in three dimensions which are able to significantly expand the resolutions in a limited avoidance space. Those methods, however, are demonstrated only in handling static or non-maneuvering obstacles. The work of [23], [26], and [123] are examples that consider maneuvering obstacles, but in a homogeneous coordinated situation where the vehicles have uniform speeds and avoidance tendencies. The work of [75] presents a Selective Velocity Obstacle method that handles heterogeneous encounters, including the random maneuvers of obstacles, but the resolution is based on implicit coordination.

This paper contributes to the literature by proposing a novel reactive avoidance method called the Three-Dimensional Velocity Obstacle (3DVO) method. The method is designed to handle uncoordinated multiple encounters by exploiting the limited space as much as possible, in a three-dimensional manner. This concept is a continuation of the work originally reported in [126] by the same authors, presented here with a simpler but more complete formalization. Additional contribution of this current paper is the incorporation of the heterogeneous situation, which is evaluated in a simulation by randomizing initial speeds and turning-rates, to truly represent an escape situation[114]. The foundation of the 3DVO method is the Velocity Obstacle method[22, 108] (VO-method), which is selected due to several advantages it has compared to other reactive methods. For instance, compared to the basic Potential Field method (PF-method)[117], the VO-method was originally designed for avoiding moving obstacles by taking into account the velocity of each obstacle. The VO-method also gives a set of possible resolutions that is less prone to problems with local minimums in multiple encounter situations. Lastly, the VO-method has a more geometrically understandable appearance, which make its three-dimensional extension straightforward while keeping all its criteria and strategies.

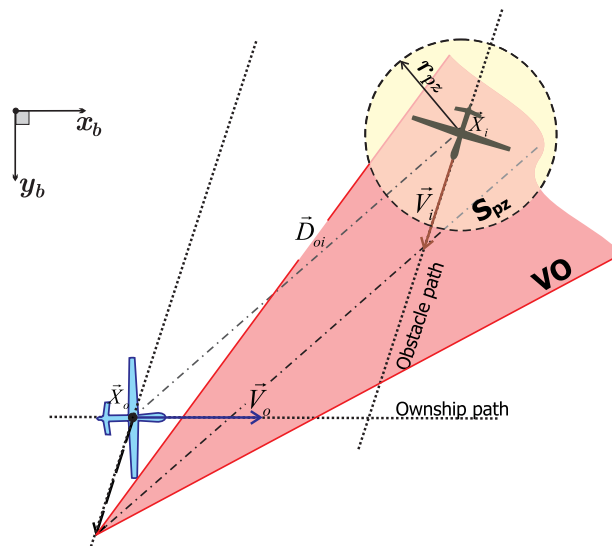
This paper is structured as follows. Section II discusses the concept of the 3DVO method by introducing the extension of the method into three-dimensions setup. The approaches to handle maneuvering obstacles are elaborated as well, along with the introduction of the Avoidance Planes concept. After that, Section III explains possible strategies for the 3DVO method, which include the avoidance algorithm, the decision process in choosing the Avoidance Plane, and the derivation of the avoidance turning rate. Section IV presents the implementation of the three-dimensional VO-method in several simulations, where the performance of the method is demonstrated. A validation process using Monte Carlo simulation is also conducted and presented in this section. Section V ends the paper with several concluding remarks.

## 5.2. THE THREE-DIMENSIONAL VELOCITY OBSTACLE METHOD

The Three-dimensional Velocity Obstacle (3DVO) method extends the use of the original VO-method[22, 75], which is applied in a two-dimensional encounter, such as shown in Figure 5.1-a. In every encounter case, a collision cone set (CC) can be drawn, which collects all relative velocity vectors between the vehicles that intersect the protected-zone ( $S_{pz}$ ): a threshold area around the obstacle. In cases of avoiding collision at a short distance, the value of  $S_{pz}$  radius,  $r_{pz}$  is typically the summation of the vehicles effective



(a)



(b)

Figure 5.1: Graphical presentation of (a) Collision Cone and (b) The Velocity Obstacle set

semi-spans. Whether the two vehicles are bound to collide or not, therefore, can be determined by the inclusion of their relative velocity  $\vec{V}_R$  to the CC. Hence to avoid collision, the ownship needs to ensure its velocity exclusion from the CC set.

The VO-method uses the inclusion of the ownship absolute velocity vector  $\vec{V}_o$  into the so-called Velocity Obstacle set (**VO**), which is the translation of **CC** along the velocity of the obstacle,  $\vec{V}_i$ , as shown in Figure 5.1-b. To avoid the obstacle, the ownship needs to change its velocity vector to a point outside the **VO**.

The VO-method extension into the 3DVO method includes the detection of three-dimensional conflicts, and the generation of possible avoiding routes that also exploit the three-dimensional space around the ownship. This section explains the detection part by converting the sets of the VO-method to a three-dimensional definition. The algorithm to reactively generate the avoiding routes, along with the strategy for avoidance, is explained in Section III.

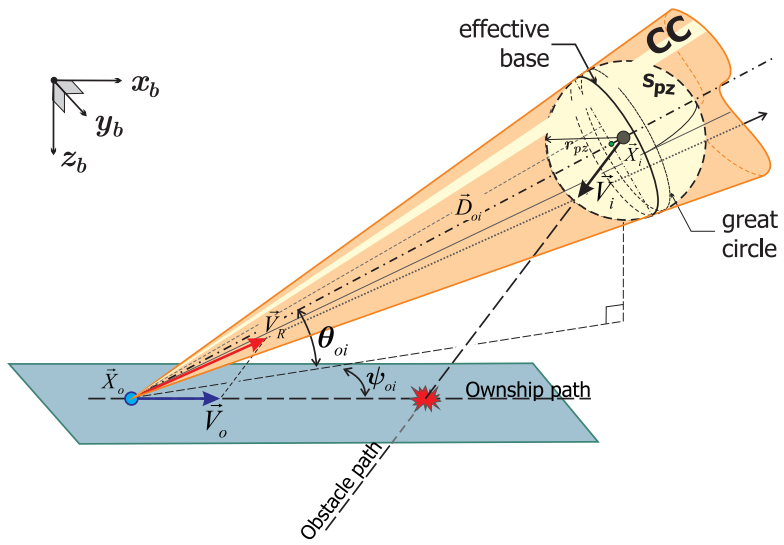
### 5.2.1. 3DVO METHOD'S VELOCITY OBSTACLE CONE

The concept of the VO-method is extended for three-dimensional cases by first redefining the protected zone,  $\mathbf{S}_{\text{pz}}$ , from a circle to a three-dimensional form. There are two types of  $\mathbf{S}_{\text{pz}}$  commonly found in the literature, either spherical[126, 127], or cylindrical[64, 123, 125]. This paper uses the spherical protected-zone definition that can represent general UAV encounters and resolutions better than a cylindrical in the three-dimensional space. The reason is that unlike manned aircraft, a UAV, especially of rotary-wing type, can have a much more flexible trajectory in any direction by exploiting the entire space around it, and hence it needs to consider collisions from any three-dimensional direction. A spherical protected zone in this case will treat encountering obstacles equally regardless of the direction and orientation.

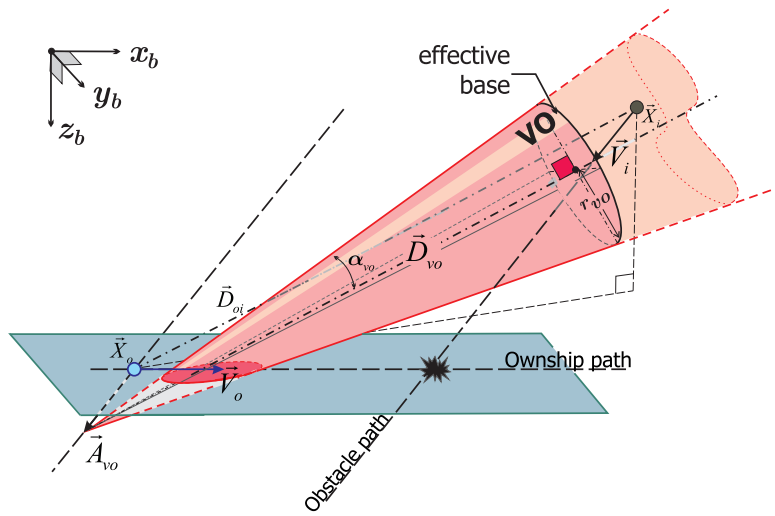
Consider a three-dimensional encounter case between an avoiding vehicle (or an ownship) and an obstacle, as depicted in figure 5.2. Similar to the two-dimensional case, the Collision Cone **CC** can be derived by collecting every relative velocity  $\vec{V}_R$  whose positive elongation intersects the  $\mathbf{S}_{\text{pz}}$  sphere. In this three-dimensional case, the **CC** takes the shape of an infinite right-cone with size and orientation corresponding to the dimension of  $\mathbf{S}_{\text{pz}}$  and the obstacle position  $\vec{X}_i$ , relative to the ownship. The apex of **CC** is the ownship position  $\vec{X}_o$ , where every tangential line from  $\vec{X}_o$  to the edge of  $\mathbf{S}_{\text{pz}}$  is a generating line of the cone (generatrix).

Similar to the two-dimensional case, the Velocity Obstacle set is obtained by translating the **CC** cone in three-dimensions along  $\vec{V}_i$  from  $\vec{X}_o$ , as shown in Figure 5.2-b. With this set, the collision criterion between two vehicles in three-dimensional space can be defined: an ownship will eventually collide if and only if its velocity vector  $\vec{V}_o$  is included in the corresponding **VO** cone, i.e.,  $\vec{V}_o \in \mathbf{VO}$ .

The three-dimensional **VO** can be defined using a cross-section perpendicular to the cone axis as an effective base. This paper uses the cross-section that is rimmed by the  $\mathbf{S}_{\text{pz}}$  intersection with the cone, as shown in Figure 5.2-a. Thus, the **VO** cone is defined by three parameters: the position of its apex,  $\vec{A}_{vo}$ , the length and orientation of the axis,  $\vec{D}_{vo}$ , and the radius of the effective base,  $r_{vo}$ . These parameters are mathematically expressed in equations (5.1) and (5.2) as functions of  $\mathbf{S}_{\text{pz}}$  radius and the obstacle position in spherical coordinates (distance  $d_{oi}$ , elevation  $\theta_{oi}$ , and azimuth  $\psi_{oi}$ ) with respect to the ownship frame of reference ( $\vec{X}_o$  as the origin). The cone opening angle,  $\alpha_{vo}$ , is also defined in equation (5.1). Note that the effective base of the cone does not coincide with the great-circle of  $\mathbf{S}_{\text{pz}}$ , as depicted in Figure 5.2-a.



(a)



(b)

Figure 5.2: Three-dimensional velocity obstacle set definition. (a) the Collision Cone  $CC$ , (b) Translated  $CC$  cone to the Velocity Obstacle set  $VO$

$$d_{vo} = \frac{d_{oi}^2 - r_{pz}^2}{d_{oi}}, \quad r_{vo} = r_{pz} \frac{\sqrt{d_{oi}^2 - r_{pz}^2}}{d_{oi}}, \quad \alpha_{vo} = \arctan\left(\frac{r_{vo}}{d_{vo}}\right) \quad (5.1)$$

$$\vec{A}_{vo} = \vec{V}_i, \quad \text{and} \quad \vec{D}_{vo} = \begin{bmatrix} \cos\theta_{oi} \cos\psi_{oi} \\ \cos\theta_{oi} \sin\psi_{oi} \\ \sin\theta_{oi} \end{bmatrix} d_{vo}. \quad (5.2)$$

The inclusion of the  $\vec{V}_o$  vector end point in the **VO** cone can be determined by checking the angle between the vector from the cone apex,  $\vec{A}_{vo}$ , and the cone axis. Equation (5.3) represents the criteria of inclusion using the vector inner product. The second term in equation (5.3) is to ensure the imminence of the encounter by the avoidance starting point,  $d_{avo}$ , since the first criterion is unbounded, representing the possible collision within infinite time in the future. Thus,

$$\vec{V}_o \in \mathbf{VO}_i \iff \left\{ \begin{array}{l} [\vec{V}_o - \vec{A}_{vo}] \cdot \vec{D}_{vo} > \cos\alpha_{vo} \quad \text{and} \quad d_{oi} < d_{avo} \\ |\vec{V}_o - \vec{A}_{vo}| d_{vo} \end{array} \right. \quad (5.3)$$

The **VO** cone expands as the two vehicles converge, and shrinks as they diverge. When the  $\alpha_{vo}$  reaches  $\pi/2$ , the ownship position is exactly on the surface of the protected zone  $\mathbf{S}_{pz}$ , or  $d_{oi} = r_{pz}$ , as indicated in equation (5.1). A singularity case happens when the two vehicles collide, or when  $d_{oi} < r_{pz}$ , in which case the **VO** cone cannot be defined.

Finally, multiple encounters are accommodated in the three-dimensional setup by taking the summation of the **VO** sets. Let  $i = 1, 2, 3, \dots, N$  be the indexes of  $N$ -imminent obstacles under consideration, then the overall **VO** for a multiple encounter case is the union of the Velocity Obstacle set, or  $\cup_i \mathbf{VO}_i$ . The ownship velocity vector is included in the overall set if it is included in at least one of the **VO**<sub>*i*</sub> or

$$\vec{V}_o \in \bigcup_i \mathbf{VO}_i \iff \exists i : \vec{V}_o \in \mathbf{VO}_i. \quad (5.4)$$

### 5.2.2. HANDLING MANEUVERING OBSTACLES: THE BUFFER VELOCITY SET

The challenges in using the VO-method in situations where the obstacles are maneuvering have been addressed in previous studies. The work of [24] describes the problem of oscillation and the reciprocal dance in cases of two-dimensional conflicts, where each of the vehicles attempts avoidance using the VO-method. These problems, which can cause a failed avoidance, are commonly solved using an implicit coordination of avoidance[26, 75, 123]. However, in an uncoordinated situation the problems reappear with an additional problem of a sudden imminence. This last problem occurs when a vehicle adversely changes its course in close proximity to another, such that there is no sufficient space or time left to conduct the sudden avoidance.

An extra set can be added to the Velocity Obstacle set in order to handle the possible maneuver of an obstacle. Consider the case shown in Figure 5.3-a. Within a certain time step, the ownship generates a **VO** set based on the instantaneous encounter geometry, and generates a resolution to avoid any corresponding conflicts. The time-step between

two **VO** generations, denoted  $\Delta t$ , is assumed to be constant and represents the detection frequency of the CD&R system. During this  $\Delta t$ , however, the obstacle might have updated its velocity vector, such as, for instance, by a rotational maneuver within the range of  $\vec{V}'_i$  to  $\vec{V}''_i$ . As shown in Figure 5.3-a, for each point on the arcs of  $\vec{V}_i$ , a new **VO** set can be defined, some of which might rule out the initially assumed safe zones.

If all possible maneuvers of the obstacle within the generation time  $\Delta t$  can be predicted, then they can be anticipated by summing all the possible **VO** sets into one big set. Figure 5.3-a shows this summation as a new triangle that originates at point  $A_{vo}^*$ , collecting all possible **VO** sets. The resulting triangular set, however, is not aligned with the axis of the original **VO**, and adds an extra degree of freedom for the combined **VO** definition, especially in three-dimensional cases.

Figure 5.3-b defines a simpler definition for the sums of **VOs** by using a circular reachable velocity set of the obstacle,  $\mathbf{RV}_i$ . This set collects every possible arc of  $\vec{V}_i$  within  $\Delta t$ , from any arbitrary bearing angle between vehicles separated by a particular distance. The resulting sum of **VO** can be defined by moving the apex in the opposite direction of the  $\vec{D}_{vo}$  until the entire  $\mathbf{RV}_i$  is included. This definition also holds in the three-dimensional setup, where the  $\mathbf{RV}_i$  is represented as a sphere as shown in the Figure 5.3-c. This paper denotes the extra layer of the **VO** as the Buffer Velocity set (**BV**). The combined resulting **VO**, denoted as the  $\mathbf{VO}^+$ , effectively takes into account the obstacle maneuver within the time-step of its generation,  $\Delta t$ .

The VO parameters in three dimensions are therefore redefined, as expressed in equation (5.5) and (5.6), i.e.,

$$\alpha_{vo^+} = \alpha_{vo}, \quad \vec{A}_{vo^+} = \vec{A}_{vo} - r_{rvi} \frac{\vec{D}_{vo}}{d_{vo} \sin \alpha_{vo^+}}. \quad (5.5)$$

The radius of the  $\mathbf{RV}_i$ ,  $r_{rvi}$ , depends on the assumed value of the change of heading of expected obstacles relative to the ownship, within the generation time-step,  $\omega_i \Delta t$ . The radius  $r_{rvi}$  can be derived using the cosines law on the isosceles triangle  $AX_oA'$  in Figure 5.3-b, as presented in equation (5.6). Note that in the triangle,  $X_oA = X_oA' = \vec{V}_i$ , and  $AA' = r_{rvi}$ . Hence,

$$r_{rvi} = |\vec{V}_i| \sqrt{2(1 - \cos(\omega_i \Delta t))}. \quad (5.6)$$

Equation (5.7) presents the  $\vec{V}_o$  inclusion criteria to the  $\mathbf{VO}^+$ . The inclusion into the **BV** zone in particular, can be derived by the subtraction of **VO** (equation (5.3)) from  $\mathbf{VO}^+$ .

$$\vec{V}_o \in \mathbf{VO}^+ \iff \left\{ \begin{array}{l} \frac{[\vec{V}_o - \vec{A}_{vo^+}] \cdot \vec{D}_{vo}}{|\vec{V}_o - \vec{A}_{vo^+}| d_{vo}} > \cos \alpha_{vo^+} \quad \text{and} \quad d_{oi} < d_{avo} \end{array} \right\} \quad (5.7)$$

For simplification, the plus (+) superscript, which indicates the addition of the **BV** set on the **VO**, is omitted in the remainder of this paper.

### 5.2.3. AVOIDANCE PLANES

Similar to the original VO-method, in order to avoid the obstacles, the ownship needs to update its velocity vector to a point outside every relevant **VO** set, into the set of the Avoidance Velocities,  $\vec{V}_{avo}$ . In the three-dimensional setup, these points of avoidance

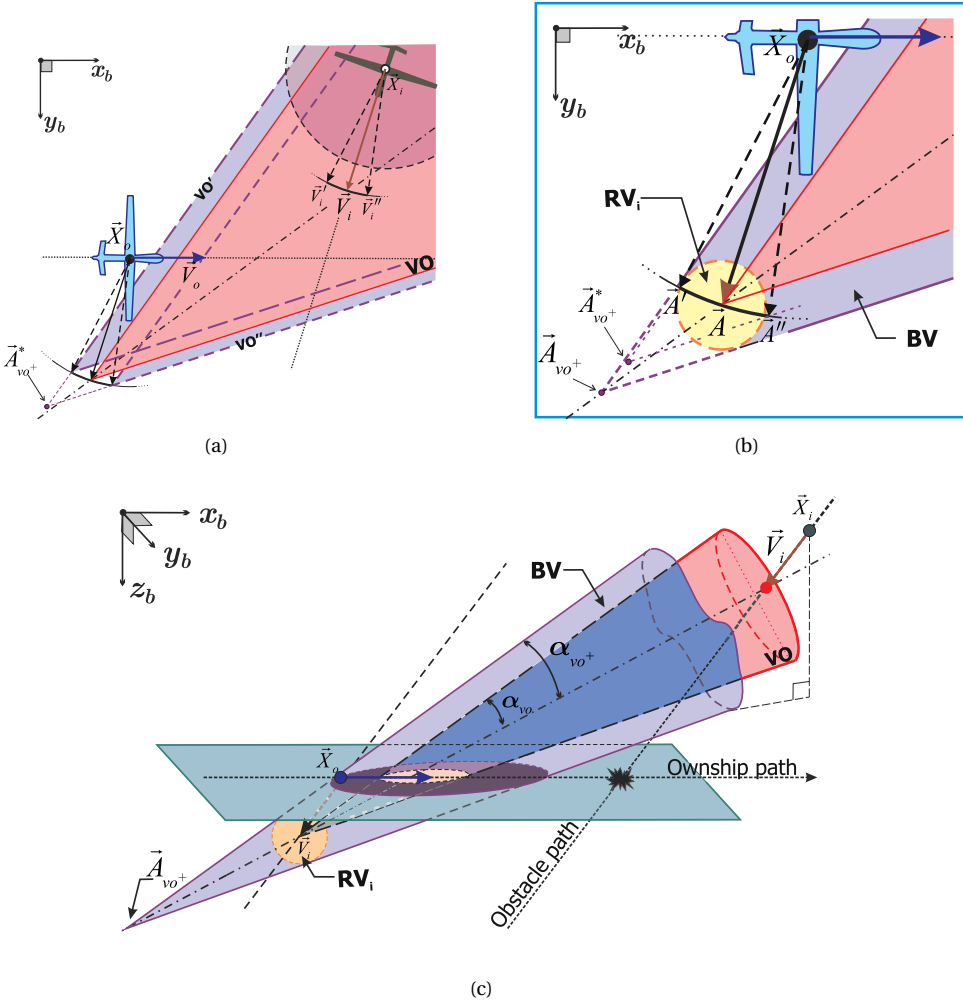


Figure 5.3: The Buffer Velocity set definition. (a) The VO sets from points in the 'arc' of possible obstacle velocities, (b) the circle of  $RV_i$  and the resulting  $VO^+$ , in two dimensions and (c) in three dimensions

become more complex to determine, since there are more options in escaping either horizontally, vertically, or by a combination of the two. If the possible velocity updates can be represented with a particular three-dimensional curve or a sphere, then the options for avoidance are given by the intersection of that curve with the VO cone. The analytical derivation of such an intersection involves a complicated quartic equation, which defeats the purpose of the VO-method as a reactive and graphically understandable method for avoidance.

Therefore, the 3DVO method is accompanied by the concept of Avoidance Planes. This concept is used as a tool to logically and graphically describe the three-dimensional

case into separate two-dimensional setups, and to find the appropriate velocity for avoidance. Therefore, instead of trying to derive all the possible resolutions for avoidance, the 3DVO method focuses only on a finite number of avoidance planes, which can be pre-defined based on the performance of the ownship. Ref [74] presents a similar method in which a three-dimensional case is broken down into two avoidance planes, which are the lateral plane (XY-Plane) and the longitudinal plane (XZ-Plane). The method presented in [73] also resembles the method with a very fine discretization of planes around the ownship X-axis.

The Avoidance Planes,  $P_\phi$ , are defined as any plane in which the ownship velocity vector  $\vec{V}_o$  lies, as shown in Figure 5.4-a. The avoidance is assumed to be conducted in one of these planes, which is parameterized by the angle of rotation of the plane,  $\phi_P$ , around the vehicle X-axis. The **VO** set, therefore, is represented as a two-dimensional cross sectional area,  $\mathbf{VO}_{P_\phi}$ . Since the **VO** is a right-cone, each  $\mathbf{VO}_{P_\phi}$ s form a conic section, as shown in the example of four Avoidance Planes where  $\phi_P = -90^\circ, -45^\circ, 0^\circ$  and  $45^\circ$ , in Figure 5.4-b. By comparing between the resulting  $\mathbf{VO}_{P_\phi}$ , the ownship can choose the most fitting plane for an optimal avoidance. Section III presents an example of a strategy that includes an approach to choose between available avoidance planes.

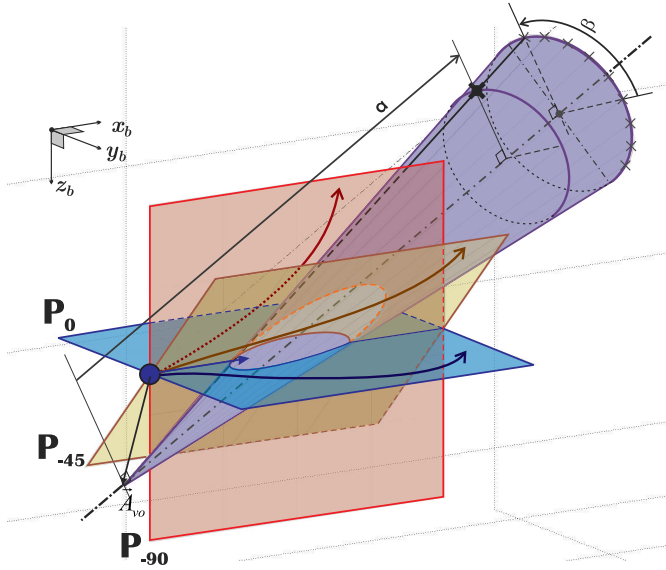
The type of conic section can be determined by comparing the **VO**'s opening angle,  $\alpha_{vo}$ , with the acute dihedral angle between the avoidance plane  $P_\phi$  and the cone effective base. This angle, denoted as  $\delta_{P_\phi}$ , is derived in equation (5.8), i.e.,

$$\delta_{P_\phi} = \arccos \left( \frac{\vec{D}_{vo}}{d_{vo}} \begin{bmatrix} 0 \\ \sin \phi_P \\ \cos \phi_P \end{bmatrix} \right). \quad (5.8)$$

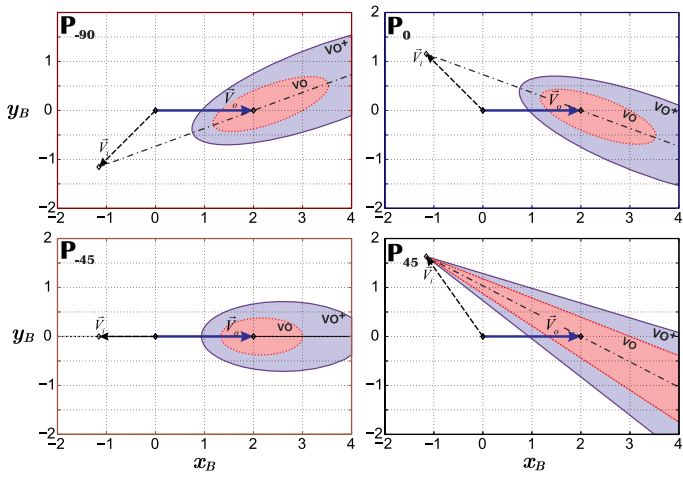
The conic section, therefore, is elliptical if  $\delta_{P_\phi} < \pi/2 - \alpha_{vo}$ , and hyperbolic otherwise. Degenerate cases occur if additionally  $A_{vo}$  lies on the corresponding  $P_\phi$ , which transforms the section into either a single point, a line, or into a triangular section. Physically, this case indicates that the obstacle are moving on the chosen avoidance plane, and thus an avoidance on this plane is less safer than others. Figure 5.4-b shows one example of this degenerate case in the  $P_{45^\circ}$ , which results in a triangular section limited by the two intersecting lines of the  $P_{45^\circ}$  and the **VO** cone surface.

To derive the conic-section in an arbitrary avoidance plane, this paper expresses the **VO** cone parameters with respect to each avoidance plane ( $P_\phi$ ) reference using parametric equations, as presented in equations (5.9) through (5.14). Here, equation (5.9) is a standard cone parametric equation in Euclidean space rotated to align it with the  $\vec{D}_{vo}$  vector, forming the Collision Cone **CC**. Adding the intended **VO** apex translates the cone into the Velocity Obstacle, as presented in equation (5.10). Finally, equation (5.11) rotates the previous **VO** with respect to each avoidance plane  $P_\phi$ , into the  $\{x_{vo}^\phi, y_{vo}^\phi, z_{vo}^\phi\}$  coordinates. Hence, the equations are

$$\begin{bmatrix} x_{cc} \\ y_{cc} \\ z_{cc} \end{bmatrix} = R_{\theta_{oi}|\psi_{oi}} \begin{bmatrix} a \\ a \tan \alpha_{vo} \cos \beta \\ a \tan \alpha_{vo} \sin \beta \end{bmatrix}, \quad (5.9)$$



(a)



(b)

Figure 5.4: The Avoidance Plane illustration intersecting the VO, (b) Conic-sections of the VO cone on several avoidance-planes.

$$\begin{bmatrix} x_{vo} \\ y_{vo} \\ z_{vo} \end{bmatrix} = \begin{bmatrix} x_{cc} \\ y_{cc} \\ z_{cc} \end{bmatrix} + \vec{A}_{vo}, \quad \text{and} \quad (5.10)$$

$$\begin{bmatrix} x_{vo}^\phi \\ y_{vo}^\phi \\ z_{vo}^\phi \end{bmatrix} = R_{p\phi} \begin{bmatrix} x_{vo} \\ y_{vo} \\ z_{vo} \end{bmatrix}, \quad (5.11)$$

where

$$0 \leq \beta < 2\pi, \quad a \geq 0, \quad (5.12)$$

$$R_{\theta_{oi}|\psi_{oi}} = \begin{bmatrix} \cos \psi_{oi} & \sin \psi_{oi} & 0 \\ -\sin \psi_{oi} & \cos \psi_{oi} & 0 \\ 0 & 0 & 1 \end{bmatrix} \times \begin{bmatrix} \cos \theta_{oi} & 0 & -\sin \theta_{oi} \\ 0 & 1 & 0 \\ \sin \theta_{oi} & 0 & \cos \theta_{oi} \end{bmatrix}, \quad \text{and} \quad (5.13)$$

$$R_{p\phi} = \begin{bmatrix} 1 & 0 & 0 \\ 0 & \cos \phi_{\mathbf{p}} & \sin \phi_{\mathbf{p}} \\ 0 & -\sin \phi_{\mathbf{p}} & \cos \phi_{\mathbf{p}} \end{bmatrix}. \quad (5.14)$$

The vertices in each avoidance-plane are derived by solving equation (5.11) for  $z_{vo}^\phi = 0$ , for every  $\beta$ . The resulting velocity obstacle conic section, denoted as  $\mathbf{VO}_{\mathbf{P}_\phi}$ , is therefore simplified into a polygon formed by a finite set of vertices,  $\{x_{vo}, y_{vo}\}$  on the limiting curves. This method is chosen instead of other methods for deriving the  $\mathbf{VO}_{\mathbf{P}_\phi}$  due to its simplicity and the required computational power, as compared to, for instance, the derivation of an exact quadric function. Moreover, it is also possible to use the parametric derivation of the  $\mathbf{VO}_{\mathbf{P}_\phi}$  from a  $\mathbf{S}_{\mathbf{p}\mathbf{z}}$  that is shaped other than a sphere, as long as the vertices that form the effective base of the  $\mathbf{VO}$  cone (or pyramid) are determined.

The parameter  $\beta$  in equation (5.9) is the free-parameter of the  $\mathbf{VO}$  effective circular base, whereas  $a$  is the free-parameter of the generating lines of the cone, which is bounded to be equal or greater than zero, to remove vertices that lie on the other nappe of the cone. Both parameters are illustrated in Figure 5.4-a. For some cases of hyperbolic cross section, the bound of  $a$  can cause the omission of a significant part of the  $\mathbf{VO}_{\mathbf{P}_\phi}$  section. Therefore, an additional extrapolation function is required in this case, so that the section can cover the reachable range of the  $\vec{V}_o$ .

The vertices that form the  $\mathbf{VO}_{\mathbf{P}_\phi}$  section in each Avoidance Plane  $\mathbf{P}_\phi$  are derived by solving the  $x_{vo}^\phi$  and  $y_{vo}^\phi$  in equation (5.11), for  $z_{vo} = 0$ . The following equation gives the value of  $a$  for the non-degenerate cases:

$$a\{z_{vo}^\phi = 0\} = \frac{A_{voz} \cos \phi_{\mathbf{p}} - A_{voy} \sin \phi_{\mathbf{p}}}{(\sin \phi_{\mathbf{p}} \cos \theta_{oi} + \cos \phi_{\mathbf{p}}) \sin \psi_{oi} + ((\cos \phi_{\mathbf{p}} \cos \theta_{oi} - \sin \phi_{\mathbf{p}} \sin \psi_{oi} \sin \theta_{oi}) \sin \beta - \sin \phi_{\mathbf{p}} \cos \psi_{oi} \cos \beta) \tan \alpha_{vo}} \quad (5.15)$$

The  $\mathbf{VO}_{\mathbf{P}_\phi}$  for the degenerate cases can also be indicated using the numerator and denominator of equation (5.15). If the numerator is zero, all  $\mathbf{VO}$  generating lines cross the

avoidance plane on its apex. In this case, the  $\{x_{vo}, y_{vo}\}$  pair is determined by the values of  $\beta$  take produce a zero value for the denominator in equation (5.15). Zero, one, or two real value root(s) can be obtained as the solutions, by which, together with the cone apex, result in a single point, a straight line, or a triangular  $\mathbf{VO}_{p_\phi}$  section, respectively.

### 5.3. STRATEGY FOR A THREE-DIMENSIONAL AVOIDANCE

The proposed Three-dimensional Velocity Obstacle (3DVO) method are based on the three-dimensional sets and criteria described in the previous section. This section gives an example of a strategy using those definitions to generate a reactive avoidance maneuver in three dimensions. This strategy resembles the two-dimensional avoidance strategy in Ref.[75], with an additional step to select the safe Avoidance Plane.

#### 5.3.1. AVOIDANCE ALGORITHM

The algorithm of avoidance is defined according to the condition of the ownship velocity vector  $\vec{V}_o$  with respect to the defined sets in the 3DVO method. The algorithm is presented graphically in Figure 5.5, differentiated by the three modes of *mission*, *avoid*, and *maintain*.

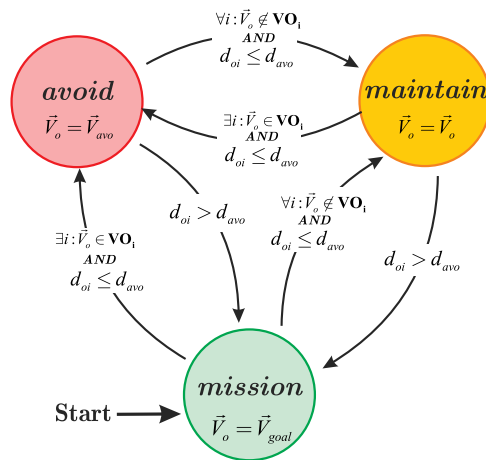


Figure 5.5: The Three-dimensional Velocity Obstacle method state diagram.

From a condition where the velocity vector is heading towards a designated goal,  $\vec{V}_o = \vec{V}_{goal}$ , whenever the  $\vec{V}_o$  is included in the corresponding  $\mathbf{VO}$ , or fulfilling equation (5.3), the ownship goes to the avoid mode. If the encounter is imminent ( $d_{oi} \leq d_{avo}$ ), but the  $\vec{V}_o$  is not included in any of the  $\mathbf{VO}$  set, the ownship can keep its heading towards its original goal in the maintain mode. In the avoiding mode, the  $\vec{V}_o$  is updated continuously in the direction to the surface of  $\mathbf{VO}$  until it steps outside the set, where the ownship is then switches to maintain mode. From maintain mode, the ownship might need to switch back to the avoid mode due to an obstacle maneuver, if the encounter is still imminent. Mission mode is restored whenever the encounters are no longer imminent, i.e.,  $d_{oi} > d_{avo}$ .

In avoid mode, the ownship velocity vector is updated to a certain  $\vec{V}_{avo}$  to get outside of the velocity obstacle set  $\mathbf{VO}$ . The original VO-method commonly updates the ownship velocity to a point on the  $\mathbf{VO}$  surface, denoted as the chosen escape point,  $\vec{E}_{vo}$ . This point can be chosen based on various strategies, such as by accelerating or decelerating while staying on the path, by turning without alteration of speed, or by simply choosing the closest point from the current velocity. This paper focuses on providing an escape route by pure turning with a certain rate of  $\omega_{avo}$ , until the velocity vector aligns with the  $\vec{E}_{vo}$ . Hence, in a constant time-step  $\Delta t$ , the  $\vec{V}_{avo}$  is defined in equation (5.16), where  $\epsilon_{vo} = \arctan\left(\frac{E_{voy}}{E_{vox}}\right)$  is the angle of the vector  $\vec{E}_{vo}$ , in the chosen direction, from the ownship X-axis.

$$\vec{V}_{avo} = \begin{bmatrix} \cos \Theta & -\sin \Theta \\ \sin \Theta & \cos \Theta \end{bmatrix} \vec{V}_o, \quad \text{where } \Theta = \arg \min \{|\omega_{avo} \Delta t|, |\epsilon_{vo}|\}. \quad (5.16)$$

By using the avoidance plane, the  $\vec{E}_{vo}$  are determined in each plane as intersection points between the  $\mathbf{VO}_{P_\phi}$  and the circle of  $\vec{V}_o$  rotation, as shown in Figure 5.6. These points are derived by solving the variables in equation (5.11) with  $z_{vo} = 0$ , where the  $\{x_{vo}^\phi, y_{vo}^\phi\}$  satisfies equation (5.17), i.e.,

$$(x_{vo}^\phi)^2 + (y_{vo}^\phi)^2 = |\vec{V}_o|^2 \quad (5.17)$$

There will be a maximum of four solutions for the  $\vec{E}_{vo}$  of the respective  $\mathbf{VO}_{P_\phi}$ . The logical common choice from the four will be the one with the smallest  $\epsilon_{vo}$  angle, which corresponds to the subtlest maneuver to avoid. No (zero) solution can result under two conditions: if either no part of the circle of  $\vec{V}_o$  rotation is included in  $\mathbf{VO}_{P_\phi}$  or the whole circle is included. The latter condition happens when the ownship is too close to the obstacle, and should be prevented by conducting the avoidance maneuver well before the condition occurs.

An additional precaution is added in the algorithm when handling multiple encounters with eight obstacles, which is to only use  $\vec{E}_{vo}$  points that are outside all other imminent  $\mathbf{VO}_\phi$ s. This is shown in Figure 5.6-b for a multiple-encounters situation, where only the two outermost points are valid  $\vec{E}_{vo}$ , from the total of six intersections of  $\vec{V}_o$  with  $\mathbf{VO}_\phi$ .

### 5.3.2. CHOOSING AN AVOIDANCE PLANE

To demonstrate the 3DVO method performance, this paper uses an example with twelve Avoidance Planes, discretized evenly around the ownship X-axis, from  $-\pi/2$  to  $\pi/2$ . The ownship therefore can choose the best avoidance plane by comparing the angle of rotation from the current velocity vector  $\vec{V}_o$  to the  $\vec{V}_{avo}$  point on the respective  $\mathbf{VO}_\phi$  section. The avoidance plane, however, can provide other information to refine this strategy, especially when taking into account the obstacle maneuvers.

Besides using the angle of rotation, the best Avoidance Plane can be chosen by considering the shape of the  $\mathbf{VO}_\phi$  section. A degenerate triangular shape, for example, is generally more dangerous than an ellipse or a circle, since it indicates that the corresponding Avoidance Plane might be the same plane the obstacle is moving in. Hence the avoidance maneuver can be nullified by an adverse movement of the obstacle. This

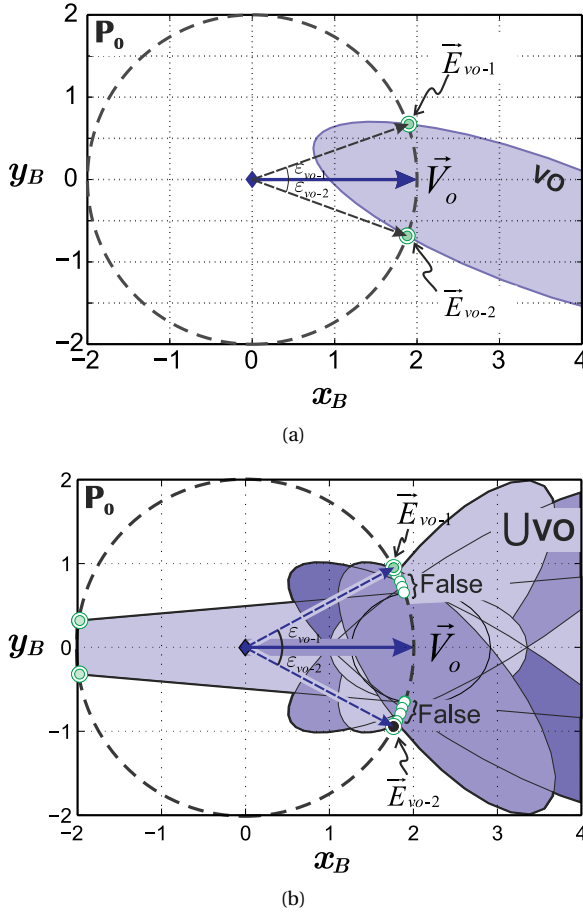


Figure 5.6: Avoidance by pure turning on  $\mathbf{P}_0$  for cases with (a) one obstacle, (b) multiple obstacles

danger can also happen in some case in avoidance on hyperbolic  $\mathbf{VO}_\phi$  sections, due to the intersection of the  $\mathbf{VO}_\phi$  with the  $\mathbf{VO}$  cone effective base.

For those reasons, the Avoidance Plane is chosen by weighing the danger of each plane based on the shape of the  $\mathbf{VO}_\phi$  section. Hyperbolic and triangular  $\mathbf{VO}_\phi$  sections are dropped, while ellipsoidal sections are preferable, and therefore the avoidance is conducted in one of the  $\mathbf{P}_\phi$  that has the particular shape. Afterwards the choice of  $\mathbf{P}_\phi$  is based on which plane can provide a  $\vec{E}_{vo}$  with the smallest rotation angle,  $\epsilon_{vo}$ . Note that eccentricity of the  $\mathbf{VO}_\phi$  section is not used as a deciding factor (which would result in a  $\mathbf{P}_\phi$  that provides a  $\mathbf{VO}_\phi$  section closest to that of a circle), since it does not necessarily correspond to the smallest  $\epsilon_{vo}$ .

In case of multiple encounters, the avoidance plane is chosen from those that can give a minimum level of danger based on the inclusion of  $\vec{V}_o$  and the shape of  $\mathbf{VO}_\phi$ , before deriving the one that has the smallest angle of rotation to a possible  $\vec{V}_{avo}$ . Simi-

larly to the single encounter case, avoidance-planes with triangular and hyperbolic  $\mathbf{VO}_\phi$  are dropped. It is possible that a hyperbolic or triangular  $\mathbf{VO}_\phi$  resulted in an avoidance plane, but does not include the  $\vec{V}_o$ . This particular plane is also dropped and considered more dangerous than those that have only ellipse sections.

### 5.3.3. AVOIDANCE TURNING RATE

Two parameters that need to be defined to apply the algorithm for 3DVO method are the avoidance distance  $d_{avo}$  and the avoidance turning rate  $\omega_{avo}$ . The latter is required in an imminent encounter conflict where the vehicle dynamics cannot be neglected. The relationship between these two parameters can be viewed physically as the required maneuverability ( $\omega_{avo}$ ) for the available sensing capability ( $d_{avo}$ ).

Consider an encounter between two vehicles, an ownship and an obstacle, initially positioned at  $\vec{X}_o(0)$  and  $\vec{X}_i(0)$ , respectively, as shown in Figure 5.7. This type of conflict is considered as the worst avoidance scenario when, hypothetically, the avoidance had to be done by turning to the opposite side of the obstacle  $\mathbf{S}_{pz}$ , or in this case, to the left. Turning to the right, on the other hand, would require the minimum effort since the vehicle is practically heading to the edge of the obstacle  $\mathbf{S}_{pz}$ . The radius required for this hypothetical left turning is therefore the smallest compared to any other colliding scenario, achievable with the largest value of avoidance turning rate,  $\omega_{avo}$ .

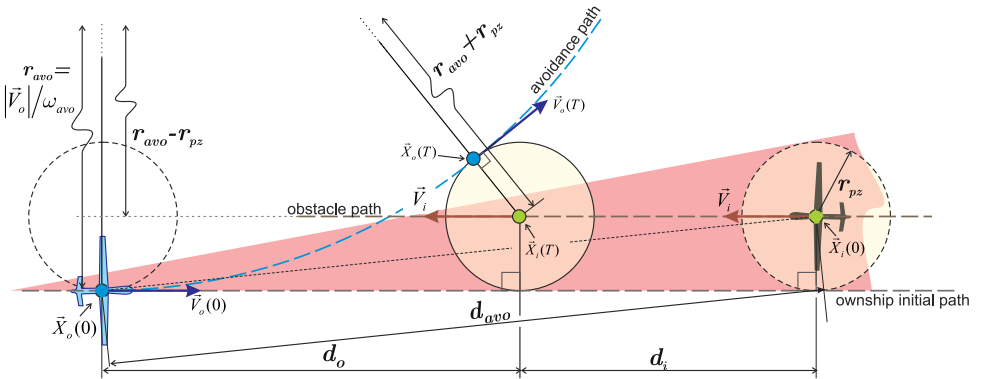


Figure 5.7: The worst scenario of conflict when the avoidance must be conducted by a hypothetical turn to the opposite direction

From the initial point at  $t = 0$ , the ownship follows a circular path with radius  $r_{avo} = |\vec{V}_o|/\omega_{avo}$ , while the obstacle keeps its straight trajectory. The vehicles meet at  $t = T$ , where the ownship grazes the obstacle protected-zone, achieved by two conditions: the ownship position,  $\vec{X}_o(T)$ , is just at the edge of the  $\mathbf{S}_{pz}$ , and its vector of velocity  $\vec{V}_o(T)$  is exactly tangential to that circle. This meeting condition is achieved when the value of the ownship avoidance turning rate,  $\omega_{a.cr}$  is critical: if it is bigger, the avoidance path will have some offset from the  $\mathbf{S}_{pz}$  edge and, if it is smaller, the ownship will penetrate the protected-zone. The critical value of  $\omega_{avo}$  that is derived in this worst case scenario should be able to ensure safety in any other conflict scenario.

The relation between the critical value of the avoidance turning rate,  $\omega_{a.cr}$ , and the

avoidance distance  $d_{avo}$ , can be derived by splitting it into two parts, the ownship part,  $d_o$ , and the obstacle part  $d_i$ . The former is derived using the critical conditions, which implies that the center of the circular avoidance path, the point of grazing,  $\vec{X}_o(T)$ , and the center of the  $\mathbf{S}_{pz}$  lie on one straight line. A right triangle, therefore, can be formed with  $r_{avo} + r_{pz}$  as the hypotenuse and  $r_{avo} - r_{pz}$  and  $d_o$  as the legs. Hence  $d_o$  can be expressed as a function of the conflict geometry, as presented in equation (5.19). The  $d_{avo}$  is then solved as the hypotenuse of the triangle with  $d_o$  and the  $\mathbf{S}_{pz}$  radius as the legs, as presented in equation (5.18).

The obstacle part of the avoidance distance,  $d_i$ , is a straight line that can be derived using the obstacle speed  $|\vec{V}_i|$  and time, as expressed in (5.20). The time here has to match the time required by the ownship to reach point  $\vec{X}_o(T)$  from its initial position. To derive the required time, the ownship  $\vec{V}_o$  rotation can be used as follows: from the initial heading,  $\psi_o(0) = 0$ , the ownship rotates using a constant turning rate  $\omega_{avo}$  until  $\psi_o(T) = \omega_{avo}T$ , which corresponds directly to the opposite angle of  $d_o$ , in the right triangle before. Equation (5.21) expresses the time in terms of the turning rate and the encounter geometry. Hence,

$$d_{avo} = \sqrt{(d_o + d_i)^2 + r_{pz}^2}, \quad (5.18)$$

$$d_o = \sqrt{(r_{avo} + r_{pz})^2 - (r_{avo} - r_{pz})^2} = 2\sqrt{\frac{|\vec{V}_o|r_{pz}}{\omega_{avo}}}, \quad (5.19)$$

$$d_i = |\vec{V}_i|T, \quad (5.20)$$

where

$$T = \frac{1}{\omega_{avo}} \arctan\left(\frac{d_o}{r_{avo} - r_{pz}}\right) = \frac{1}{\omega_{avo}} \arctan\left(\frac{d_o}{|\vec{V}_o|/\omega_{avo} - r_{pz}}\right). \quad (5.21)$$

Figure 5.8 shows the relation between the avoidance distance  $d_{avo}$  and the critical value of the avoidance turning rate  $\omega_{a.cr}$ , for the worst-case scenario explained before. The resulting curve is somewhat similar to the graph of the same parameter in Ref [75], which is obtained using a different method. The graph can also be viewed as a simplification of the Reachable Avoidance Velocity set (**RAV**) [22], or the command parameter space [122, 124] employed in previous VO-method. In this case, the ownship need to choose an avoidance preference, i.e., by choosing a combination of  $d_{avo}$  and  $\omega_{avo}$ , that is above the  $\omega_{a.cr}$  curve.

Figure 5.8 is derived for a constant ownship speed,  $|\vec{V}_o|$ , of 5 m/s, facing head-on obstacles with speeds,  $|\vec{V}_i|$ , from 5 to 10 m/s. The required turning rate increases with obstacle speed, which suggest that to provide an adequate turning rate, the ownship needs to estimate first the speed of obstacle it might encounter during its operation. Furthermore,  $\omega_{a.cr}$  increases exponentially with  $d_{avo}$  and practically sets a minimum distance of avoidance for a range of obstacle speeds. For instance, if it is estimated that the obstacle has speeds greater than 10 m/s, avoidance at 5 m from the obstacle by a pure turning would be impossible. These resulting  $\omega_{a.cr}$  and the corresponding avoidance distances are used in the 3DVO method implementation, presented in the next section.

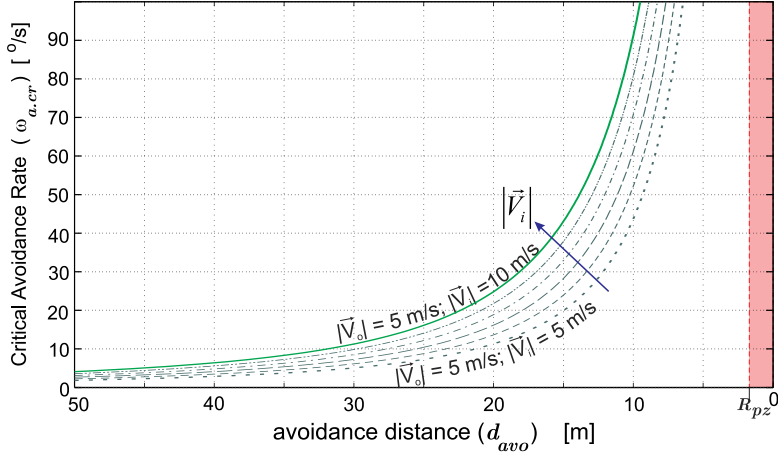


Figure 5.8: The curve of the critical avoidance turning rate,  $\omega_{a,cr}$ , along the corresponding avoidance distance  $d_{avo}$

5

## 5.4. IMPLEMENTATION

To evaluate its performance, the Three-dimensional Velocity Obstacle (3DVO) method and the proposed strategy are implemented in three different simulated cases. These cases are designed to test the method on generating three-dimensional resolutions, on handling maneuvering obstacles, and on handling multiple encounters. Each vehicle is modeled as a point-mass with designated initial velocity vector in the Euclidean space, moved in a constant time-step,  $\Delta t = 0.1$  second. Note that to focus more on the method performance, these simulation does not include the dynamics of the vehicles, or the effect of the environment, e.g., wind and gravity.

Each vehicle independently generates conflict resolutions using the 3DVO method, based on their own detection of encounters in proximity. This detection includes the measurements for both ownship's and obstacles' states, which are listed together in Table 5.1, along with the assumptions used in the simulations. Every parameter is acquired seamlessly in every time-step, without delay or errors.

The simulations are presented in a global frame of reference, such as shown in Figure 5.9, where each protected zone,  $\mathbf{S}_{pz}$ , is represented by a sphere with radius  $r_{pz} = 1$  meter, and each velocity vector is visualized with a small cone. Note that the time slices in the frames are not ordered uniformly, instead, they are selected such that they show important phases of the simulation progression.

### 5.4.1. TWO VEHICLES CONVERGING

Figure 5.9 shows the simulation of the case that has been used to explain the 3DVO method in previous sections, shown in Figure 5.2 to 5.3. This case serves as a proof of concept and the strategy of the 3D resolution generation using the avoidance planes. Two conflicting vehicles are involved, where the ownship is using the 3DVO method and conducts avoidance at  $d_{avo}$  of 10 meters and the obstacle stays on its initial flight path.

Table 5.1: Parameters required in the 3DVO method implementation

| Parameter   | Notes and Assumptions  | Unit  |
|---|--|-------|
| 1 Ownship Position $\vec{X}_o$                    | Treated as the origin for all 3DVO implementation  | [m]   |
| 2 Ownship Velocity $\vec{V}_o$                    | On ownship body axis, therefore only requires the initial speed, $ \vec{V}_o $   | [m/s] |
| 3 Avoidance distance, $d_{avo}$                   | Avoidance distance preference for each vehicle is explicitly stated in each simulation setup   | [m]   |
| 4 Avoidance turning rate, $\omega_{avo}$          | Avoiding turning rate is set at 10% above $\omega_{a.cr}$ , corresponding to the preference of $d_{avo}$ , as presented in Figure 5.7                      | [m/s] |
| 5 Obstacle- $i$ position, $\vec{X}_i$             | Derived from the obstacle's angular position, i.e., the distance $d_{oi}$ , azimuth $\psi_{oi}$ , and elevation $\theta_{oi}$ angle, from the ownship axis | [-]   |
| 6 Obstacle- $i$ velocity, $\vec{V}_i$             | Obstacle- $i$ absolute velocity, referred to the ownship axis  | [m/s] |
| 7 Obstacle- $i$ possible turning rate, $\omega_i$ | For the derivation of the Buffer Velocity set <b>BV</b> . Assumed to be the same as the $\omega_{avo}$ of the ownship                                      | [-/s] |
| 8 Radius of protected-zone, $r_{pz}$              | Every vehicle in the simulation assumes 1 meter as the radius of the protected-zone  | [m]   |

Both vehicles move at 5 meters/second in a straight line, heading to a point far away from the initial position.

From the twelve avoidance planes provided by the 3DVO method's strategy, four avoidance-planes, i.e.,  $\mathbf{P}_{-90^\circ}$ ,  $\mathbf{P}_{-45^\circ}$ ,  $\mathbf{P}_0^\circ$ , and  $\mathbf{P}_{45^\circ}$ , are shown. For each plane, both right and left turning are tested, making a total of eight resolution paths for the encounter case, as shown in a composite time-lapse frame in Figure 5.9. Every resolution successfully avoids the obstacle, as shown by the distance between the two vehicles in Figure 5.10-a. An offset from the obstacle  $r_{pz}$  results from the use of the buffer velocity set.

Figure 5.10-b shows the ownship drifting distance over time on each plane and each direction of avoidance. The figure shows almost the same maneuvering slope for every generated resolution. The vehicle's drift from its initial path can be evaluated by calculating the total path length of the drifting profile,  $\Delta l$ , as shown in the inset of the Figure 5.10-b. The value can be used to determine the efficiency of the avoidance maneuver. By comparison, turning to the right on  $\mathbf{P}_{45^\circ}$  is the least efficient way to avoid for the encounter case. The more efficient way of avoidance is resulted by turning to the left on  $\mathbf{P}_{45^\circ}$ ,  $\mathbf{P}_0^\circ$  and  $\mathbf{P}_{-45^\circ}$ , or by turning to the right on  $\mathbf{P}_{-90^\circ}$  and  $\mathbf{P}_{-45^\circ}$ , each differentiated by just a small margin. These results correspond to the  $\mathbf{VO}_{\mathbf{p}_\phi}$  section of each avoidance plane, shown in Figure 5.4-b, where the least efficient avoidance happens on the plane

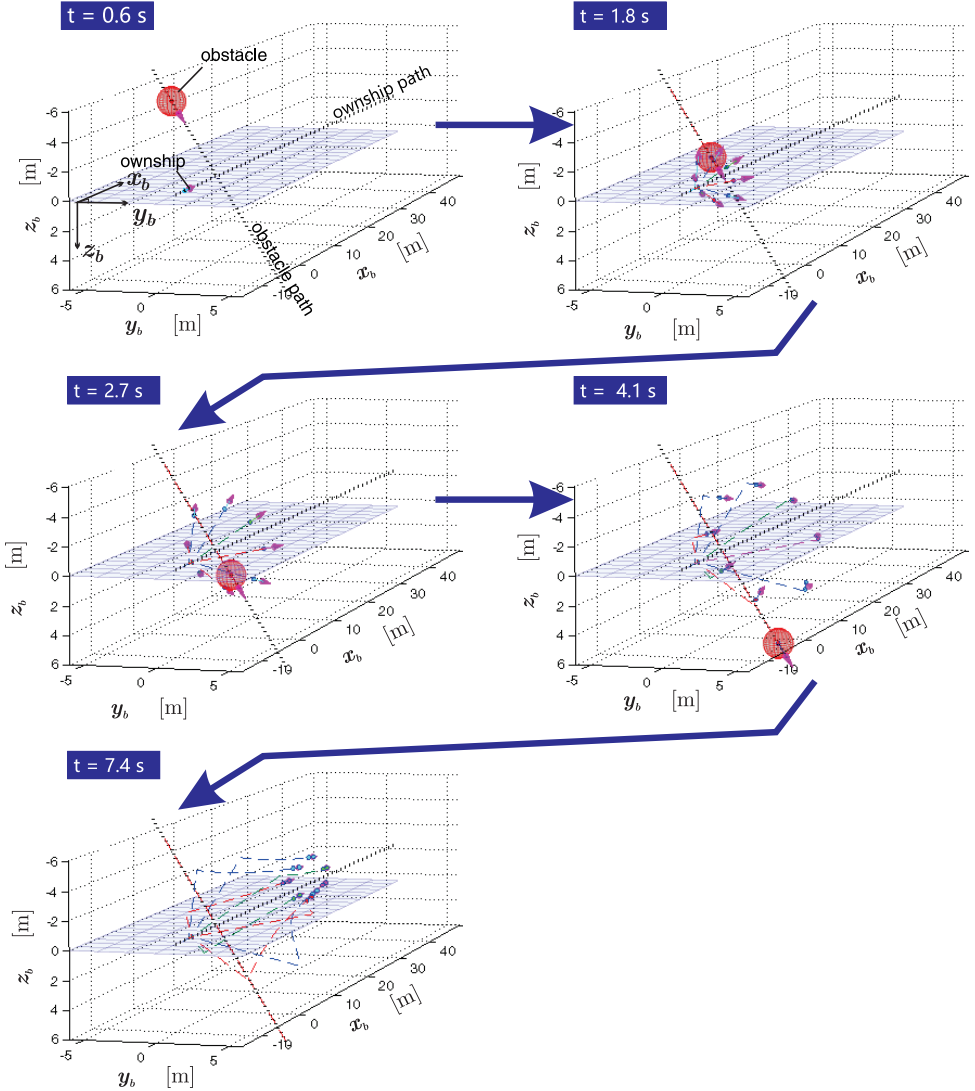
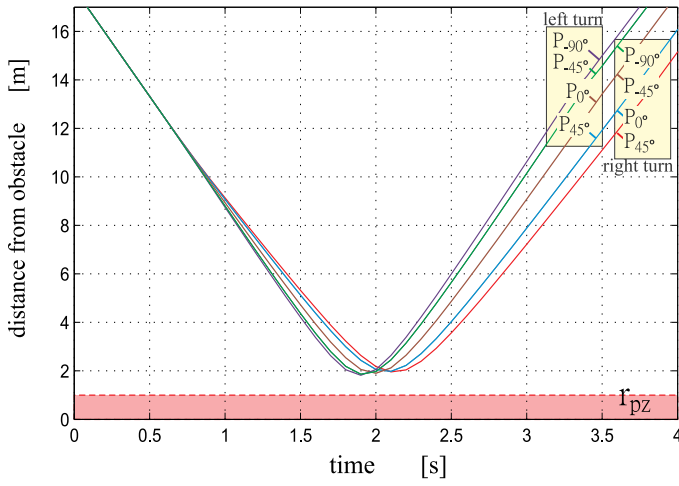


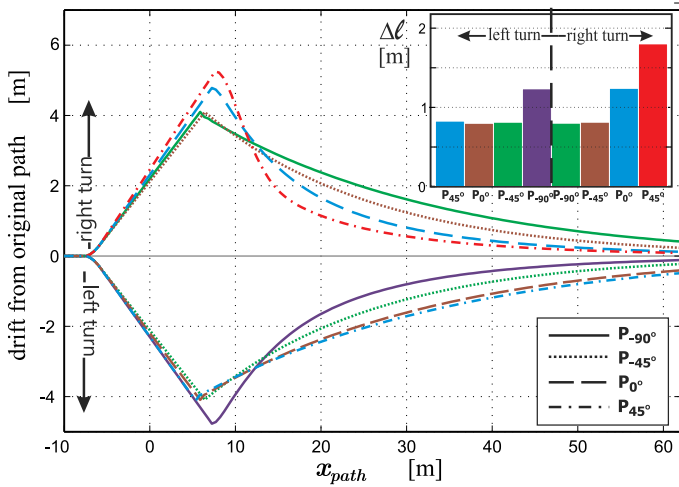
Figure 5.9: Simulation-1: The same case shown in Figure 5.2. Several choices of avoidance plane are given,  $\mathbf{P}_{-90^\circ}$ ,  $\mathbf{P}_{-45^\circ}$ ,  $\mathbf{P}_{0^\circ}$ , and  $\mathbf{P}_{45^\circ}$ .

that has a triangular  $\mathbf{VO}_{\mathbf{P}_\phi}$  section,  $\mathbf{P}_{45^\circ}$ .

As a reactive avoidance method, the 3DVO is less computationally intensive compared to optimal control approaches, which require many iterations across control parameters for just one resolution. In contrast, compared to a simpler reactive method such as a basic PF-method that only requires one matrix summation from the obstacle relative position, the 3DVO is slower. However, the 3DVO process only starts when the criteria in equation (5.7) are fulfilled, while the basic PF-method, such as presented in



(a)



(b)

Figure 5.10: Simulation-1: (a) Distance between vehicles and (b) ownship drifting from original path

[117], starts whenever the vehicles are close enough, even for cases without possibility of collisions. This indicates that the 3DVO is more efficient in terms of the resulting avoidance path.

If an ownship only has a certain predefined avoidance plane to escape, e.g., always turn on its horizontal plane, then the only calculation is the criteria check in equation (5.7). The results are then used to determine the ownship states as depicted in Figure 5.5. On the other hand, when the ownship needs to decide which, among the available Avoidance Planes, is the best for the escape maneuver, the complexity of the 3DVO method increases. For this case, it requires four steps to determine a resolution, one of which con-

sist of a series of matrix manipulations (one summation and two multiplications). This step depends directly on the number of vertices involved when determining the  $\mathbf{VO}_{\mathbf{p}_\phi}$ , and on the number of available Avoidance Planes. The simulations in this research use at most 36 vertices and twelve Avoidance Planes, for which the number of calculations is still far less than the number of iterations across parameters in an optimal control scheme for avoidance, such as dynamic programming[8].

#### 5.4.2. MULTIPLE HETEROGENEOUS CONFLICTS

This simulation tests the overall capability of the 3DVO method: generating resolutions in a multiple and dynamic encounter situation. Here, eight vehicles are tested in a cube-like setup, as shown in Figure 5.11. Each sphere in the figure represents half the radius of the protected-zone to conserve the visualization of the collision, such that vehicle collisions are shown by two touching spheres, instead of two coincident spheres. This setup is a three-dimensional extension of the eight-vehicle super-conflict case used in previous studies [39, 75, 87], which tested the two-dimensional collision-avoidance method.

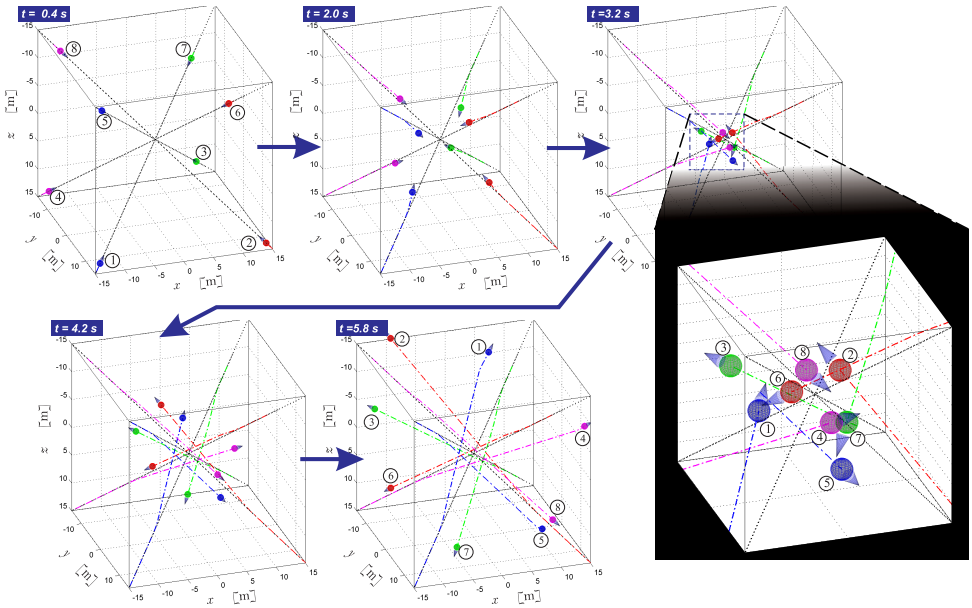


Figure 5.11: Simulation-2: Multiple 3-dimensional conflicts, in randomly heterogeneous setup.

The vehicles in this simulation are heterogeneous, meaning that each of them has a different speed,  $|\vec{V}|$ , and a different preference of where to start the avoidance,  $d_{avo}$ . The speed of each of the vehicles is uniformly randomized within a range of 5 – 10 meters/second. Furthermore, the  $d_{avo}$  is uniformly randomized as well, within 10 - 15 meters, with avoidance turning-rate,  $\omega_{avo}$  that is 10% higher than the critical turning rate shown in Figure 5.8. The initial positions in the cube are selected along the respecting space diagonals, to make all vehicles reach the center of the cube at the same time.

The 3DVO method and strategy are used in each vehicle, which enable it to avoid oth-

ers by turning on one of the twelve possible avoidance-planes. With all vehicles avoiding in a random and uncoordinated manner, the situation becomes dynamic: each vehicle is facing obstacles that can change direction at an arbitrary time. Figure 5.11 shows one example result of the random scenario.

The simulation shows that the heterogeneous setup produces a variation of resolution maneuvers, which ultimately resolves the conflict independently for every vehicle. The work of the 3DVO method can be represented by the change of the flight path and the heading angle, as shown in Figure 5.12. Here, each vehicle has a different preference of avoidance, with vehicle 3 and 5 having the biggest change of direction. The dynamic situations are shown by the modes of the vehicles, where the avoidance mode occurs more than once for some of the vehicles. The change of direction between the avoidance modes also demonstrates the variation of the avoidance-plane chosen during the maneuver, exploiting the three-dimensional space.

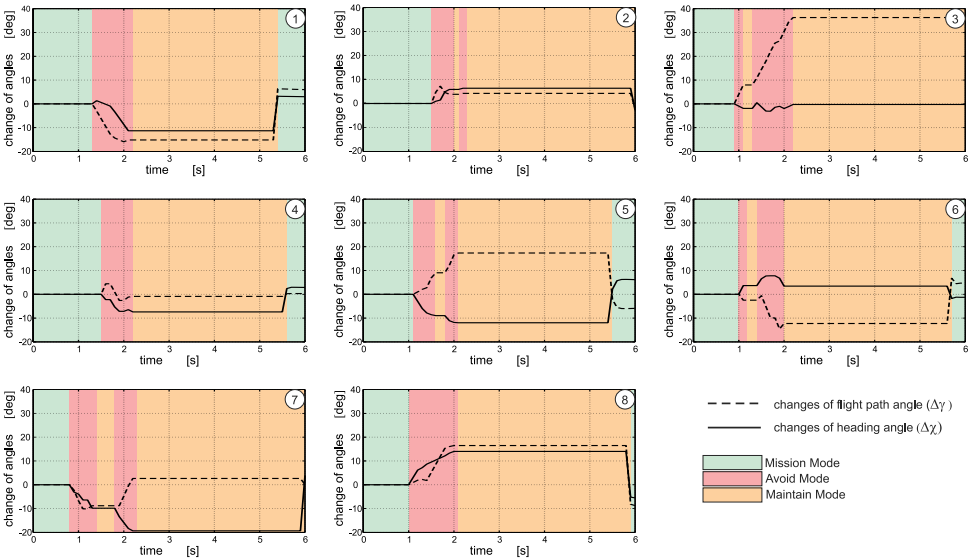


Figure 5.12: Simulation-2: Changes of vehicles directional angle and the modes of the 3DVO method, during avoidance

### 5.4.3. 3DVO METHOD VALIDATION

This third implementation is used to validate the performance of the 3DVO method in generating three-dimensional resolutions for various three-dimensional conflicts by using Monte Carlo simulations. The eight-vehicle super-conflict scenario in the previous subsection is used again with an additional random factor for the vehicle position. As shown in an example in Figure 5.13, besides the vehicle speeds and the avoidance distances, the unit vector of the positions,  $\hat{x}$ ,  $\hat{y}$ , and  $\hat{z}$ , are also uniformly randomized, while keeping each octant of the Euclidean space having one representative vehicle. The space-diagonal paths for each vehicles, therefore, vary in orientation and thus results in more stressful scenarios than those in the previous subsection. The initial positions are

then adjusted to force all vehicles to reach the origin at the same time. Moreover, an exception is added to drop any generated scenario that starts with two vehicles or more that are already in an imminent encounter, or in a collision.

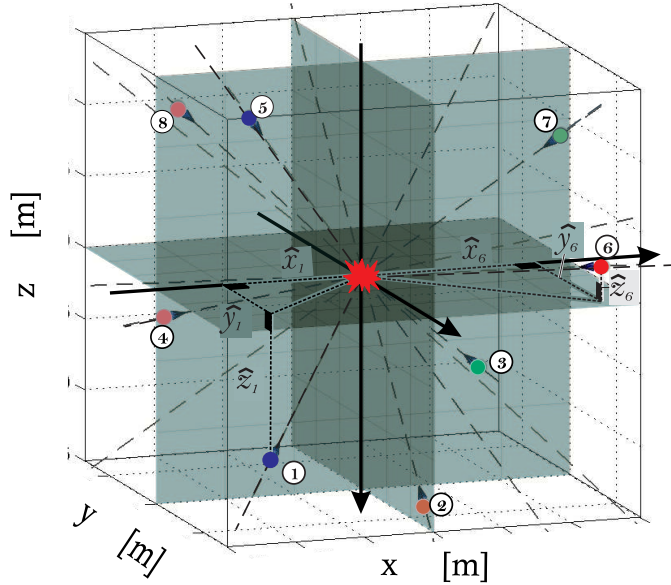


Figure 5.13: Simulation-3: Initial parameter randomization setup for the super-conflict scenarios

For a limited time frame, the expected value of collision probability and its variance are calculated using equations (5.22) and (5.23). Along with the complete 3DVO method simulation, five other variations of the method are also tested for comparison, as listed in Table 5.2. The last row of the table presents the results of the PF-method implementation to the super-conflict setup, in order to have an exact comparison of the 3DVO with other reactive methods. It should be noted, however, that the PF-method[117] implemented is only in its most basic form with a 3D realization, i.e., adding a negative gain to the ownship velocity vector based on the relative position of each imminent obstacle.

A total of 25,000 different initial condition samples,  $N_{MC}$ , are considered. The number is selected by observing the convergence of the expected value of  $P_{col}$  results for each series of the simulations. A collision is marked when at least two vehicles have a distance less than the designated radius  $r_{pz} = 1$  meter, where the simulation is stopped and added to the collision occurrence,  $N_{col}$ . Any collision that may occur afterwards is neglected. Equation (5.24) gives the precision of the Monte Carlo runs with a 99.95% confidence interval. Note that the result does not follow one vehicle in particular, but rather the general probability in the airspace sample. The equations to derived the Monte Carlo parameters are

$$E[P_{col}] = \frac{1}{N_{MC}} \sum_{i=1}^{N_{MC}} n_{col_i}, \quad (5.22)$$

$$\sigma_{col}^2 = \frac{1}{N_{MC}} \sum_{i=1}^{N_{MC}} (n_{col_i} - E[P_{col}])^2, \quad \text{and}, \quad (5.23)$$

$$P_{col} = E[P_{col}] \pm \frac{3.3\sigma_{col}}{\sqrt{N_{MC}}}. \quad (5.24)$$

The result of the Collision Frequency is presented in Table 5.2. It is shown that two-dimensional avoidance is not enough to solve a three-dimensional uncoordinated conflict. The use of multiple avoidance planes, which exploits the three-dimensional space more, gives a lower collision occurrences even without considering the obstacle maneuver. However, it is shown that the use of the Buffer Velocity for the collision reduction is more effective than the addition of Avoidance Planes. Ultimately, the 3DVO method and the proposed strategy resulted in zero collision occurrence for the 25,000 samples of random three-dimensional, uncoordinated, dynamic multiple conflicts. The probability of collisions, however, cannot be determined within the tested samples due to the insufficient variation of results.

Table 5.2: Comparison of collision occurrences in various method, for the 25,000 random samples

| Methods | Predefined Avoidance Plane | BV add | Collision Occurrence | Collision Probability | note            |
|---------|----------------------------|--------|----------------------|-----------------------|-----------------|
| 1       | XY-plane                   | NO     | 1428                 | 5.75 ± 0.48 %         | VO-method       |
| 2       | XY-plane                   | YES    | 260                  | 1.04 ± 0.21 %         |                 |
| 3       | XY & YZ -planes            | NO     | 386                  | 1.52 ± 0.26 %         |                 |
| 4       | XY & YZ -planes            | YES    | 23                   | 0.09 ± 0.06 %         |                 |
| 5       | 12 planes (distributed)    | NO     | 256                  | 1.02 ± 0.21%          |                 |
| 6       | 12 planes (distributed)    | YES    | 0                    | not available         | 3DVO            |
| 7       | -                          | -      | 4521                 | 18.03 ± 0.80 %        | basic PF-method |

The basic PF-method result is evidently inferior, even if it is compared with the two-dimensional VO-method. This, however, is expected since the basic PF-method is not designed either for multiple encounters, or for dynamic maneuvering obstacles.

## 5.5. CONCLUSIONS

This paper described a novel conflict resolution method called the Three-Dimensional Velocity Obstacle (3DVO) method. The method is designed to generate a reactive three-dimensional avoidance maneuver for an Unmanned Aerial Vehicle (UAV) to resolve three-dimensional conflicts. The method takes into account uncoordinated obstacle movement, as well as multiple obstacle encounters. The overall 3DVO method performance has been demonstrated using a series of simulations, which resulted in zero collisions for all given conflict scenarios.

The performance of the 3DVO method is the result of three key features: the addition of the Buffer Velocity zone, the concept of the Avoidance Planes, and the derivation

of the required avoidance turning-rate. The Buffer Velocity zones ensures safety of the UAV when facing obstacles with adverse movement during the avoidance process. The Avoidance Planes enables the three-dimensional exploitation that reduces the frequency of collision. These planes can be linked directly to the maneuverability of the UAV. Lastly, the required avoidance turning rate derivations give a quantitative relationship between the UAV maneuverability (turning-rate) and available sensing capability (avoidance distance). This relationship can be used to determine a safety measure in UAV design.

While the 3DVO method shows many promising results, there is still room for improvement. The method has yet to be tested in higher-density super-conflict cases. The influence of uncertainty has yet to be considered, which is necessary for conflict scenarios that assume the use of on-board sensors. Real-life flight testing is also required before the 3DVO can be considered ready to be implemented in a UAV. Nevertheless, the 3DVO method has been demonstrated and performed as intended to aid UAV's Conflict Detection and Resolution system, towards its integration into the airspace system.

# 6

## DISCUSSION, CONCLUSION, AND RECOMMENDATION

*Its time to see what drones can do,  
to test their limit and breakthrough,  
no right no wrong no rules for them, they're free...  
Let them go!*

Elsa of Arendelle (mod.)

*Interconnecting discussions of results are presented in this final chapter, based on the research performed throughout previous chapters, along with a brief reflection on the situation at the time the research ended, in mid 2016. Following those discussions, final conclusions and recommendations are drawn to conclude this entire research, which aims to define and evaluate systems for detecting and resolving possible mid-air conflicts of Unmanned Aerial Vehicles, specifically to support safe beyond visual line-of-sight operations in an integrated airspace. The chapter closes this dissertation with several suggestions for the continuation of this research.*

## 6.1. DISCUSSION

THIS dissertation started off with the definition of four research problems that prevent the realization of a safe integration of Unmanned Aerial Vehicles (UAVs) into the airspace system. Those problems, i.e., the airspace incompatibility, the UAV Conflict Detection and Resolution (CD&R) system diversity, the safety analysis difficulty, and the autonomous CD&R inadequacy, are all included in the main goal of this dissertation, written again in this section as follows:

**To define and evaluate systems for detecting and resolving possible mid-air conflicts of Unmanned Aerial Vehicles, specifically to support safe beyond visual line-of-sight operations in an integrated airspace.**

The goal is achieved within the four main chapters of this research with the definition of a taxonomy for UAV CD&R protocols along with a proposition of a multi-layered architecture for its implementation in Chapter 2, with an evaluation of safety using Monte Carlo simulations in a high density airspace in Chapter 3, and with the introduction of two novel CD&R algorithms for UAV Beyond the Visual-Line-of-Sight (BVLOS) operations in Chapters 4 and 5. This section discusses how the research problems are tackled by analyzing the interconnected results and conclusions of the chapters, along with a brief reflection on the current situation (mid 2016). An extra subsection is added, in the end of this section, to present discussions about the main methodology used throughout this research.

6

### 6.1.1. ON AIRSPACE INCOMPATIBILITY

Compared to back in mid 2011, when this research was initiated, UAVs are increasingly getting exposed to the general public. Regulations, as well as experiments, have been made which steadily define UAVs' airworthiness and widens their area of operations. Operator awareness of the regulations is also increasing as shown by the decline of drone sightings in unwanted areas, such as near to runways<sup>1</sup>, and the booming of registered drone owners, which have outnumbered the plane and helicopter owners<sup>2</sup>. At the same time, drone advocacy groups, consisting of many big player such as Alphabet's Google X, and Amazon Prime Air, help to push regulatory policies to allow UAV operations, especially for BVLOS<sup>3</sup>.

The current airspace system is still incompatible for UAVs, as indicated by the non-existence of commercial BVLOS operations, while on the other hand, the VLOS UAVs are flourishing. The main problem remains the same, that the procedures of CD&R, in the current (manned-flight) airspace management, are unfamiliar with how UAVs operate. As the newcomer, efforts to lessen the incompatibility should be more on the UAV

<sup>1</sup>McFarland, M. "Why America's drone problem may not be as bad as some think", June 2016, retrieved June 2016 from <https://www.washingtonpost.com/news/innovations/wp/2016/06/07/why-americas-drone-problem-may-not-be-as-bad-as-everyone-thinks/>

<sup>2</sup>Blake, A. "Drones registered with FAA outnumber manned aircraft at 325,000 and growing", February 2016, retrieved June 2016 from <http://www.washingtontimes.com/news/2016/feb/9/drones-registered-with-faa-outnumber-manned-aircraft/>

<sup>3</sup>Vanian, J. "New Drone Advocacy Group Launches With Cisco and CNN as Members", May 2016, retrieved June 2016 from <http://fortune.com/2016/05/03/commercial-drone-alliance-cisco-cnn/>

side, and therefore, adopting the current procedures of CD&R is the key requirement to a safe integration. This is the original reason of this dissertation in proposing an exhaustive multi-layered architecture for UAV CD&R system, indicating the relevancy of this research to the current situation. This architecture consists of layers, containing CD&R methods that are compatible and known with the manned flights, while also embracing those that are unique to UAV flights. Six layers are defined based on a comprehensive taxonomy, denoted as: (1) Procedural, (2) Manual, (3) Cooperative, (4) Non-cooperative (5) Escape, and (6) Emergency, ensuring that even in cases when an outer layer fails, there are still inner layers available to maintain safety.

Therefore, the proposed CD&R architecture from Chapter 2 can be an appropriate way to accelerate the integration process for commercial BVLOS UAVs. This view is in accordance with the project at NASA's Ames Research Center<sup>4</sup> that tests the first nationwide UAVs Traffic Management (UTM) system, which is able to track simultaneously 24 UAVs flying within Visual-Line-of-Sight (VLOS) in the lower airspace. The experiment apparently also demonstrates the first two layers of the proposed CD&R architecture, i.e., the Procedural and the Manual Layer. The remaining layers appear to match the project as well, as it will gradually test other capability levels including cooperative and non-cooperative safety assurance, and specific tasks for UAVs, such as news gathering and package delivery. The end result of this project is planned to be transferred to the FAA in 2019, which will be a great milestone in the progress of eliminating the incompatibility of UAV flights.

Furthermore, with the NASA UTM project continuation that will involve BVLOS flights, the results of Chapter 3 might give some insight on how the experiment can be conducted. For an area as large as the whole United States (9.8 million kilometer-square), using 24 UAVs are actually very conservative, since, according to the result in Chapter 3, for just an area with 8000 kilometer-square such as the sky above the city of New York Metro, there can exist 57 UAVs flying in one altitude level, while maintaining a certain Target Level of Safety (TLS) requirements of less than  $10^{-2}$  Near Mid Air Collision (NMAC) occurrences [7]. Therefore, testing a more localized UTM with higher density of UAV traffic is recommended.

### 6.1.2. ON UAV CD&R SYSTEM DIVERSITY

Currently, the diversity of CD&R preferences apparently only exists in research labs, since most of the available commercial UAVs rely only on their pilot for the task of mitigating conflicts and collisions. As the consequence of VLOS flight limitation, there is practically no need to have an autonomous CD&R system on-board, let alone one that is uniquely optimized for each UAV. While there is indeed a variation of pilot skills and UAV performance, the concern of diversity is not actualized yet to be managed or standardized.

The taxonomy in Chapter 2 is proposed more to anticipate the probable CD&R diversity in the future, once BVLOS flights of UAVs in the airspace are allowed. This situation is very much plausible due to at least three reasons. Firstly is due to the availability of various research in the CD&R systems, as it is presented in Chapter 2. Moreover, new CD&R approaches are constantly emerging with the innovation of airframes and sensors. The

<sup>4</sup>Atherton, K. D. "NASA is making a drone-traffic control system", April 2016, retrieved June 2016 from <http://www.popsci.com/nasa-drone-traffic-control>

second reason is the increasing interest on UAVs by 'big players', such as Alphabet, Amazon, Cisco, and CNN, which have also assembled as an advocacy group<sup>3</sup> with a main agenda to push for regulatory policies for their (various) BVLOS operations. Thirdly is the increasing value of the UAV industry in the world market, predicted to increase to \$127 billion by the 2020<sup>5</sup>, which in end attracts even more interested parties.

The proposed taxonomy, therefore, can aid both developers and authorities in deciding whether a UAV has an adequate CD&R system or not. Since it classifies approaches based on factors that directly affect the airspace management, the taxonomy can determine the role of a CD&R system in an overall mission, identifying redundancies, and spotting the system incompatibilities for an integrated airspace. For example, a system that uses the Potential Field Method [18–20] with a LASER range finder [12], a system that uses Visual Servoing method [21] with a camera, and a system that uses Velocity Obstacle Method[22–26] with an ultrasonic sensor [10], are in the same category of CD&R systems as long as they are autonomously avoiding obstacles in close range without any coordination.

Within a category in the taxonomy, however, variations on the detection and maneuver can still exist, for instance, the accuracy of a camera can differ from that of an ultrasonic sensor, or, while using the same Velocity Obstacle Method, the turning rate of two vehicles can vary. Hence, the CD&R variation across vehicles is an inseparable part of the heterogeneity of the future integrated airspace. This characteristic is featured in every simulation in Chapter 3 to derive safety parameters, and in Chapter 4 and 5 to validate the newly introduced SVO and 3DVO method, respectively.

### 6.1.3. ON UAV CD&R SYSTEM SAFETY

The fact that current regulations have not been easy for BVLOS flight reflects on the lingering dubiety in the safety of UAV operations from authorities and, by extension, the public. General media are rarely in favor of UAVs, as shown by many reports on drones flying too close to a passengers plane near airports<sup>6</sup>, or drones that obstruct firefighter's responding aircraft, which lead to a campaign 'if you fly, we can't' in California<sup>7</sup>. At the same time, many anti-UAV measures are being developed, such as the anti-drone guns<sup>8</sup>, or the drone catching eagles<sup>9</sup>.

To prove BVLOS flight safety, it is dubbed that the CD&R system needs to be able to reach a certain Target Level of Safety (TLS), which should be better or equivalent to the safety of manned-flight[7]. The exact quantitative value of the TLS and what tests need to be conducted on a CD&R system to demonstrate its fulfillment, however, have not been mentioned in any regulatory document. Only pilots are currently the subject

<sup>5</sup>Moskwa, W., "World drone market to near \$127 billion in 2020", May 2016, retrieved May 2016 from <http://www.sltrib.com/home/3871762-155/world-drone-market-to-near-127>

<sup>6</sup>Bachman, J., "Drones Are the New Threat to Airline Safety", April 2016, retrieved June 2016 from <http://www.bloomberg.com/news/articles/2016-04-04/drones-are-the-new-threat-to-airline-safety>

<sup>7</sup>Zorthian, J., "Drones Are a Big Problem for Firefighters Battling Massive Blazes", June 2016, retrieved June 2016 from <http://time.com/4383769/drones-firefighters-wildfires/>

<sup>8</sup>Novak, M., "These Anti-Drone Guns Are The Future of Messing With Your Neighbors", May 2016 in retrieved June 2016 from <http://gizmodo.com/these-anti-drone-guns-are-the-future-of-messing-with-yo-1777086208>

<sup>9</sup>Castle, S., "Dutch Firm Trains Eagles to Take Down High-Tech Prey: Drones", May 2016 retrieved June 2016 from <http://www.nytimes.com/2016/05/29/world/europe/drones-eagles.html>

of certification<sup>10</sup>, started in the end of 2016, which is to be expected since, during VLOS flight, the main system to mitigate collisions is, in fact, the pilot.

Hence, at the current moment, the only source of TLS quantification for UAVs flight is the research on safety analysis [7], including the method presented in Chapter 3. The main parameter commonly used to measure safety, is the frequency of the Near Mid-Air Collisions (NMAC) under the effect of a CD&R protocols. Due to the heterogeneity in the airspace, this parameter is difficult to obtain analytically, that this research utilizes an exhaustive series of Monte Carlo simulations instead. The simulation is conducted in a high density situation in order to converge the results rapidly in a reasonable number of samples. A Similar simulation method is also employed in the validation process of the methods introduced in Chapter 4 and 5. This dissertation proposes a target of NMAC occurrences to happen less than  $10^{-2}$  per hour, taken from the equivalent value in the history of manned flight.

As presented in Chapter 3, the distributed cooperative CD&R protocol is able to increase the maximum number of operating UAV in one flight level to almost ten times the number when no CD&R is applied, in order to maintain the NMAC frequency below the TLS requirement. A city like Chicago that has an area of more than five-thousand kilometer-square can have 45 UAVs flying independently at one altitude, and can be a whole lot if airspace flight levels are applied, such as described in [101] The much better result for the cooperative protocol in the chapter, compared to the non-cooperative one, also justifies the necessity of order in the airspace, which in this case is the implementation of the Right-of-way rules [86].

Simulation results, however, are not enough for public and authority to remove all their lingering doubts about UAV operational safety in an integrated airspace. Experiments, such as conducted by NASA<sup>4</sup>, are commonly more trusted and acceptable. Therefore, each results in this dissertation need to be reinforced with experimental conjugates, which already can be realized using the various test sites all over the globe. Since a full experiment for simulations, such as in Chapter 3, can be extremely unpractical, combinations of simulations and experiments is required to complement each other into one specific procedure to accurately measured the performance of a CD&R protocol.

#### 6.1.4. ON AUTONOMOUS CD&R SYSTEM INADEQUACY

Naturally, since they are not yet allowed to operate except within VLOS, there are not many examples of autonomous CD&R systems in current commercial UAVs. One of the very few examples is DJI's Geofencing feature, which automatically prevents their drones to fly or take off in locations that raise safety or security concerns, determined from a continuously updated on-line map<sup>11</sup>. DJI also has embedded an object detection and automatic avoidance ability for its newest drone, the Phantom 4, relying on forward-facing cameras that can recognize large objects<sup>12</sup>. The particular system works, regardless of the pilot skills, accurately in forward flying, but not as reliable in any other directions, as well as against small objects such as power lines. Despite these imperfection, the Phantom 4 is among the first commercial drones with a working autonomous

<sup>10</sup>Liptak, A., "The FAA Relaxes Some Rules For Commercial Drone Pilots", 2016, accessed June 2016, <http://gizmodo.com/the-faa-relaxes-some-rules-for-commercial-drone-pilots-1768692392>

CD&R system, which opens a lot more possibilities in its future development.

The examples reveal the underlying mindset of most of the UAVs CD&R system developments that are only optimized for a flight in a secluded area, instead of considering the characteristics of integrated airspace, as listed in Chapter 2. Presented also in the same chapter, a similar mindset is also present in the studies of autonomous CD&R systems, where most of the proposed methods are commonly focused on avoiding static obstacles in indoor applications. Some of them that actually focuses on dynamic obstacles, mostly only being demonstrated to avoid vehicles of the same type and with the same protocol, such as a swarming maneuver. This tendency persists mainly because VLOS UAVs, those that are allowed, do not really need such autonomous CD&R systems, and instead, they can rely solely on the pilot capability.

In order to change the mindset of secluded airspaces, this dissertation develops and tests two new CD&R algorithms based on the characteristics of the integrated airspace as listed in Chapter 2. The first algorithm is the Selective Velocity Obstacle (SVO) method, introduced in Chapter 4, an extension of the VO-method with additional criteria for implicit coordination. This CD&R method is developed based on the unlikeliness of the future airspace to exist without some sort of order, such as implementing common rules of the air. Chapter 5 introduces the Three-dimensional Velocity Obstacle (3DVO) method that represents the VO-method in three-dimensional space to obtain a much wider possibility for resolutions. Furthermore, taking account of a possibly uncoordinated encounter in the airspace, the 3DVO is equipped with an additional algorithm to anticipate adverse movements of the obstacle. These SVO and 3DVO methods are validated comprehensively using series of Monte Carlo simulations in a heterogeneous airspace, where speeds and avoidance preferences vary across vehicles.

Nevertheless, several experiments that do consider the integrated airspace characteristics have also been conducted in recent years, by cooperation between authorities and hopeful companies. The Pathfinder project by the FAA<sup>13</sup>, for example, collaborates with PrecisionHawks, one of the few companies they are currently working with, in testing the safety of its agricultural UAV and at the same time, building more acceptable regulations for BVLOS operation. The drone is accompanied by a Low Altitude Tracking and Avoidance System (LATAS), an ADS-B based dynamic on-board data system that can automatically guide the drone to land or turn if it gets too close to a forbidden area, or if a conventional aircraft suddenly appears. Another example is the experiment in Europe under the guidance of the Single European Sky ATM Research (SESAR) initiative<sup>14</sup>, focuses on ADS-B system based self-separation ability of several UAVs with addition of one manned-aircraft. The latest is the nationwide experiment conducted by NASA Ames<sup>4</sup> that has a similar idea to the multi-layered architecture proposed in Chap-

<sup>11</sup>Leswing, K., "Why Your Drone Can't Fly Near Airports Anymore", November 2015, retrieved in June 2016 from <http://fortune.com/2015/11/18/dji-geofencing-airport/>

<sup>12</sup>Gilbertson, S., "Review: DJI Phantom 4", April 2016, retrieved in June 2016 from <http://www.wired.com/2016/04/review-dji-phantom-4/>

<sup>13</sup>Atherthon, K.D., "FAA tests system to let drones Sense and Avoid obstacles", November 2015, retrieved in June 2016 from <http://www.popsci.com/faa-tests-drone-obstacle-avoidance-system>

<sup>14</sup>Stevenson, B., "UAVs and MSA carry out Spanish self-separation tests", May 2016, retrieved in June 2016 from <https://www.flightglobal.com/news/articles/uavs-and-msa-carry-out-spanish-self-separation-tests-425693/>

ter 2, that is, instead of only relying on one CD&R approach, UAVs can have multiple layers of safety that stretch from a centralized UTM system to an independent sense and avoid system. The SVO and 3DVO methods, therefore, can be a part of this experiment to support cooperative and non-cooperative BVLOS flights, which are already planned as the continuation of the experiment for the end of 2016.

### 6.1.5. ON RESEARCH METHODOLOGY

There are two methodologies that keep recurring in the previous discussions and become the mathematical core of this dissertation in achieving its main goal. The first is the Velocity Obstacle method (VO-method) [22–26] that is the base of all CD&R algorithms proposed in this dissertation. The second methodology is the Monte Carlo simulation that is used to test and validate the premises of all CD&R methods in the chapters.

#### THE VELOCITY OBSTACLE METHOD

Instead of generating one specific solution, the main feature of the VO-method is providing avoidance criteria to determine whether an ownship is in a conflict or not. Maneuvers for avoidance, therefore, are generated based on that criteria, in conjunction with the ownship dynamics and a chosen strategy. In this dissertation, the ownship dynamics are represented by a fix turning rate value, while the strategy is determined by the starting point of avoidance and the intended Closest Point of Approach (CPA). Heterogeneity, therefore, can easily be modeled by diversifying those parameters in each vehicle, on top of the already diverse initial speeds and headings. The maneuver generated is a reactive maneuver, which is based only on the instantaneous encounter geometry, i.e., the positions and velocities of every involved vehicle, without any prediction or optimization processes.

In the UAV domain, as well as in general robotics, the VO-method is not as popular as its peers in the autonomous reactive avoidance methods, especially compared to methods such as the Potential Field method or the Optical Flow (or Visual Servoing) method. One of the reasons is because it is commonly regarded as a visualization tool of relative constraints between encountering vehicles, rather than a generator of specific avoidance directives. Another reason is that the method requires two states from the obstacle, i.e., the position and velocity, which warrants either more sensors on-board, or more computational time for an additional derivative process. Hence, the VO-method, and other methods with similar traits, are more common in the field of displays and instruments that rely on a dependent surveillance system, such as radio communication or ADS-B, to assist pilots of aircraft and ships in making their decision [64].

Considering its natural ability to handle multiple moving (dynamic) obstacles simultaneously, the VO-method is more appropriate for an integrated airspace than other autonomous avoidance methods. This potential is the main reason the method is chosen as the basis of the Selective Velocity Obstacle (SVO) method and the Three-dimensional VO-method (3DVO), introduced in Chapter 4 and 5, respectively. The two novel methods handle the problem in the integrated airspace, specifically for the Cooperative and Escape layers of the CD&R procedures prescribed in Chapter 2. With the satisfying simulation results throughout chapters in this dissertation, there is an open possibility to use the VO-method and its extension in real autonomous flights. While several experi-

ment have already been conducted to test the method in actual flight, a lot more tests are required specifically for BVLOS flights, before a VO-method based CD&R system can be mature enough to ensure safety in an integrated airspace.

#### THE MONTE CARLO SIMULATION

Monte Carlo simulation is a numerical method to derive certain parameters from repeated but randomly initialized simulation samples of a defined model [128]. In this dissertation, Monte Carlo simulations are mainly used to derive two safety parameters of the airspace, i.e., the frequency of the Near Mid-Air Collision (NMAC), and the frequency of the Mid-Air Collision (MAC). Those two parameters are especially difficult to determine in a heterogeneous airspace setup, where each vehicle independently reacts to each other based on their own CD&R preferences. Available analytical solutions in literature [28, 99–101] on the other hand, are not applicable in this dissertation since they mostly assume fix flight paths of vehicles during simulations.

To be able to perform the Monte Carlo simulation, a model of the heterogeneous airspace needs to be built, in which inputs can be randomly initialized for each vehicle. In this dissertation, the model is implemented in the MATLAB programming environment as a script that is used and continuously improved throughout Chapter 3, 4 and 5. To create numerous variations of airspace conditions, the vehicles can be independently initialized in either two or three dimensional space, with specific positions, headings, and speeds. The VO-method is used as the base of the CD&R system, distributed in each vehicle with its own preferences of avoidance distance and CPA. CD&R protocols in the airspace, such as following an implicit rule for coordination, or being truly uncoordinated, can also be selected in the model.

The main downside of using Monte Carlo simulations is its requirement for a considerably large amount of samples and computational time to obtain a significant result, especially when it needs to collect collisions in a realistic airspace setup. This is shown especially in the validation of the SVO in Chapter 4, where for the cases with only five UAVs randomly initiated in a  $5 \times 5$  kilometer-square area, more than 36 hours are needed to simulate all  $10^6$  samples, on a standard desktop PC. The significance of the result is further reduced by the number of unavailing cases in which vehicle are initialized in diverging directions from each other and immediately leave the area of interest without any chance to perform an avoidance maneuver. Nevertheless, relative performances, by comparison with the same setup of Monte Carlo simulation using other CD&R methods, can still be obtained to measure the improvement offered by the SVO.

Chapter 5 attempts to reduce the unavailing cases in its 3DVO validation, by using a super conflict configurations, i.e, eight evenly distributed vehicles converging to a point in a three-dimensional space. While being less realistic, the super conflict strategy succeeded in reducing the number of simulations needed to reach convergence to less than  $2.5 \times 10^4$  samples. Chapter 3, on the other hand, initializes the UAVs randomly but in a high density airspace to increase the number of conflicts, and with a Periodic Boundary Condition setup to suppress the unavailing cases. The final results from several high densities are then charted to obtain their relation with the less dense but more realistic airspace. This technique allows for the validation of a CD&R protocol in achieving a certain Target Level of Safety (TLS) by using the Monte Carlo simulation method in a reasonable amount of computational time.

Throughout the dissertation, whilst being the main method for validation, the Monte Carlo simulation also aids in the development of the SVO and 3DVO method, by quickly revealing unpredicted scenarios in which the two methods failed, allowing the isolation of bugs in the algorithm. With the continuously improving computer performances, Monte Carlo simulation has potential to be validate a CD&R algorithm, especially for autonomous operations where conflicts can be triggered by interaction between different algorithms without any human supervision. Moreover, with actual flight experiments that are most likely limited and costly, the Monte Carlo simulation will be a most viable method to validate CD&R protocol to support BVLOS operation in an integrated airspace.

## 6.2. FINAL CONCLUSION

On the basis of the research performed in this dissertation, it can be concluded that safe integration of Unmanned Aerial Vehicles (UAVs) into the airspace is very much feasible. This is elaborated further in the following paragraphs in three categories for the key stakeholders in this field, along with specific recommendations for implementing the dissertation results.

### FOR RESEARCHERS

This dissertation has demonstrated a method to determine the number of UAVs that can possibly fly in a certain area, by determining the NMAC frequency using Monte Carlo simulations. The method has been tested for three types of distributed CD&R protocols, i.e., no CD&R, where no avoidance is conducted, uncoordinated, where the preferences of avoidance in each vehicle are randomized, and implicitly-coordinated, where every avoidance is governed by a common set of rules. The simulation method is developed especially to overcome the difficulty of using analytic methods, such as the Gas Model, in predicting NMAC occurrences in an airspace under the influence of CD&R protocols. The large number of samples and long processing time that are commonly needed in a Monte Carlo simulation setup are reduced by simulating extreme conditions that promote collisions, such as in high density or super conflict setups. As it has been demonstrated in this dissertation, the results can be scaled to a realistic airspace condition in a specific area.

A taxonomy for UAV CD&R systems has been built, defining feasible generic approaches for operation in an integrated airspace, that can be attributed to any CD&R method in literature, based on their type of surveillance, coordination, maneuver and autonomy. Six of the generic approaches have been arranged into an example of a multi-layered architecture, providing safety with a fail-safe concept: when one approach fails, there are still others available to ensure safety. The diverse CD&R approaches in literature, therefore, can be implemented accordingly based on their roles in the entire operation of UAVs, especially in Beyond Visual Line-of-Sight (BVLOS) flights. Being adopted from, and hence compatible with, the current manned-flight CD&R arrangement, the use of this multi-layered architecture can potentially accelerate integration of UAVs into the airspace.

Two novel distributed autonomous CD&R methods, which have been designed with consideration of the characteristics of an integrated airspace, have been introduced, formalized, and validated in this dissertation. The first one is the Selective Velocity Obstacle (SVO) method that handles conflicts with cooperative vehicles, which share flight data with each other and conduct avoidance based on a set of common rules, such as the manned-flight right-of-way rules. The second method introduced is the Three-Dimensional Velocity Obstacle (3DVO) method that mitigates collisions in a short range without any coordination between vehicles, such that it requires to exploit the remaining space in a three-dimensional manner, taking into account the possible adverse maneuvers from the opposing vehicles. Both methods have been validated by series of Monte Carlo simulations in a stressful heterogeneous airspace setup, in which they were able to significantly reduce the occurrence of NMACs and MACs, and hence are promising to support BVLOS operation in an integrated airspace.

#### FOR UAV CD&R DEVELOPERS

The taxonomy proposed in this dissertation has revealed that most of the available CD&R approaches in literature are inadequate for a UAV BVLOS operation in an integrated airspace, since they have only been developed for flights in a secluded environment. Therefore, it is important for UAV developers to choose approaches that have more consideration for characteristics of an integrated airspace such as the heterogeneity of UAV performances, missions, and CD&R preferences. Nevertheless, some of the inadequate approaches can be extended to fit the integration scheme, such as demonstrated and validated in this dissertation with the extension of the VO-method into SVO and 3DVO methods.

Both the SVO and 3DVO method have been designed based on the requirements set in the proposed multi-layered architecture, specifically the Cooperative and Escape layers. Similar procedures can be applied to extend other algorithms, or to develop a whole new algorithm, for other layers. This will enrich the available CD&R approaches that can be selected for UAV operation in an integrated airspace.

#### FOR PUBLIC AND AUTHORITIES

This dissertation has demonstrated the possibility of reaching the airspace's Target Level of Safety (TLS) by resorting to an autonomous Conflict Detection and Resolution (CD&R) system in an extremely high density setup. This has been validated by numerous simulations in a heterogeneous airspace, where the UAVs fly with diverse preferences for their CD&R system, on top of having variations in their speeds and headings. The low risk of UAV operations has been demonstrated even more by the rarity of near mid-air collision (NMAC) and mid-air collision (MAC) occurrences in all of the simulations, to the point that they need to resort to an artificially exaggerated setup in order to measure safety. Hence, the method using Monte Carlo simulation has been proven to be a powerful tool to test the algorithm in all possible conditions and can be the most defining certification tool for an autonomous CD&R algorithm of UAVs operating in such a heterogeneous airspace, in which experiments in actual flights can be unpractical.

Simulations, experiments, or the combination of both, however, might never perfectly result in a satisfying validation of a CD&R system in ensuring safety. Therefore, at one point perhaps it is best for the authorities to begin accommodating BVLOS flights of

UAVs, integrated into the airspace, that will allow both UAV operators and CD&R developers to gain experience and mature their systems in real situations. This is comparable with the history of deregulation in manned-flight, which actually creates a competitive environment that pushes both manufacturers and operators to continuously strive for safety improvements.

### 6.3. FUTURE WORKS

Along with the obtained results, several challenges and limitations in methodologies throughout the chapters are noted. These are the basis for the formulation of future works that can be done to extend the research in this dissertation, presented in the following paragraphs.

The proposed multi-layered CD&R architecture in Chapter 2 can be more practical with definitions of physical thresholds between layers, such as the distance, time-to-collision, or combinations between them. These thresholds, which might need to be defined specifically for each type of UAV, are also required to conduct a comprehensive simulation to quantitatively validate such an architecture.

While being set to mimic the heterogeneous situation in an integrated airspace, simulations in this dissertation have neglected several details that are prone to happen in real flight. The SVO method implementation in Chapter 4, for instance, can be further validated if the simulation includes the dynamics of each vehicle, uncertainties in measurements, and disturbances from the environment. Furthermore, a three-dimensional space representation of the SVO method is also recommended, due to the characteristics of UAV flights and missions. This extension can also be applied to widen the scope of the NMAC and MAC frequencies results from Chapter 3.

The 3DVO method, on the other hand, has offered a three-dimensional uncoordinated maneuver that fits with the agility of UAVs. However, as a reactive short ranged avoidance algorithm, it is most critical for the method to incorporate vehicle dynamics and environmental disturbances, since it can result in a significantly different outcome. Furthermore, the heterogeneity of CD&R systems can be more realistically represented if the avoidance planes in the 3DVO method are defined for each type of UAV, corresponding directly to each of the UAVs' performance.

Other extensions of the VO-method can be made for other layers in the proposed architecture. The Non-cooperative layer, for instance, can be filled by the SVO-method with an addition of algorithms to anticipate adverse movement of the counterparts, such as the Buffer Zone that is explained in Chapter 5. Likewise, the Manual layer can be aided using the VO-method, if the conflict imminence, which corresponds to the VO set base angle, can be transferred as a haptic feedback to the controller on ground.

Conducting experiments to strengthen the results in SVO and 3DVO implementation is also suggested, especially in testing an actual flight where a UAV autonomously interacts with the diverse traffic in the airspace. This is particularly to identify factors that might not be predicted in the mathematical model of the simulations, such as random disturbances from the systems and from the environments. The interaction between the pilot and the autonomous system can also be analyzed in this experiment setup.

These works are warranted, as it has also been stated in many recent parallel studies, to mature the autonomous CD&R concepts, especially for BVLOS flights. Nevertheless, this dissertation has achieved its main goal, contributing in the definition and evaluation of possible CD&R systems, in order to support safe UAV operations in an integrated airspace.

# REFERENCES

- [1] R. A. Hull and R. B. Bourne, *Radio Control of Model Aircraft*, QST **10**, 9 (October, 1937).
- [2] F. Gudaitis, *The First Days of Radio Control*, Model Airplane News Airplane News Magazine **1**, 9 (January, 1994).
- [3] M. T. DeGarmo and G. M. Nelson, *Prospective Unmanned Aerial Vehicle Operations in the Future National Airspace System*, in *AIAA 4th Aviation Technology, Integration, and Operations Forum, ATIO* (AIAA, 2004) pp. 172–179, AIAA 2004-6243, doi:10.2514/6.2004-6243.
- [4] *Operation and Certification of Small Unmanned Aircraft Systems; Final Rule, Federal Register Vol. 81 No. 124, (June 28, 2016), 14 CFR Parts 21, 43, 61, et al.*, DEPARTMENT OF TRANSPORTATION, Federal Aviation Administration ().
- [5] *Remotely Piloted Aircraft Systems (RPAS) in The Netherlands*, Ministerie van Infrastructuur en Milieu, Inspectie Leefomgeving en Transport ().
- [6] *CAP722, Unmanned Aircraft System Operations in UK Airspace – Guidance*, UK Civil Aviation Authority ().
- [7] K. Dalamagkidis, K. P. Valavanis, and L. A. Piegl, *On Integrating Unmanned Aircraft Systems into the National Airspace System*, in *International Series on Intelligent Systems, Control, and Automation: Science and Engineering*, Vol. 36 (Springer Science+Business Media, 2009) 1st ed., doi: 10.1007/978-94-007-2479-2.
- [8] M. J. Kochenderfer, J. E. Holland, and J. P. Chryssanthacopoulos, *Next Generation Airborne Collision Avoidance System*, Lincoln Laboratory Journal **19**, 55 (2012), doi: 10.2747/1548-1603.48.1.24.
- [9] G. Fasano, D. Accardo, A. Moccia, G. Carbone, U. Ciniglio, F. Corraro, and S. Lungo, *Multi-sensor-based Fully Autonomous Non-cooperative Collision Avoidance System for Unmanned Air Vehicles*, Journal of Aerospace Computing, Information and Communication **5**, 338 (2008), doi: 10.2514/1.35145.
- [10] J. Müller, A. Ruiz, and I. Wieser, *Safe and Sound: A Robust Collision Avoidance Layer for Aerial Robots based on Acoustic Sensors*, in *Record - IEEE PLANS, Position Location and Navigation Symposium* (2014) pp. 1197–1202, doi: 10.1109/PLANS.2014.6851492.

- [11] E. Tijs, G. De Croon, J. Wind, B. Remes, C. De Wagter, H.-E. De Bree, and R. Ruijsink, *Hear-and-Avoid for Micro Air Vehicles*, in *International Micro Air Vehicle conference and competitions (IMAV 2010)* (2010).
- [12] S. Hrabar, *Reactive Obstacle Avoidance for Rotorcraft UAVs*, in *IEEE International Conference on Intelligent Robots and Systems* (2011) pp. 4967–4974, doi: 10.1109/IROS.2011.6094560.
- [13] A. Moses, M. Rutherford, M. Kontitsis, and K. Valavanis, *UAV-borne X-band RADAR for Collision Avoidance*, *Robotica* **32**, 97 (2014), doi: 10.1017/S0263574713000659.
- [14] R. Beard, T. McLain, M. Goodrich, and E. Anderson, *Coordinated Target Assignment and Intercept for Unmanned Air Vehicles*, *Robotics and Automation, IEEE Transactions on* **18**, 911 (2002), doi:10.1109/TRA.2002.805653.
- [15] H. bin Duan, X. yin Zhang, J. Wu, and G. jun Ma, *Max-Min Adaptive Ant Colony Optimization Approach to Multi-UAVs Coordinated Trajectory Replanning in Dynamic and Uncertain Environments*, *Journal of Bionic Engineering* **6**, 161 (2009), doi:10.1016/S1672-6529(08)60113-4.
- [16] R. Klaus and T. McLain, *A Radar-Based, Tree-Branching Sense and Avoid System for Small Unmanned Aircraft*, in *AIAA Guidance, Navigation, and Control Conference 2013* (AIAA, Boston, MA, 2013) aIAA 2013-4789, doi:10.2514/6.2013-4789.
- [17] I. Nikolos, K. Valavanis, N. Tsourveloudis, and A. Kostaras, *Evolutionary Algorithm Based Offline/Online Path Planner for UAV Navigation*, *IEEE Transactions on Systems, Man, and Cybernetics, Part B: Cybernetics* **33**, 898 (2003), doi: 10.1109/TSMCB.2002.804370.
- [18] Y. Kitamura, T. Tanaka, F. Kishino, and M. Yachida, *3-D Path Planning in a Dynamic Environment using an Octree and an Artificial Potential Field*, in *Intelligent Robots and Systems 95. 'Human Robot Interaction and Cooperative Robots', Proceedings. 1995 IEEE/RSJ International Conference on*, Vol. 2 (1995) pp. 474–481 vol.2, doi: 10.1109/IROS.1995.526259.
- [19] T. Lam, H. Boschloo, M. Mulder, and M. Van Paassen, *Artificial Force Field for Haptic Feedback in UAV Teleoperation*, *Systems, Man and Cybernetics, Part A: Systems and Humans, IEEE Transactions on* **39**, 1316 (2009), doi: 10.1109/TSMCA.2009.2028239.
- [20] T. M. Lam, M. Mulder, M. van Paassen, J. Mulder, and F. van der Helm, *Force-Stiffness Feedback in Uninhabited Aerial Vehicle Teleoperation with Time Delay*, *AIAA Journal of Guidance, Control, and Dynamics* **32**, 821 (2009), doi: 10.2514/1.40191.
- [21] A. Beyeler, J.-C. Zufferey, and D. Floreano, *Vision-based Control of Near-obstacle Flight*, *Autonomous Robots* **27**, 201 (2009), doi: 10.1109/CDC.2002.1184695.

- [22] P. Fiorini and Z. Shiller, *Motion Planning in Dynamic Environments Using Velocity Obstacles*, The International Journal of Robotics Research **17**, 760 (1998), doi: 10.1177/027836499801700706.
- [23] B. Kluge and E. Prassler, *Recursive Probabilistic Velocity Obstacles for Reflective Navigation*, in *Field and Service Robotics*, Springer Tracts in Advanced Robotics, Vol. 24, edited by S. Yuta, H. Asama, E. Prassler, T. Tsubouchi, and S. Thrun (Springer Berlin Heidelberg, 2006) pp. 71–79, doi: 10.1007/10991459\_8.
- [24] J. van der Berg, M. Lin, and D. Manocha, *Reciprocal Velocity Obstacles for Real-Time Multi-Agent Navigation*, in *International Conference on Robotics and Automation* (IEEE, Pasadena, CA, USA, 2008) doi:10.1109/ROBOT.2008.4543489.
- [25] S. B. J. van Dam, M. Mulder, and M. Van Paassen, *Ecological Interface Design of a Tactical Airborne Separation Assistance Tool*, Systems, Man and Cybernetics, Part A: Systems and Humans, IEEE Transactions on **38**, 1221 (2008), doi: 10.1109/TSMCA.2008.2001069.
- [26] J. Snape, J. van den Berg, S. Guy, and D. Manocha, *The Hybrid Reciprocal Velocity Obstacle*, Robotics, IEEE Transactions on **27**, 696 (2011), doi: 10.1109/TRO.2011.2120810.
- [27] P. G. Reich, *Analysis of Long-Range Air Traffic Systems: Separation Standards — I*, The Journal of Navigation **50**, 436 (1997), doi:10.1017/S0373463300019068.
- [28] G. May, *A Method for Predicting the Number of Near Mid-Air Collisions in a Defined Airspace*, Operational Research Quarterly (1970-1977) **22**, 237 (1971), doi:10.2307/3007993.
- [29] B. Alexander, *Aircraft density and midair collision*, Proceedings of the IEEE **58**, 377 (1970), doi:10.1109/PROC.1970.7643.
- [30] *Federal Aviation Regulations (FAR) Chapter I, Designation Of Class A, Class B, Class C, Class D, And Class E Airspace Areas; Airways; Routes; And Reporting Points*, Federal Aviation Administration ().
- [31] *NextGen Implementation Plan 2015*, Federal Aviation Administration.
- [32] *European ATM Master Plan*, European Union and Eurocontrol.
- [33] L. F. Winder and J. K. Kuchar, *Evaluation of Collision Avoidance Maneuvers for Parallel Approach*, AIAA Journal of Guidance, Control, and Dynamics **22**, 801 (1999), doi: 10.2514/2.44818.
- [34] M. Prandini, J. Hu, J. Lygeros, and S. Sastry, *A Probabilistic Approach to Aircraft Conflict Detection*, Intelligent Transportation Systems, IEEE Transactions on **1**, 199 (2000), doi:10.1109/6979.898224.
- [35] J. M. Hoekstra, R. C. J. Ruijgrok, and R. N. H. W. van Gent, *Free Flight in a Crowded Airspace ?* in *3rd USA/Europe Air Traffic Management R & D Seminar - Proceedings* (EUROCONTROL, Napoli, 2000).

- [36] A. Bicchi and L. Pallottino, *On Optimal Cooperative Conflict Resolution for Air Traffic Management Systems*, Intelligent Transportation Systems, IEEE Transactions on **1**, 221 (2000).
- [37] C. Tomlin, I. Mitchell, and R. Ghosh, *Safety Verification of Conflict Resolution Manoeuvres*, Intelligent Transportation Systems, IEEE Transactions on **2**, 110 (2001), doi:10.1109/6979.928722.
- [38] Z.-H. Mao, E. Feron, and K. Bilimoria, *Stability and Performance of Intersecting Aircraft Flows under Decentralized Conflict Avoidance rules*, Intelligent Transportation Systems, IEEE Transactions on **2**, 101 (2001), doi:10.1109/6979.928721.
- [39] J. Hoekstra, R. van Gent, and R. Ruigrok, *Designing for Safety: the Free Flight Air Traffic Management Concept*, Reliability Engineering & System Safety **75**, 215 (2002), doi: 10.1016/S0951-8320(01)00096-5.
- [40] L. Pallottino, E. Feron, and A. Bicchi, *Conflict Resolution Problems for Air Traffic Management Systems Solved with Mixed Integer Programming*, Intelligent Transportation Systems, IEEE Transactions on **3**, 3 (2002), doi:10.1109/6979.994791.
- [41] D. Rathbun, S. Kragelund, A. Pongpunwattana, and B. Capozzi, *An Evolution Based Path Planning Algorithm for Autonomous Motion of a UAV through Uncertain Environments*, in *Digital Avionics Systems Conference, 2002. Proceedings. The 21st*, Vol. 2 (2002) pp. 8D2-1-8D2-12 vol.2, doi:10.1109/DASC.2002.1052946.
- [42] A. Richards and J. How, *Model Predictive Control of Vehicle Maneuvers with Guaranteed Completion Time and Robust Feasibility*, in *American Control Conference, 2003. Proceedings of the 2003*, Vol. 5 (2003) pp. 4034-4040 vol.5, doi:10.1109/ACC.2003.1240467.
- [43] R. A. Paielli, *Modeling Maneuver Dynamics in Air Traffic Conflict Resolution*, AIAA Journal of Guidance, Control, and Dynamics **26**, 407 (2003), doi: 10.2514/2.5078.
- [44] H. I. Yang and Y. J. Zhao, *Trajectory Planning for Autonomous Aerospace Vehicles amid Known Obstacle and Conflicts*, AIAA Journal of Guidance, Control, and Dynamics **27**, 997 (2004), doi: 10.2514/1.12514.
- [45] R. Teo, J. Jang, and C. Tomlin, *Automated Multiple UAV Flight - The Stanford DragonFly UAV Program*, in *Proceedings of the IEEE Conference on Decision and Control*, Vol. 4 (2004) pp. 4268-4273, doi: 10.1109/CDC.2004.1429422.
- [46] A. Richards and J. How, *Decentralized Model Predictive Control of Cooperating UAVs*, in *Proceedings of the IEEE Conference on Decision and Control*, Vol. 4 (2004) pp. 4286-4291, doi: 10.1109/CDC.2004.1429425.
- [47] C. Le Tallec, *VFR General Aviation Aircraft and UAV Flights Deconfliction*, Aerospace Science and Technology **9**, 495 (2005), doi: 10.1016/j.ast.2005.01.001.

- [48] T. McGee, R. Sengupta, and K. Hedrick, *Obstacle Detection for Small Autonomous Aircraft Using Sky Segmentation*, in *Robotics and Automation, 2005. ICRA 2005. Proceedings of the 2005 IEEE International Conference on* (2005) pp. 4679–4684, doi:10.1109/ROBOT.2005.1570842.
- [49] A. Visintini, W. Glover, J. Lygeros, and J. Maciejowski, *Monte Carlo Optimization for Conflict Resolution in Air Traffic Control*, *Intelligent Transportation Systems, IEEE Transactions on* **7**, 470 (2006), doi:10.1109/TITS.2006.883108.
- [50] F. Borrelli, D. Subramanian, A. Raghunathan, and L. Biegler, *MILP and NLP Techniques for Centralized Trajectory Planning of Multiple Unmanned Air Vehicles*, in *Proceedings of the American Control Conference*, Vol. 2006 (2006) pp. 5763–5768, doi: 10.1109/ACC.2006.1657644.
- [51] M. Christodoulou and S. Kodaxakis, *Automatic Commercial Aircraft-collision Avoidance in Free Flight: the Three-dimensional Problem*, *Intelligent Transportation Systems, IEEE Transactions on* **7**, 242 (2006), doi:10.1109/TITS.2006.874684.
- [52] A. Kelly, A. Stentz, O. Amidi, M. Bode, D. Bradley, A. Diaz-Calderon, M. Happold, H. Herman, R. Mandelbaum, T. Pilarski, P. Rander, S. Thayer, N. Vallidis, and R. Warner, *Toward Reliable Off Road Autonomous Vehicles Operating in Challenging Environments*, *International Journal of Robotics Research* **25**, 449 (2006), doi: 10.1177/0278364906065543.
- [53] Z.-H. Mao, D. Dugail, and E. Feron, *Space Partition for Conflict Resolution of Intersecting Flows of Mobile Agents*, *Intelligent Transportation Systems, IEEE Transactions on* **8**, 512 (2007), doi:10.1109/TITS.2007.902646.
- [54] A. Zeitlin and M. McLaughlin, *Safety of Cooperative Collision Avoidance for Unmanned Aircraft*, *IEEE Aerospace and Electronic Systems Magazine* **22**, 9 (2007), doi: 10.1109/MAES.2007.351714.
- [55] J. W. Langelaan, *State Estimation for Autonomous Flight in Cluttered Environments*, *AIAA Journal of Guidance, Control, and Dynamics* **30**, 1414 (2007), doi:10.2514/1.27770.
- [56] S. Bouabdallah and R. Siegwart, *Full Control of a Quadrotor*, in *IEEE International Conference on Intelligent Robots and Systems* (2007) pp. 153–158, doi: 10.1109/IROS.2007.4399042.
- [57] K. Treleaven and Z.-H. Mao, *Conflict Resolution and Traffic Complexity of Multiple Intersecting Flows of Aircraft*, *Intelligent Transportation Systems, IEEE Transactions on* **9**, 633 (2008), doi:10.1109/TITS.2008.2006771.
- [58] J.-W. Park, H.-D. Oh, and M.-J. Tahk, *UAV Collision Avoidance Based on Geometric Approach*, in *Proceedings of the SICE Annual Conference* (2008) pp. 2122–2126, doi: 10.1109/SICE.2008.4655013.

- [59] A. Vela, S. Solak, J. Clarke, W. Singhose, E. Barnes, and E. Johnson, *Near Real-Time Fuel-Optimal En Route Conflict Resolution*, Intelligent Transportation Systems, IEEE Transactions on **11**, 826 (2010), doi:10.1109/TITS.2010.2051028.
- [60] L. Peng and Y. Lin, *Study on the Model for Horizontal Escape Maneuvers in TCAS*, Intelligent Transportation Systems, IEEE Transactions on **11**, 392 (2010), doi:10.1109/TITS.2010.2044790.
- [61] D. Sislak, P. Volf, and M. Pechoucek, *Agent-Based Cooperative Decentralized Airplane-Collision Avoidance*, Intelligent Transportation Systems, IEEE Transactions on **12**, 36 (2011), doi:10.1109/TITS.2010.2057246.
- [62] S. Devasia, D. Iamratanakul, G. Chatterji, and G. Meyer, *Decoupled Conflict-Resolution Procedures for Decentralized Air Traffic Control*, Intelligent Transportation Systems, IEEE Transactions on **12**, 422 (2011), doi:10.1109/TITS.2010.2093574.
- [63] M. Lupu, E. Feron, and Z.-H. Mao, *Influence of Aircraft Maneuver Preference Variability on Airspace Usage*, Intelligent Transportation Systems, IEEE Transactions on **12**, 1446 (2011), doi:10.1109/TITS.2011.2159267.
- [64] J. Ellerbroek, M. Visser, S. B. J. van Dam, M. Mulder, and M. M. van Paassen, *Design of an Airborne Three-Dimensional Separation Assistance Display*, IEEE Transactions on Systems, Man, and Cybernetics, part A: Systems and Humans **41**, 863 (2011), doi: 10.1109/TSMCA.2010.2093890.
- [65] G. C. H. E. De Croon, C. De Wagter, B. D. W. Remes, and R. Ruijsink, *Sky Segmentation Approach to Obstacle Avoidance*, in *Aerospace Conference, 2011 IEEE* (2011) pp. 1–16, doi:10.1109/AERO.2011.5747529.
- [66] A. Mujumdar and R. Padhi, *Reactive Collision Avoidance Using Nonlinear Geometric and Differential Geometric Guidance*, AIAA Journal of Guidance, Control, and Dynamics **34**, 303 (2011), doi: 10.2514/1.50923.
- [67] R. B. Patel and P. J. Goulart, *Trajectory Generation for Aircraft Avoidance Maneuvers Using Online Optimization*, AIAA Journal of Guidance, Control, and Dynamics **34**, 218 (2011), doi: 10.2514/1.49518.
- [68] C. G. Prevost, A. Desbiens, E. Gagnon, and D. Hodouin, *Unmanned Aerial Vehicle Optimal Cooperative Obstacle Avoidance in a Stochastic Dynamic Environment*, Journal of Guidance, Control, and Dynamics **34**, 29 (2011), doi: 10.2514/1.50800.
- [69] R. Chipalkatty, P. Twu, A. Rahmani, and M. Egerstedt, *Merging and Spacing of Heterogeneous Aircraft in Support of NextGen*, Journal of Guidance, Control, and Dynamics **35**, 1637 (2012), doi:10.2514/1.54076.
- [70] G. Chowdhary, D. M. Sobers Jr., C. Pravitra, C. Christmann, A. Wu, H. Hashimoto, C. Ong, R. Kalghatgi, and E. N. Johnson, *Self-Contained Autonomous Indoor Flight with Ranging Sensor Navigation*, Journal of Guidance, Control and Dynamic **35**, 1843 (2012), doi:10.2514/1.55410.

- [71] K. J. Obermeyer, P. Oberlin, and S. Darbha, *Sampling-Based Path Planning for a Visual Reconnaissance Unmanned Air Vehicle*, Journal of Guidance, Control, and Dynamics **35**, 619 (2012), doi: 10.2514/1.48949.
- [72] G. De Croon, E. De Weerd, C. De Wagter, B. Remes, and R. Ruijsink, *The Appearance Variation Cue for Obstacle Avoidance*, Robotics, IEEE Transactions on **28**, 529 (2012), doi:10.1109/TRO.2011.2170754.
- [73] R. D. Hurley, R. Lind, and J. J. Kehoe, *A Torus Based Three Dimensional Motion Planning Model for Very Maneuverable Micro Air Vehicles*, in *AIAA Guidance, Navigation, and Control Conference 2013* (AIAA, Boston, MA, 2013) aIAA 2013-4938, doi:10.2514/6.2013-4938.
- [74] J. Ellerbroek, K. C. R. Brantegem, M. M. van Paassen, and M. Mulder, *Design of a Co-Planar Airborne Separation Display*, IEEE Transactions on Human-Machine Systems **43**, 277 (2013), doi: 10.1109/TSMC.2013.2242888.
- [75] Y. I. Jenie, E.-J. v. Kampen, C. C. de Visser, J. Ellerbroek, and J. M. Hoekstra, *Selective Velocity Obstacle Method for Deconflicting Maneuvers Applied to Unmanned Aerial Vehicles*, Journal of Guidance, Control, and Dynamics **38**, 1140 (2015).
- [76] D. Jung and P. Tsiotras, *On-Line Path Generation for Unmanned Aerial Vehicles Using B-Spline Path Templates*, Journal of Guidance, Control, and Dynamics **36**, 1642 (2013), doi: 10.2514/1.60780.
- [77] S. Huang, E. Feron, G. Reed, and Z.-H. Mao, *Compact Configuration of Aircraft Flows at Intersections*, IEEE Transactions on Intelligent Transportation Systems **15**, 771 (2014), doi: 10.1109/TITS.2013.2287205.
- [78] L. Schmitt and W. Fichter, *Collision-avoidance Framework for Small Fixed-wing Unmanned Aerial Vehicles*, Journal of Guidance, Control, and Dynamics **37**, 1323 (2014), doi: 10.2514/1.G000226.
- [79] G. Mercado Velasco, C. Borst, J. Ellerbroek, M. van Paassen, and M. Mulder, *The Use of Intent Information in Conflict Detection and Resolution Models Based on Dynamic Velocity Obstacles*, Intelligent Transportation Systems, IEEE Transactions on **16**, 2297 (2015), doi:10.1109/TITS.2014.2376031.
- [80] CAP722, *Unmanned Aircraft System Operations in UK Airspace – Guidance*, UK Civil Aviation Authority.
- [81] ICAO Cir 328, *Unmanned Aircraft System (UAS)*, International Civil Aviation Organization.
- [82] Y. I. Jenie, E. van Kampen, J. Ellerbroek, and J. M. Hoekstra, *Conflict Detection and Resolution System Architecture for Unmanned Aerial Vehicles in Civil Airspace*, in *AIAA Infotech @ Aerospace, AIAA Scitech Conference 2015* (AIAA, Kissimmee, FL, 2015) aIAA 2015-0483, doi:10.2514/6.2015-0483.

- [83] J. Kuchar and L. Yang, *A Review of Conflict Detection and Resolution Modeling Methods*, *Intelligent Transportation Systems, IEEE Transactions on* **1**, 179 (2000), doi:10.1109/6979.898217.
- [84] P. Brooker, *Introducing Unmanned Aircraft Systems into a High Reliability ATC System*, *Journal of Navigation* **66**, 719 (2013), doi: 10.1017/S0373463313000337.
- [85] D. McCallie, J. Butts, and R. Mills, *Security Analysis of the ADS-B Implementation in the Next Generation Air Transportation System*, *International Journal of Critical Infrastructure Protection* **4**, 78 (2011), doi: 10.1016/j.ijcip.2011.06.001.
- [86] *Federal Aviation Regulations (FAR) Chapter I, subchapter F Air Traffic and General Operating Rules, Section 91.113 Right-of-way rules: Except water operations*, Federal Aviation Administration ().
- [87] J. M. Hoekstra, *Designing for Safety: the Free Flight Air Traffic Management concept*, (2001).
- [88] F. Barfield, *Autonomous Collision Avoidance. The Technical Requirements*, in *National Aerospace and Electronics Conference (NAECON)* (2000) pp. 808–813, doi:10.1109/NAECON.2000.894998.
- [89] A. Colozza and J. Dolce, *Initial Feasibility Assessment of a High Altitude Long Endurance Airship*, Tech. Rep. (NASA/CR—2003-212724, 2003).
- [90] A. Colozza and J. Dolce, *High-Altitude, Long-Endurance Airships for Coastal Surveillance*, Tech. Rep. (NASA/TM—2005-213427, 2005).
- [91] G. Romeo, G. Frulla, E. Cestino, and G. Corsino, *HELIPLAT: Design, Aerodynamic, Structural Analysis of Long-endurance Solar-powered Stratospheric Platform*, *Journal of Aircraft* **41**, 1505 (2004), doi: 10.2514/1.2723.
- [92] A. Girard, A. Howell, and J. Hedrick, *Border Patrol and Surveillance Missions using Multiple Unmanned Air Vehicles*, in *Decision and Control, 2004. CDC. 43rd IEEE Conference on*, Vol. 1 (2004) pp. 620–625 Vol.1, doi: 10.1109/CDC.2004.1428713.
- [93] T. Meester, T. Oomkens, and A. Rudgley, *The Future is Unmanned: Part 4*, *Maritime by Holland* **62**, 32 (2013).
- [94] D. Casbeer, R. Beard, T. McLain, S.-M. Li, and R. Mehra, *Forest Fire Monitoring with Multiple Small UAVs*, in *American Control Conference, 2005. Proceedings of the 2005* (2005) pp. 3530–3535 vol. 5, doi: 10.1109/ACC.2005.1470520.
- [95] E. Frew, T. McGee, Z. Kim, X. Xiao, S. Jackson, M. Morimoto, S. Rathinam, J. Padiyal, and R. Sengupta, *Vision-based Road-following using a Small Autonomous Aircraft*, in *Aerospace Conference, 2004. Proceedings. 2004 IEEE*, Vol. 5 (2004) pp. 3006–3015 Vol.5, doi: 10.1109/AERO.2004.1368106.

- [96] S. Herwitz, R. Berthold, S. Dunagan, D. Sullivan, M. Fladeland, and J. Brass, *UAV Homeland Security Demonstration*, in *AIAA 3rd "Unmanned Unlimited" Technical Conference, Workshop and Exhibit, Infotech@Aerospace Conferences* (AIAA, Illinois, MA, 2004) aIAA 2004-6473, doi:10.2514/6.2004-6473.
- [97] R. D'Andrea, *Guest Editorial Can Drones Deliver?* *Automation Science and Engineering*, IEEE Transactions on **11**, 647 (2014), doi: 10.1109/TASE.2014.2326952.
- [98] T. Netter and N. Francheschini, *A Robotic Aircraft that Follows Terrain using a Neuromorphic Eye*, in *Intelligent Robots and Systems, 2002. IEEE/RSJ International Conference on*, Vol. 1 (2002) pp. 129–134 vol.1, doi:10.1109/IRDS.2002.1041376.
- [99] W. Graham and R. H. Orr, *Terminal Air Traffic Flow and Collision Exposure*, Proceedings of the IEEE **58**, 328 (1970).
- [100] S. Endoh, *Flight Transportation Laboratory report R82-2 aircraft collision models*, (Massachusetts Institute of Technology, Cambridge, MA, 1982).
- [101] J. M. Hoekstra, J. Maas, M. Tra, and E. Sunil, *How Do Layered Airspace Design Parameters Affect Airspace Capacity and Safety?* in *Proceedings of the 7th International Conference on Research in Air Transportation (ICRAT 2016)* (AIAA, Philadelphia, PA, 2016).
- [102] R. Weibel and R. J. Hansman, *Safety Considerations for Operation of Different Classes of UAVs in the NAS*, in *AIAA 3rd "Unmanned Unlimited" Technical Conference, Workshop and Exhibit, Infotech@Aerospace Conferences* (AIAA, Chicago, IL, 2004) aIAA 2004-6421, doi:10.2514/6.2004-6421.
- [103] Y. I. Jenie, E.-J. van Kampen, and B. Remes, *Cooperative Autonomous Collision Avoidance System for Unmanned Aerial Vehicle*, in *Advances in Aerospace Guidance, Navigation and Control*, edited by Q. Chu, B. Mulder, D. Choukroun, E.-J. Kampen, C. Visser, and G. Looye (Springer Berlin Heidelberg, 2013) pp. 387–405, doi: 10.1007/978-3-642-38253-6\_24.
- [104] Y. I. Jenie, E. van Kampen, C. C. de Visser, and Q. P. Chu, *Selective Velocity Obstacle Method for Cooperative Autonomous Collision Avoidance System for UAVs*, in *AIAA Guidance, Navigation, and Control Conference 2013* (AIAA, Boston, MA, 2013).
- [105] *Advisory Circular No:20-165: Subject: Airworthiness Approval of Automatic Dependent Surveillance - Broadcast (ADS-B) Out Systems*, Federal Aviation Administration.
- [106] S. C. Mohleji and G. Wang, *Modeling ADS-B Position and Velocity Errors for Airborne Merging and Spacing in Interval Management Application*, in *Technical Paper* (The MITRE Corporation, 2010).
- [107] *FAA Aviation Safety Information Analysis and Sharing (ASIAS)*, .

- [108] A. Chakravarthy and D. Ghose, *Obstacle Avoidance in a Dynamic Environment: a Collision Cone Approach*, Systems, Man and Cybernetics, Part A: Systems and Humans, IEEE Transactions on **28**, 562 (1998), doi:10.1109/3468.709600.
- [109] L. Schmitt and W. Fichter, *Collision-Avoidance Framework for Small Fixed-Wing Unmanned Aerial Vehicles*, Journal of Guidance, Control, and Dynamics, **1** (2014), doi: 10.2514/1.G000226.
- [110] H. Choi, Y. Kim, and I. Hwang, *Reactive Collision Avoidance of Unmanned Aerial Vehicles Using a Single Vision Sensor*, Journal of Guidance, Control, and Dynamics **36**, 1234 (2013), doi: 10.2514/1.57131.
- [111] Y. Watanabe, A. Calise, E. Johnson, and J. Evers, *Minimum-Effort Guidance for Vision-Based Collision Avoidance*, in *AIAA Atmospheric Flight Mechanics Conference and Exhibit* (Keystone, CO, USA, 2006) aIAA 2006-6641, doi:10.2514/6.2006-6641.
- [112] A. Mujumdar and R. Padhi, *Reactive Collision Avoidance of Using Nonlinear Geometric and Differential Geometric Guidance*, Journal of Guidance, Control, and Dynamics **34**, 303 (2012), doi: 10.2514/1.50923.
- [113] S. Graham, W.-Z. Chen, J. De Luca, J. Kay, M. Deschenes, N. Weingarten, V. Raska, and X. Lee, *Multiple Intruder Autonomous Avoidance Flight Test*, (2011) aIAA 2011-1420, doi:10.2514/6.2011-1420.
- [114] Y. Jenie, E.-J. van Kampen, J. Ellerbroek, and J. Hoekstra, *Conflict Detection and Resolution System Architecture for Unmanned Aerial Vehicles in Civil Airspace*, in *AIAA Infotech @ Aerospace, SciTech Forum and Exposition* (Kissimmee, FL, USA, 2015) aIAA 2015-0483, doi:10.2514/6.2015-0483.
- [115] S. Tenoort, *D1.1 Definition of the Environment for Civil UAS Applications*, INOUI Innovative Operational UAS Integration Project, European Commission (2008), doc. No. INOUI\_WP1.1\_DFS\_D1.1\_PU\_v1.0.
- [116] *JO 7110.65U, Air Traffic Control, Chapter 1: General*, Federal Aviation Administration ().
- [117] O. Khatib, *Real-Time Obstacle Avoidance for Manipulators and Mobile Robots*, The International Journal of Robotics Research **5**, 90 (1986), doi: 10.1177/027836498600500106.
- [118] F. A. Cosío and M. P. Castañeda, *Autonomous robot navigation using adaptive potential fields*, Mathematical and Computer Modelling **40**, 1141 (2004), doi: 10.1016/j.mcm.2004.05.001.
- [119] T. Lam, H. Boschloo, M. Mulder, and M. Van Paassen, *Artificial Force Field for Haptic Feedback in UAV Teleoperation*, Systems, Man and Cybernetics, Part A: Systems and Humans, IEEE Transactions on **39**, 1316 (2009), doi:10.1109/TSMCA.2009.2028239.

- [120] A. Chakravarthy and D. Ghose, *Generalization of the Collision Cone Approach for Motion Safety in 3-D Environments*, *Autonomous Robots* **32**, 243 (2012), doi:10.1007/s10514-011-9270-z.
- [121] F. M. Heylen, S. B. J. van, M. Mulder, and M. M. van Paassen, *Design and Evaluation of a Vertical Separation Assistance Display*, in *AIAA Guidance, Navigation, and Control Conference and Exhibit* (Honolulu (HI), 2008) aIAA 2008-6969, doi:10.2514/6.2008-6969.
- [122] D. Wilkie, J. van den Berg, and D. Manocha, *Generalized Velocity Obstacles*, in *Intelligent Robots and Systems, 2009. IROS 2009. IEEE/RSJ International Conference on* (2009) pp. 5573–5578, doi:10.1109/IROS.2009.5354175.
- [123] J. Ellerbroek, M. Mulder, and M. M. van Paassen, *Evaluation of a Separation Assistance Display in a Multi-actor Experiment*, in *Proceedings of the 16th International Symposium on Aviation Psychology* (2011).
- [124] C. Peterson and J. Barton, *Virtual Structure Formations of Cooperating UAVs using Wind-compensation Command Generation and Generalized Velocity Obstacles*, in *Aerospace Conference, 2015 IEEE* (2015) pp. 1–7, doi:10.1109/AERO.2015.7118926.
- [125] S. Luongo, F. Corraro, U. Ciniglio, V. Di Vito, and A. Moccia, *A Novel 3D Analytical Algorithm for Autonomous Collision Avoidance considering Cylindrical Safety Bubble*, in *Aerospace Conference, 2010 IEEE* (2010) pp. 1–13, doi:10.1109/AERO.2010.5446780.
- [126] Y. I. Jenie, E.-J. V. Kampen, C. C. de Visser, J. Ellerbroek, and J. M. Hoekstra, *Three-dimensional Velocity Obstacle Method for UAV Deconflicting Maneuvers*, in *AIAA Guidance, Navigation, and Control Conference* (AIAA, Kissimmee, FL, 2015) aIAA 2015-0592, doi:10.2514/6.2015-0592.
- [127] A. Chakravarthy and D. Ghose, *Collision Cones for Quadric Surfaces*, *Robotics, IEEE Transactions on* **27**, 1159 (2011), doi:10.1109/TRO.2011.2159413.
- [128] G. S. Fishman, *Monte Carlo. Concepts, Algorithm, and Applications*, (Springer-Verlag, 175 Fifth Avenue, New York, NY, 100010, United States of America, 1996) Chap. 1. The Axioms, Part I, p. 26.



# SAMENVATTING

## **AUTONOMO CONFLICT DETECTIE EN RESOLUTIE SYSTEEM VOOR ONBEMANDE LUCHTVAARTUIGEN**

IN DE CONTEXT VAN INTEGRATIE IN HET LUCHTRUIM

**Yazdi Ibrahim JENIE**

In het afgelopen decennium is de commerciële waarde van onbemande luchtvaartuigen (UAVs), gedefinieerd als apparaten die vliegen in de atmosfeer zonder personen (piloten) aan boord, algemeen erkend dankzij de technologische ontwikkelingen van materialen, sensoren, computers en telemetrie. Nu UAVs goedkoper en gebruiksvriendelijker worden, zijn veel bedrijven gemotiveerd om UAVs in te zetten voor hun activiteiten, zoals voor pakketbezorging, filmopnames en het leveren van internet-dekking.

De commerciële toepassingen van UAVs kunnen echter pas gerealiseerd worden wanneer deze toestellen volledig geïntegreerd zijn in het luchtruim. Dit is momenteel niet het geval, aangezien vliegen met UAVs in de meeste landen streng gereguleerd is en vaak beperkt tot vluchten binnen het gezichtsveld van de grond-piloot (VLOS). Vliegen tot buiten het zicht van de grond-piloot (BVLOS) is in het algemeen niet toegestaan. Een hoofdreden voor de strenge regulatie is de bezorgdheid om de veiligheid van UAV vluchten, mede dankzij de grote verscheidenheid aan soorten toestellen, ieder met hun eigen voorkeur voor interactie met andere UAVs en met de huidige bemande luchtvaart. Hierdoor wordt verwacht dat management van het luchtruim, in het bijzonder het mitigeren van conflicten en botsingen, veel complexer gaat worden, wat de veiligheid in het geding kan brengen.

Om deze reden is dit proefschrift gericht op het probleem van een veilige integratie van UAVs in het luchtruim, specifiek op de ontwikkeling van conflict detectie en resolutie (CDR)systemen. Een CDR systeem bestaat uit apparaten en procedures die conflicten en botsingen in de lucht kunnen mitigeren. Voor UAVs moet dit systeem overweg kunnen met verschillende types obstakels, van statische objecten tot andere luchtvaartuigen met zeer uiteenlopende vliegeigenschappen. Bovendien kunnen er interacties optreden tussen twee UAVs met verschillende CDR systemen aan boord. Pas wanneer CDR systemen volledig gedefinieerd en gereguleerd zijn om overweg kunnen met deze verscheidenheid aan scenario's, kunnen UAVs geïntegreerd worden in het luchtruim. Het hoofddoel van dit proefschrift is het definiëren en evalueren van systemen voor detectie en resolutie

van mogelijke conflicten van UAVs, specifiek om BVLOS UAV vluchten in een geïntegreerd luchtruim te ondersteunen. Dit doel wordt bereikt door de aanpak van vier uitdagingen met betrekking tot: incompatibiliteit van het luchtruim, CDR diversiteit, twijfel over UAV veiligheid en de ontoereikendheid van autonome UAV CDR systemen. Uit deze vier problemen volgen direct de onderzoeksvragen:

1. Welke structuren kunnen gedefinieerd worden om CDR systemen voor UAVs in een geïntegreerd luchtruim te beheren?
2. Hoe kunnen de verschillende CDR systemen geclassificeerd worden in een alomvattende taxonomie die verenigbaar is met het huidige luchtruim?
3. Hoe kan de veiligheid van een geïntegreerd luchtruim met heterogene CDR systemen bepaald worden?
4. Hoe kunnen autonome CDR systemen voor UAVs ontworpen worden om overweg te gaan met conflicten in een geïntegreerd luchtruim?

Om de eerste onderzoeksvraag te beantwoorden wordt in dit proefschrift een taxonomie van CDR systemen voorgesteld voor UAVs in een geïntegreerd luchtruim. Mogelijke oplossingen worden in kaart gebracht en opgesplitst naar het type van toezicht, coördinatie, manoeuvre en de mate van autonomie. Deze factoren worden gecombineerd tot enkele generieke benaderingen, zo kan bijvoorbeeld het Traffic Warning and Collision Avoidance System (TCAS) uit de bemande luchtvaart gezien worden als een combinatie van een gedistribueerde afhankelijke toezichthouding, een expliciete coördinatie, een ontwijkmanoeuvre en een handmatige vluchtuitvoering. De combinaties die passen bij het doel van integratie van UAVs worden dan geselecteerd, wat resulteert in een innovatieve taxonomie van UAV CDR benaderingen.

Vanuit de generieke benaderingen wordt in dit proefschrift een uit meerdere lagen bestaande architectuur ontwikkeld, die CDR procedures beheert welke verenigbaar zijn met het huidige luchtruim en tevens CDR procedures die uniek zijn voor UAVs. Door de meerlaagse architectuur zijn UAVs niet van een enkele CDR procedure afhankelijk, maar zijn er meerdere CDR benaderingen in een fail-safe opstelling, zodat er bij het falen van een enkele laag, nog meerdere CDR benaderingen over zijn om conflicten te voorkomen. Zes CDR benaderingen uit de taxonomie worden geselecteerd als de veiligheidslagen: (1) Procedureel, (2) Handmatig, (3) Coöperatief, (4) Non-Coöperatief, (5) Ontwijk, (6) Nood.

Uit implementatie van de meerlaagse CDR aanpak blijkt dat het gebruik afhangt van het type missie: in bepaalde missies kunnen sommige lagen minder noodzakelijk zijn, terwijl deze in andere missies juist belangrijker zijn. De voorgestelde architectuur mist echter definities van de fysieke scheiding tussen de lagen, zoals de tijd-tot-botsing, die voor ieder type UAV gedefinieerd moeten worden. Het fysiek scheiden van de CDR lagen is een toekomstige taak van het luchtruimbeheer voor UAVs, maar zal pas echt gedefinieerd kunnen worden wanneer BVLOS vluchten van UAVs toegelaten zijn in het luchtruim.

Om de tweede onderzoeksvraag te beantwoorden wordt de voorgestelde taxonomie toegepast op de beschikbare CDR methodes uit de literatuur, om zo te bepalen of ze complementair of onderling uitwisselbaar zijn. In totaal zijn 64 CDR methodes geëvalueerd, variërend van berekeningen op basis van deterministische kaarten, zoals Global

Path Planning, tot reactieve ontwijkmethodes op basis van sensorinformatie, zoals bij de Velocity Obstacle methode. Met behulp van de taxonomie kan de positie van iedere aanpak gedefinieerd worden in een algemeen veiligheidsbeheersysteem, zoals de meerlaagse architectuur.

Het toepassen van de taxonomie op de bestaande methodes laat zien dat veel van de bestaande methodes buiten de taxonomie vallen, wat suggereert dat onderzoek meer gericht moet worden op de delen van de taxonomie waar de bestaande methodes achterblijven. Het is ook gebleken dat, vanwege de huidige beperking tot VLOS vluchten, de verscheidenheid aan CDR methodes zich slechts voordoet in de laboratoriumomgeving. Desalniettemin kan de taxonomie ontwikkelaars en autoriteiten helpen bij beslissingen over veiligheid van CDR methodes en kan het helpen om de veiligheid van toekomstige BVLOS vluchten te waarborgen.

De derde onderzoeksvraag wordt beantwoord met behulp van een set Monte Carlo simulaties waaruit twee veiligheidsparameters bepaald worden: de frequentie van bijna-botsingen (NMAC) en de frequentie van botsingen (MAC). De eerste parameter geeft aan hoe vaak twee UAVs dicht bij elkaar vliegen dan een bepaalde minimale afstand, die in de meeste discussies in dit proefschrift op 50 meter is gezet. De tweede parameter geeft het aantal botsingen tussen UAVs weer. De Monte Carlo methode overkomt de limitaties van de analytische methodes uit de literatuur, zodat het effect van een gedistribueerd CDR systeem meegenomen kan worden alsook heterogene condities in het luchtruim. Echter heeft de Monte Carlo methode niet vaak de voorkeur gehad voor het bepalen van de veiligheidsparameters, vanwege de lange rekentijd die nodig is om tot significante resultaten te komen. Dit probleem wordt in dit proefschrift opgelost door een hoge dichtheid van UAVs in het luchtruim te simuleren en de resultaten vervolgens terug te schalen naar realistische dichtheden.

Twee CDR protocollen zijn gemodelleerd in de simulaties. De eerste is het coöperatieve protocol, waarin iedere UAV ontwijkt door impliciet gecoördineerde luchtvaartregels. De tweede is het niet-coöperatieve protocol, waarin iedere UAV ontwijkt op basis van willekeurige voorkeuren. Een doel voor het veiligheidsniveau (TLS) is gedefinieerd in dit proefschrift om de gezamenlijke prestatie van de CDR systemen te meten, waarbij de frequentie van NMAC en MAC respectievelijk kleiner moet zijn dan  $10^{-2}$  en  $10^{-7}$  per uur. Deze TLS waardes zijn afgeleid van equivalente waardes in de bemande luchtvaart in het laatste decennium.

Uit de resultaten van het onderzoek in dit proefschrift blijkt dat het gedistribueerde coöperatieve CDR protocol het maximaal aantal UAV op één hoogte bijna tien keer kan vergoten vergeleken met de situatie zonder CDR en bij gelijkblijvende TLS. Dit betekent dat voor een stad als Chicago, die een oppervlakte heeft van meer dan vijfduizend vierkante kilometers, in totaal 45 UAVs op één hoogte kunnen vliegen. Geconcludeerd kan worden dat veel betere resultaten bereikt worden met het coöperatieve protocol, wat de noodzaak tot orde in het luchtruim rechtvaardigt, in dit geval in de vorm van de luchtvaartvoorangsregels. Dit proefschrift toont de kracht van Monte Carlo simulaties voor het testen van CDR algoritmes en protocollen voor een groot aantal mogelijke condities, zelfs voor onvoorspelbare condities die pas opgemerkt worden tijdens de simulatie. Het nadeel van de methode blijft echter bestaan, aangezien er geen significante resul-

taten bepaald kunnen worden voor frequenties van MAC binnen de simulaties vanwege de zeldzaamheid van MACs, zelfs bij een hoge dichtheid van UAVs. Het wordt daarom aanbevolen om langere simulaties te doen en tevens om de dynamische eigenschappen door middel van vliegtuigmodellen toe te voegen aan de simulaties.

De vierde onderzoeksvraag wordt beantwoord door het introduceren van twee innovatieve CDR algoritmes die specifieke lagen in de eerder besproken CDR architectuur invullen. Het eerste algoritme is de Selective Velocity Obstacle (SVO) methode, een uitbreiding van de Velocity Obstacle (VO) methode met extra criteria voor impliciete coördinatie. Deze CDR methode is speciaal ontworpen voor de coöperatieve laag van de CDR architectuur, aangezien het onwaarschijnlijk is dat een toekomstig luchtruim zal bestaan zonder enige vorm van orde of coördinatie, zoals de luchtvaartvoorangsregels. De SVO methode wordt ook gebruikt als basis voor het coöperatieve CDR protocol in de hiervoor besproken afleiding van de NMAC frequentie met behulp van Monte Carlo simulaties.

Het tweede algoritme is de driedimensionale Velocity Obstacle (3DVO) methode, die een uitbreiding is van de VO methode naar de driedimensionale ruimte, wat zorgt voor een grotere hoeveelheid resolutiemogelijkheden. De driedimensionale resolutie wordt uitgevoerd in willekeurige ontwijkvlakken, waarvan het aantal en de oriëntatie vastgesteld kan worden aan de hand van de manoeuvreerbaarheid van de UAV. Aangezien de 3DVO methode ontworpen is om de Ontwijk-laag in de CDR architectuur te vervullen, wordt tevens gebruik gemaakt van Buffer Velocity Zones, een extra algoritme dat de bewegingen van ongecoördineerde obstakels anticipeert. Het is ontdekt dat het toevoegen van de Buffer Velocity Zones de prestaties van het algoritme significant meer vergroten dan een toename van het aantal ontwijkvlakken.

Zowel de SVO als de 3DVO methode zijn gevalideerd met een set Monte Carlo simulaties in een heterogeen luchtruim, waarin beide methode de frequenties van NMACs en MACs significant konden verminderen. Dit geeft aan de beide methodes veelbelovend zijn voor de ondersteuning van BVLOS vluchten in een geïntegreerd luchtruim. Beide methodes maken echter geen gebruik van een dynamisch vliegtuigmodel, wat de resultaten significant kan veranderen, vooral in de Ontwijk-laag waar ontwijken dient te gebeuren bij korte onderlinge afstand. Bovendien wordt aangeraden om in de toekomst testvluchten te doen met beide concepten, vooral in echte BVLOS situaties waar UAVs autonoom reageren in het heterogene luchtruim. Verder zijn adequate algoritmes voor de overige lagen in de architectuur nodig om een complete BVLOS vlucht te ondersteunen. Dit zal het aantal beschikbare CDR benaderingen voor UAV operaties in een geïntegreerd luchtruim verrijken.

Op basis van het onderzoek dat uitgevoerd is in dit proefschrift wordt geconcludeerd dat veilige integratie van UAVs in het luchtruim heel goed mogelijk is. Deze conclusie wordt ondersteund door de vele uitgevoerde simulaties, die aantonen dat het mogelijk is om de TLS van het luchtruim te behalen met behulp van een autonoom CDR systeem dat gedistribueerd is en onafhankelijk werkt in iedere UAV. Het lage risico van UAV vluchten, zelf in een heterogeen luchtruim, is gevalideerd door de zeldzaamheid van NMACs en MACs, tot het punt waar een overdreven dichtheid of een super-conflict nodig is om de

operationele veiligheid te meten.

Hoewel veel UAV CDR benaderingen uit de literatuur niet ontworpen zijn voor BVLOS vluchten in een geïntegreerd luchtruim, kunnen de meeste wel aangepast worden tot adequate benaderingen zoals voorgeschreven door de voorgestelde taxonomie. Een voorbeeld van een dergelijke aanpassing is in dit proefschrift gepresenteerd met de uitbreiding van de VO methode tot de SVO methode, die past in een Coöperatieve benadering, en de uitbreiding tot de 3DVO methode, die past in de Ontwijk-laag. Met de grote verscheidenheid aan CDR benaderingen in de literatuur is een validatie in een heterogene opstelling vereist, ofwel door simulaties ofwel door testvluchten.

Vergeleken met halverwege 2011, toen het onderzoek in dit proefschrift gestart werd, is het commerciële gebruik van UAVs nu in 2016 nog verder doorgedrongen tot het algemene publiek. De wetgeving wordt aangepast om de luchtwaardigheid van UAVs te definiëren om zo het toepassingsgebied te vergroten. UAV eigenaren zijn zich ook steeds meer bewust van de regelgeving rondom UAVs, wat blijkt uit een toename in het aantal geregistreerde UAVs. Tegelijkertijd zijn er UAV lobbygroepen opgericht die de autoriteiten proberen te overtuigen om BVLOS vluchten toe te staan. Zij geven aan dat integratie van UAVs in het luchtruim onontkoombaar is en dat er een urgente noodzaak is voor CDR systemen die de veiligheid van het luchtruim ondersteunen. Op een bepaald moment is het daarom wellicht het beste als de autoriteiten beginnen met het accommoderen van BVLOS vluchten in het luchtruim, zodat UAVs en hun CDR systemen verder ontwikkeld kunnen worden op basis van ervaringen in het echte luchtruim. Gelijk aan de geschiedenis van deregulering in de bemande luchtvaart, kan dit een competitieve omgeving creëren die zowel de fabrikanten als de operators van UAVs zal aansturen tot continue verbetering van de veiligheid in een geïntegreerd luchtruim.



# ACKNOWLEDGEMENT

**A**LHAMDULILLAHIRABBIL'AALAMIIN, all praise is to Allah, the Cherisher and Sustainer of the universe, for without His help and guidance, this thesis, as well as my PhD program, would never be completed. This thesis is the crystallization of my ( $\pm$ )five years of work in my PhD program in the Control and Simulation group, of the Control and Operation division, of the Faculty of Aerospace Engineering, of the Delft University of Technology. I would like to dedicate these two pages to acknowledge people whom I benefited from the most, scientifically, technically, and socially, during my PhD period.

First of all I need to express my gratitude to Prof. Said D. Jenie, my dearest late uncle, who had pushed me in the first place to the wonderful world of Aerospace Engineering, and whose shoulder I have always been standing on right until I finished my master in 2008. Afterwards, thanks to Prof. Hari Muhammad, I began to be involved in many projects in ITB to apply the knowledge and hone the skills I have been taught off. It was Prof. Hari, together with Prof. Bob Mulder, who then opened a path to continue my education, by introducing me to the Control and Simulation group of TU Delft. Shortly after, with the help of Prof. Max Mulder whom I truly appreciate, I was granted a PhD scholarship from the Islamic Development Bank (IDB), went to the Netherlands, joined the group, got a desk, and was given a kick start research topic I should be working on for the next 'four' years. And thus, my PhD life began.

I owe most of my research development to my daily supervisor, Dr. Erik-Jan van Kampen, who provides me almost every weeks with valuable ideas, insights, advises, and critiques. I'm grateful for every discussion I have had with him, which occasionally extended to unscientific daily things. The topic of my research only began to mature and solidify after Prof. Jacco M. Hoekstra was appointed to be my promotor. Thanks to his expertise, and also with additional help from Dr. Joost Ellerbroek, I was able to further exploit the path I have decided to take, and mold it nicely into this very thesis. I also want to acknowledge Bertine Markus for her assist in all administration stuffs, Bart Remes who introduced me to the MAVLAB, Christophe De Wagter from whom the idea to work on UAV integration came from, and Dr. Coen Visser for his help with many fine details in my works.

To all my former and current colleagues in the group, I am grateful for all coffee corner talks, barbecues, conference travels, and every 'good morning' and 'see you' I have received in the past five years. In somewhat chronological order: Jan, Lauren, Wouter, Deniz, Ligu, Jia, and Rolf, the 'original' 0.11 roommates; Jaime, Sophie, Ye, Kirk, Ivan, Ewoud, Kimberly, and Lodewijk, the 'new' roommates; Daan, Rita, Herman, Ajenk, Jan,

Peng, Maarten, Gustavo, Joao, Han Woei, Tommasso, Tao, Ye, Kasper, Henri, Emanuel, and Junzi; and all other colleagues in the C&S group: You have all broadened my perspective of the world in so many aspects, and I really wish I have more time to know you all better. My special gratitude goes out to mBak Ajenk, or AKA Dyah, who acted as a big sister to me during this last five years.

To my Indonesian friends in Delft and the surroundings, thank for the friendship and kindness that sometimes makes me forgot that I'm very far from home. Thanks to Mas Patar, mBak Anna, Pak Jun, Bu Idha, Pak Wied, Pak Agus, Pak Senot, Bu Pungky, Pak Widya, Bu Reni, Pak Agung, Pak Zul, Pak Dudi, Mas Saputra, Bu Lasmini, Bu Ochi, Pak Marwan, Mas Andri, mas Pandu, mas Tofan, mbak Ajenk, Budi, pak Dieky, Pak Stevie, masbro Dwi, Pak Adhi, Mas Sayuta, mas Juli, Yudha, Mas Hedi, mas Data, mas Dito, and others whom I can proudly say that it is impossible to mention you all due to space limitations. Special thanks for Bu Reni and the family of Sekolah Indonesia Den-Haag (SIDH) who makes the last year of my PhD life much less stressful (yes, really). Another special is for Budi for the discussion about education, life, and nationality that we occasionally have. Hopefully someday we all can meet and collaborate again in a much higher level.

Finally, to my family, I will never be able to perfectly express how grateful I am for all the love that has been given to me. Thanks to Papa, Mama, mBak Ak, and Iik who always be there for me, and have been the greatest supporters and main motivators for me to keep pushing forward to the highest level of my education. To my wife Elly, I am truly grateful to have you as my best friend, my life partner, my keeper, my soul mate, and I wish that together we can establish a true *sakiinah, mawaddah wa rahmah* family. Grand-finally, thank you to my son Hanz, who taught me to have fun in seriousness, and to my daughter Hana, who always reminds me to be serious in having fun.

Thank you, thank you, thank you. And I wish you all all the best!!

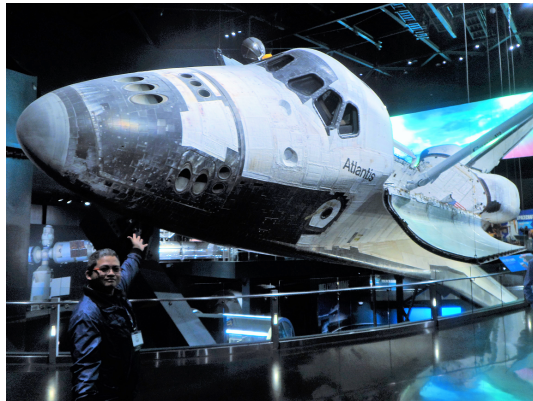
Delft, 23 January 2017

**Yazdi Ibrahim Jenie**

# CURRICULUM VITÆ

**Y**AZDI IBRAHIM JENIE was born in Surakarta, Indonesia, on April 19th, 1983. From 1989 to 2001 he did his formal education in Yogyakarta, and afterward moved to Bandung and started his study in Aerospace Engineering at Institut Teknologi Bandung (ITB). He spent a year in 2005 to work on his Final Task in Toyohashi University of Technology, Japan, before obtaining his Sarjana Teknik (B.Sc) degree from ITB in 2006.

Shortly after he started his master program as a part of the development of the national Wing in Surface Effect (WiSE) craft, in cooperation with the Agency for the Assessment and Application of Technology (BPPT) of Indonesia. He obtained his Magister Teknik (M.Sc) degree with honors in 2008 for his work on developing a full mathematical model of the WiSE craft for flight simulator implementation.



He immediately joined the Flight Physics research group of the Faculty of Mechanical and Aerospace Engineering of ITB as an academic assistant. Here he was also involved in various projects, especially on mathematical models and simulators, including for WiSE craft, ducted-fan UAVs, cruise missiles, satellite launch vehicles, and fighters.

In the mid of 2011 he was granted the Merit Scholarship Programme for High Technology from the Islamic Development Bank, which allowed him to start his PhD at the Faculty of Aerospace Engineering in Delft University of Technology, in the Netherlands. His research focused on Unmanned Aerial Vehicles (UAV) System, especially on the autonomous conflict detection and resolution system, in preparation for UAV integration into the airspace system.

From 2015 he became an assistant professor in his faculty in ITB, also under the Flight Physics research group. His current research interest is on flight dynamics, simulations, and autonomous systems.



# LIST OF PUBLICATIONS

## Journal Articles

4. **Y.I. Jenie**, E. van Kampen, J. Ellerbroek, and J.M. Hoekstra, *Safety Assessment of UAV CD&R System in a High Density Airspace using Monte Carlo Simulations*, IEEE Transactions on Intelligent Transportation Systems, [SUBMITTED-2016].
3. **Y.I. Jenie**, E. van Kampen, J. Ellerbroek, and J.M. Hoekstra, *Taxonomy of Conflict Detection and Resolution Approaches for Unmanned Aerial Vehicle in an Integrated Airspace*, IEEE Transactions on Intelligent Transportation Systems, **vol. PP**, no.99, pp.1-10 (July 2016).
2. **Y.I. Jenie**, E. van Kampen, C.C. de Visser, J. Ellerbroek, and J.M. Hoekstra, *Three-Dimensional Velocity Obstacle Method for Uncoordinated Avoidance Maneuvers of Unmanned Aerial Vehicles*, AIAA Journal of Guidance, Control, and Dynamics, **Vol. 39**, No. 10 pp. 2312-2323 (July 2016).
1. **Y.I. Jenie**, E. van Kampen, C.C. de Visser, J. Ellerbroek, and J.M. Hoekstra, *Selective Velocity Obstacle Method for Deconflicting Maneuvers Applied to Unmanned Aerial Vehicles*, AIAA Journal of Guidance, Control, and Dynamics, **Vol. 38**, No 6, pp 1140-1146 (April 2015).

## Book Chapters

1. **Y.I. Jenie**, E. van Kampen, and B. Remes, *Cooperative Autonomous Collision Avoidance System for Unmanned Aerial Vehicle*, Advances in Aerospace Guidance, Navigation and Control, pp.387-405, edited by Q. Chu, B. Mulder, D. Choukroun, E.-J. Kampen, C. Visser, and G. Looye; Springer Berlin Heidelberg, (2013).

## Conference Papers

10. C. Cheung, **Y.I. Jenie**, and E. van Kampen, *Experimental Validation of the Selective Velocity Obstacle method for Autonomous Collision Avoidance*, AIAA Guidance, Navigation, and Control Conference, SciTech 2017, Grapevine, TX, (January 2017).
9. **Y.I. Jenie**, E. van Kampen, J. Ellerbroek, and J.M. Hoekstra, *Safety Assessment of Unmanned Aerial Vehicle Operations in an Integrated Airspace*, AIAA @Infotech Conference, SciTech 2016, San Diego, CA, (January 2016).
8. **Y.I. Jenie**, E. van Kampen, C.C. de Visser, J. Ellerbroek, and J.M. Hoekstra, *Three-Dimensional Velocity Obstacle Method for UAV's Uncoordinated Avoidance Maneuver*, AIAA Guidance, Navigation, and Control Conference, SciTech 2016, San Diego, CA, (January 2016).
7. **Y.I. Jenie**, E. van Kampen, C.C. de Visser, J. Ellerbroek, and J.M. Hoekstra, *Three-Dimensional Velocity Obstacle Method for UAV Deconflicting Maneuvers*, AIAA Guidance, Navigation, and Control Conference, SciTech 2015, Kissimmee, FL, (January 2015).

6. **Y.I. Jenie**, E. van Kampen, J. Ellerbroek, and J.M. Hoekstra, *Conflict Detection and Resolution System Architecture for Unmanned Aerial Vehicles in Civil Airspace*, AIAA @Infotech Conference, SciTech 2015, Kissimmee, FL, (January 2015).
5. **Y.I. Jenie**, E. van Kampen, C.C. de Visser, and Q. Chu, *Velocity Obstacle Method for Non-cooperative Autonomous Collision Avoidance System for UAVs*, AIAA Guidance, Navigation, and Control Conference, SciTech 2014, National Harbor, MD, (January 2014).
4. **Y.I. Jenie**, E. van Kampen, C.C. de Visser, and Q. Chu, *Selective Velocity Obstacle Method for Cooperative Autonomous Collision Avoidance System for UAVs*, AIAA Guidance, Navigation, and Control Conference 2013, Boston, MA, (August 2013).
3. **Y.I. Jenie**, E. van Kampen, C.C. de Visser, and Q. Chu, *Hybrid Modeling of Velocity Obstacle Method in Autonomous Collision Avoidance System for UAVs*, AIAA Modeling and Simulation Technology Conference 2013, Boston, MA, (August 2013).
2. **Y.I. Jenie** and E. van Kampen, *An Autonomous Collision Avoidance Strategy for Unmanned Air Vehicle Guidance*, 5TH European Conference for Aeronautics and Space Sciences (EU-CASS) 2013, Munich, (June 2013).
1. **Y.I. Jenie**, E. van Kampen, and B. Remes. *Cooperative Autonomous Collision Avoidance System for Unmanned Aerial Vehicle*, CEAS EuroGNC 2013 Conference, Delft, (April 2013).

### Scientific Posters

2. **Y.I. Jenie**, *Autonomous Collision Avoidance System for UAVs, Towards Integration into the National Airspace System*, PhD Poster Day 2014, Faculty of Aerospace Engineering, Delft University of Technology (April 2014)
1. **Y.I. Jenie**, *Autonomous Collision Avoidance System for UAVs, Towards Integration into the National Airspace System*, PhD Poster Day 2013, Faculty of Aerospace Engineering, Delft University of Technology (April 2013)